1. Effective Date	04/27/2021	**Professional Engineer's Stamp**
2. Does this ECAR involve a Safety SSC?	No	
3. Safety SSC Determination Document ID	N/A	Not required per LWP-10010, Sec. 4.1, par. cc
4. SSC ID	N/A	
5. Project No.	23747	
6. Engineering Job (EJ) No.	N/A	
7. Building	TRA-670	
8. Site Area	ATR Complex	

9. Objective / Purpose

The Advanced Graphite Capsule (AGC) irradiation experiment will provide irradiation creep rate data for the new graphite proposed for the Next-Generation Nuclear Plant (NGNP) program. The fourth experiment in the series (AGC-4) was designed to irradiate various types of graphite specimens at 900ºC and targeted displacements per atom (DPA) of 6. This experiment has been irradiated in the east flux trap of the Advanced Test Reactor (ATR) during the 157D, 158A, 162A, 162B, 164A, 164B, 166A, and 166B cycles. Temperatures were monitored using 12 thermocouples (TC) located at various elevations in the reactor core, and variable helium-argon gas mixtures were used for gas gap temperature control of the specimens.

The purpose of this Engineering Calculation and Analysis Report (ECAR) is to calculate the specimen temperature after the model is calibrated by the measured TC data with the as-run heating rates of the components, the DPA of the graphite, and the gas mixture compositions during the experiment. As-run specimen mean temperature and the tolerance will be obtained.

10. If revision, please state the reason and list sections and/or page being affected.

N/A

11. Conclusion / Recommendations

A finite element, steady-state heat transfer analysis of the entire AGC-4 test train was performed using Abaqus. The analysis was performed on three selected days during each cycle (one cycle has two days), using the measured east source power, measured gas flows, as-run heating rates, and as-run graphite DPA, to obtain best-estimate temperatures of the specimens and TCs. The accuracy of the model was assessed by comparing the measured and calculated TC temperatures. The difference between these temperature values was used to estimate the mean and standard deviation of the error. Setting the uncertainty equal to the mean ± two standard deviations corresponding to a 95% confidence interval, the

results indicate that the maximum uncertainty in the calculated thermocouple temperature is ±30°C.

The temperature of each creep specimen is desired to be maintained at 900°C ±50°C. However, the results of this analysis show that the temperatures of the specimen stacks are outside the desired range. In general, the specimen average temperatures over the cycles vary from 800 to 900°C. The total specimen mean temperature is 838°C with ±106°C uncertainty (two standard deviation). Specifically, the lower stack mean temperature is 818°C, upper stack mean temperature is 843°C, and center stack mean temperature is 870°C. The maximum specimen temperature occurs in the center stack, reaching close to 980°C, and the lowest occurs at the ends of the peripherical stacks, dropping to around 670°C.

CONTENTS

TABLE OF TABLES

TABLE OF FIGURES

1. PROJECT ROLES AND RESPONSIBILITIES

Project Role	Name	Organization	Pages Covered (if applicable)
Performer	Changhu Xing	C140	All
Checker[a]	Casey J. Jesse	C140	All
Independent Reviewer[b]			
CUI Reviewer[c]	Michael E. Davenport	C640	All
Manager[d]	Richard H. Howard	C140	All
Requestor[ef]	Michael E. Davenport	C640	All
Nuclear Safety[f]			
Document Owner[f]	Michael E. Davenport	C640	All
Reviewer[f]	William E. Windes	B612	All
Reviewer[f]	David T. Rohrbaugh	D520	All

Responsibilities:

a. Confirmation of completeness, mathematical accuracy, and correctness of data and appropriateness of assumptions.

b. Concurrence of method or approach. See definition, LWP-10106.

c. Concurrence with the document's markings in accordance with LWP-11202.

d. Concurrence of procedure compliance. Concurrence with method/approach and conclusion.

e. Authorizes the commencement of work of the engineering deliverable. See Appendix A.

f. Concurrence with the document's assumptions and input information. See definition of Acceptance, LWP-10200.

2. SCOPE AND BRIEF DESCRIPTION

The Advanced Graphite Creep (AGC) irradiation experiment will provide irradiation creep rate data for the new graphite proposed for the Next-Generation Nuclear Plant (NGNP) program. In order to develop this data, matched pairs of stressed and unstressed specimens will be irradiated, and their pre- and post-irradiation dimensional and other thermomechanical properties will be measured to ascertain the effects of irradiation on these properties [1].

The AGC-4 experiment was designed to irradiate various types of graphite specimens at 900ºC and a targeted DPA of 6. This experiment has been irradiated in the east flux trap of the Advanced Test Reactor (ATR) during the 157D, 158A, 162A, 162B, 164A, 164B, 166A, and 166B cycles. Temperatures were monitored using 12 thermocouples (TCs) located at various elevations in the reactor core, and variable helium-argon gas mixtures were used for gas gap temperature control of the specimens.

As-run specimen temperatures are calculated in this Engineering Calculations and Analysis Report (ECAR) after the model is calibrated by the measured TC data with the in-situ heating rates of the component, the DPA of the graphite, and the gas mixture compositions during the experiment.

3. DESIGN OR TECHNICAL PARAMETER INPUT AND SOURCES

Technical and functional requirements of the AGC-4 experiment are given in TFR-875 [2]. The AGC-4 experiment is the fourth in a series of irradiation experiments to obtain data on fine-grained isotropic graphite used in the next-generation very high temperature reactor (VHTR). Figure 1 presents an illustration of the cross section (height/axial direction) of the test train.

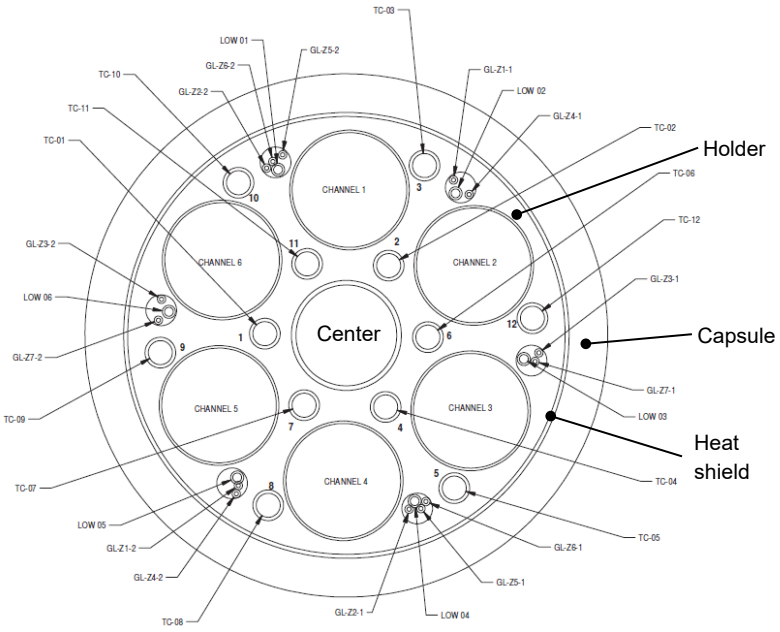

Figure 1. Illustration of the AGC-4 experiment (DWG-604554).

The test train consists of seven stacks of cylindrical graphite specimens having a diameter of 0.5 inches. They are placed in Channels 1–6 and the center channel of the graphite holder shown in Figure 1. The center stack contains unstressed specimens, while the peripheral stacks contain stressed specimens above the core mid-plane and unstressed specimens below the core mid-plane. The holder is contained in a stainless-steel capsule, with a HAYNES 230 heat shield placed between them. The holder has a stepped outside diameter to provide an axially varying temperature control gas gap to compensate for the axial variation in heating. All specimens should be irradiated at the same temperature, while corresponding stressed and unstressed specimens should be irradiated to the same DPA. Temperature is monitored using TCs, and five gas zones containing separate helium-argon gas mixtures are used for gas gap temperature control of the specimens. Other capsule internal components include tungsten spacers that provide heat generation at the top and bottom of the test train. TCs and gas tubing are located in the holes of the holder.

4. RESULTS OF LITERATURE SEARCHES AND OTHER BACKGROUND DATA

Table 1 presents the drawings used in the analysis. Some revisions of the drawings occurred after the design thermal analysis of ECAR-2494 and they are incorporated in the current as-run analysis.

Table 1. Drawing numbers and descriptions.

Drawing #	Description	Revision
443027	ATR South and East Flux Trap Chopped Dummy In-Pile Tube Assembly	12
600862	ATR Advanced Graphite Capsule (AGC) Gas Control System Test Train Top Head Gas Line Interconnection Diagram	2
603523	ATR Advanced Graphite Capsule (AGC) Miscellaneous Graphite Component Assemblies and Details	1
603533	ATR Advanced Graphite Capsule (AGC) Gas Zone Supporting Details	0
603539	ATR Advanced Graphite Capsule (AGC-3) Specimen Stack Heater Details	1
603541	ATR Advanced Graphite Capsule (AGC) Specimen Spacer, End Cap and Pin Details	0
604534	ATR Advanced Graphite Capsule (AGC-4) Thermal Heat Shield and Split Ring Details	1
604551	ATR Advanced Graphite Capsule (AGC-4) Graphite Specimen Holder Machining Details	0
604552	ATR Advanced Graphite Capsule (AGC-4) Hole Details for Upper and Lower Specimen Holders	1
604553	ATR Advanced Graphite Capsule (AGC-4) Specimen Stack-Up Arrangements	2
604554	ATR Advanced Graphite Capsule (AGC-4) Test Train Facility Assembly	0
604555	ATR Advanced Graphite (AGC-4) Test Train Installation	0
630428	ATR Advanced Graphite Capsule (AGC) Stainless Steel and Aluminum Component Details	8
630434	ATR Advanced Graphite Capsule (AGC) Capsule Facility In-Core Pressure Boundary Tube	3
778033	ATR Advanced Graphite Capsule (AGC) AGC-4 Graphite Specimen Cutout Diagrams	1

5. ASSUMPTIONS

1) Heating rate of each component is computed by averaging the heating rates of the azimuthal segments. For instance, for the holder at each capsule position, six segments were considered in the neutronic analysis [3] at the same elevation. In the thermal analysis, one average value is employed. The past sensitivity studies showed that the azimuthal variations in heating rates in the test train do not have a significant effect on temperature because conduction heat transfer between components tends to equalize the temperature.

Heating rates of the specimen stacks are treated separately to get more precise temperature evaluation. Because the specimens are separated by gas gaps, no averaging over the azimuthal is performed.

2) Axial profile of the heating rates used an asymmetric distribution from previous AGC series experiments instead of the distribution from the regression. Only the regressed amplitude is applied to the simulation model.

3) The length of the specimen stacks under axial compression will change during irradiation due to irradiation-induced creep. In this analysis, temperature is evaluated in the undeformed configuration as a function of elevation. For a given specimen, its temperature at a particular time during irradiation may be determined by estimating its location with respect to the core mid-plane, including the effect of axial compression, and then using the results of this analysis to obtain the temperature at that location.

4) One significant uncertainty is the gap between the heat shield and capsule, which can vary from the case where the inside surfaces of the heat shield contact the nubs on the holder to the case where the dimples on the outside surface of the heat shield contact the capsule. The nominal gap between heat shield and capsule is 0.011 inch. The resulting temperature control gas gaps between the heat shield and holder are determined by accounting for thermal expansion and shrinkage of the holder.

   The nominal gas gap between the heat shield and capsule is adjusted to account for uncertainty in the exact location of the heat shield, the increased thermal conductance due to contact between the capsule and dimples on the heat shield, and the uncertainty in the control gas composition due to gas leakage around the rings separating adjacent gas zones. The variable gas gap between the heat shield and capsule was adjusted in order to bring into agreement the measured and calculated TC temperatures. Moreover, the control gases in adjacent gas zones may mix since the seals are not gas tight. In some cases, an argon-rich mixture in one zone was assumed to mix with a helium-rich mixture in an adjacent zone in order to bring into agreement the measured and calculated TC temperatures.

5) Another uncertainty is the gas gap between the graphite specimens and graphite holder, which increases during irradiation due to graphite shrinkage. The bore diameter measurements of the irradiated holders showed a significant difference in the dimensional changes occurring in the lower and upper holders (INL/EXT-14-32060 [4]), suggesting that the compressive loading of the upper holder had affected the measured dimensional change. Moreover, the position of the specimens in the bore channels of the graphite holder is not fixed, and the diameter of the stressed specimens is also changing due to creep. These uncertainties preclude an accurate calculation of the gas gap between the specimens and holder. Therefore, the gas gap is set to its nominal design value of 0.010 inch and is assumed not to change during irradiation. A previous analysis of the temperature uncertainty in the AGC experiments reported that the uncertainty in the gap between the specimens and holder will add approximately 12°C to the uncertainty in the temperature of the center specimen stack (ECAR-3017 [5]).

6) An additional uncertainty is the gas gap between the TCs and graphite holder, which may vary due to the loose fit of the TC inside the holder. The gas gap assumed in this analysis is based on the experiment reported in ECAR-2429 [6] and is discussed in the as-run analyses of the AGC-1 and AGC-2 experiments (ECAR-2562 [7], ECAR-2322 [8]).

7) The AGC-4 test train was rotated 180° after the first four cycles of irradiation. The effect of test train rotation on the azimuthal position of the specimens and TCs was included in the analysis.

8) TC holes in the holder have a counterbore diameter that is different from the diameter where the TC beads are located. In the model, a uniform diameter is assumed.

9) The TC sheath is made of Inconel (DWG-604554); however, stainless steel was used in the past Abaqus models. This analysis aligns with the past AGC series analyses.

10) The legacy dimension discrepancies of the TC & gas line holes between the Abaqus model and the drawings were not changed because Tie constraints were applied between the TC & gas line and the holes.

6. COMPUTER CODE VALIDATION

A finite element heat transfer analysis of the experiment was performed using Abaqus Version 6.14-2 on an SGI ICE X distributed memory cluster with 972 compute nodes (“Falcon” on the Idaho National Laboratory (INL) network). The operating system is SUSE Linux Enterprise Server 12 Service Pack 4, and each compute node has two 18-core 2.10 GHz Intel Xeon processors. Abaqus is listed in the INL Enterprise Architecture (EA) repository of qualified scientific and engineering analysis software (EA Identifier 336418). Abaqus has been validated for the thermal analysis of ATR experiments by solving several test problems and verifying the results against analytical solutions provided in heat transfer textbooks. A complete description of the validation test problems is given in ECAR-131 [9]. It should be noted that ECAR-131 was performed for validating Abaqus 6.7-3; however, the test problem descriptions are still accurate for the test problems run for Version 6.14-2. The test problems were run on Falcon and the verification report can be found in ECAR-4673 [10]. The Mathcad and Excel calculations have been independently verified by visual inspection and random hand calculation checking during the review process as allowed by LWP-10200, Appendix E [11].

7. DISCUSSION/ANALYSIS

7.1. Background information

The thermal analysis was performed using a detailed finite element model of the experiment created in ECAR-2494 and was updated with the current drawings.

The material properties are obtained from the handbooks and databases listed in the references and are given in Appendix A1. The gas gaps between capsule components, accounting for the change in the capsule component diameter due to thermal expansion and the change in graphite diameter due to irradiation-induced shrinkage, are calculated in Appendix A2. The resulting heat transfer coefficients for the fluence-dependent “hot” gas gaps are computed using various helium-argon gas mixtures and various DPA values and are given in Appendix A3.

The primary coolant flow in the annular gap between the capsule and chopped dummy in-pile tube is calculated for two-pump operation. Heat transfer coefficients for the turbulent forced convection are given in Appendix A4 and applied to the coolant/capsule and coolant/tube interfaces.

The average lobe power in the east flux trap is 20.8 MW over the eight cycles [3]. Heating rates for each component in the test train were obtained as a function of position with respect to the core mid-plane. For the capsule, heat shield, graphite holder and specimens, TCs, and primary coolant, a cosine-shaped profile was used to represent the axial variation in heating. The axial profile was split into separate profiles above and below core mid-plane, producing an asymmetric profile that preserves total core heating. The asymmetric heating profile improves temperature calculations as compared to the symmetric profile. Heating rates at an instantaneous power during each cycle are obtained by linear scaling to the average lobe power. Details are given in Appendix A5.

Reactor power, temperature control gas flows, and TC temperatures are obtained from the Nuclear Data Management and Analysis System (NDMAS). Spreadsheets containing data recorded at 10-minute intervals were downloaded from the NDMAS website (ndmashome.inl.gov or htgr.inl.gov, but authorization is needed). Reactor power, temperature control gas flows, and TC temperatures at selected days during each cycle are computed by averaging the data over the entire day. The peak DPA on those days was obtained from the as-run reactor physics analysis [3]. The original Excel data files from NDMAS and the data-processed file are stored in the reference folder. Selected data is given in Appendix A6.

7.2 Simulation model

A finite element, steady-state heat transfer analysis of the AGC-4 test train, including the capsule and all internal components, was performed using Abaqus. The 8-node linear brick element was used to model all solid components except the heat shield, which was modeled using the 4-node linear shell element. The 8-node convection brick element was used to model the primary coolant with a prescribed mass flow rate (the unit is mass flux). The model geometry and finite element mesh of the experiment cross section at the top of the test train where all TCs are visible is shown in Figure 2. A 3D cutaway view of the experiment is shown in Figure 3. In these figures, the capsule is blue, specimen holder is green, specimens are red, and TCs are orange. The heat shield is modeled as a thin shell and is not clearly visible in the figure. The primary coolant (outside of the capsule) and chopped dummy in-pile tube (enclosing the coolant) are not shown.

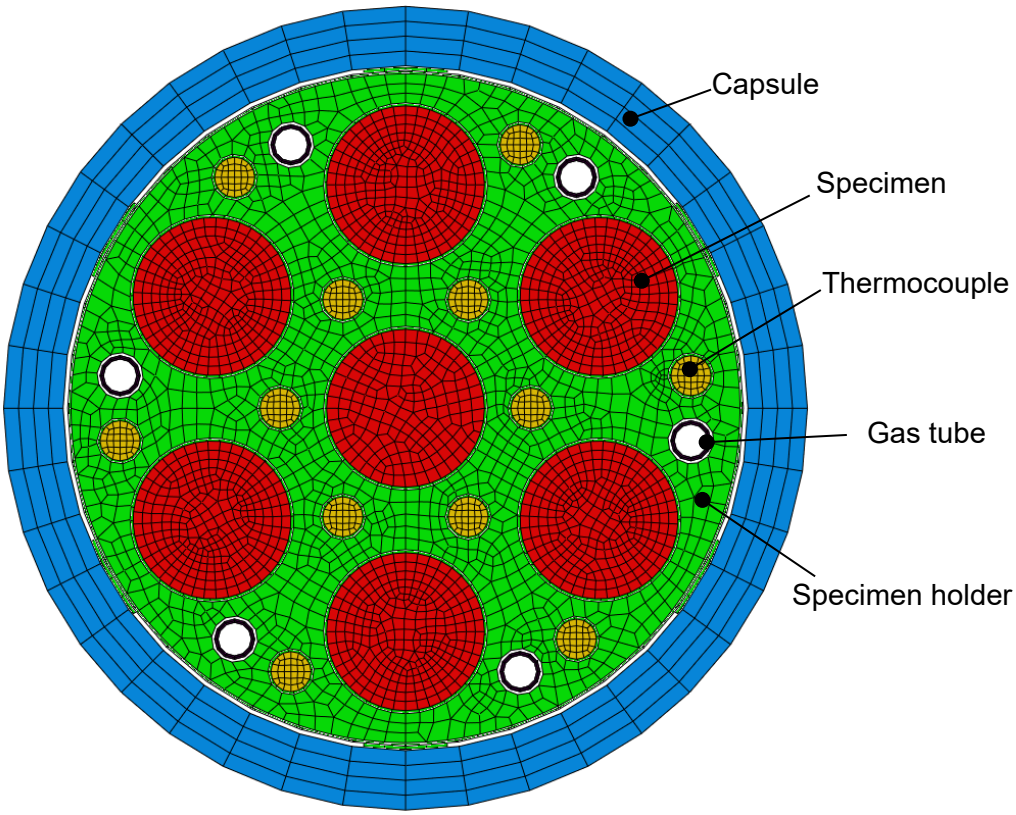

Figure 2. Model geometry and finite element mesh in Abaqus (axial).

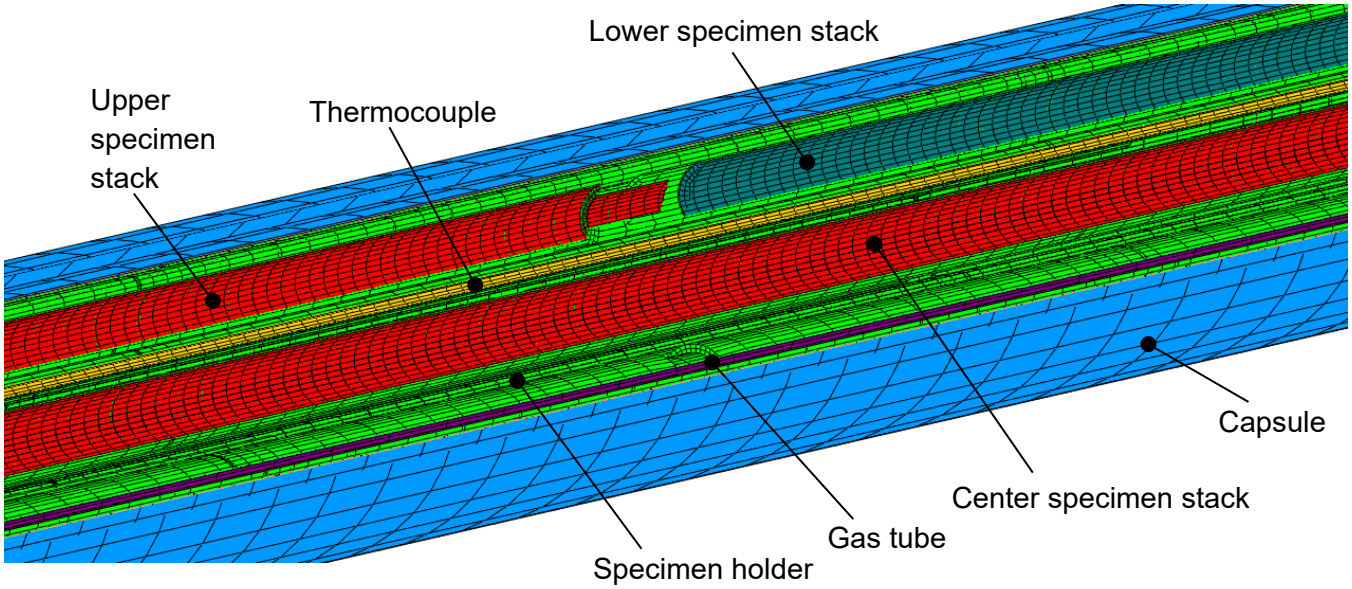

Figure 3. Model geometry and finite element mesh in Abaqus (cutaway view).

7.3 Calibration of the model

Calibration/correlation of the model is performed by comparing the simulated TC temperature with the measured ones (guess and check). In each cycle, three days (only Cycle 162B has two selected days) were selected for the correlation. The selection of the calibration days in the cycles are determined by several factors. Firstly, two to three days are selected with an interval of 17–20 days tending to be evenly distributed in each cycle. The intervals are not the same because the durations of the ATR cycles are not equal. For the eight cycles, the duration ranges from 38 to 64 days. Secondly, some days, for instance, the start of a cycle or restart after a scram is avoided because the temperature response is much slower than the ATR power. Some cycles do not have a scram, but some have one to two scrams (see the recorded plots). Thirdly, the days when the gas mixture and lobe power data were missing are skipped. This may be due to the recording malfunction. Lastly, the days when the gas mixture changes are not selected. Since the temperature and gas mixture cannot be synchronized simultaneously (gas mixture determines the boundary condition, but the temperature response requires time), the selected days are in the middle or at the end of the same gas mixture.

TC used in the experiment is type N, purchased from Idaho Labs Corp based on item 64 in DWG-604554. According to the specifications of the type N TC, the accuracy is 2.2 ºC or 0.75% (whichever is greater) (thermocoupleinfo.com). The maximum measured temperature is 1002 ºC thus the TC maximum uncertainty is 7.5 ºC. The TC wires were calibrated by the vendor following ASTM E235. Lot calibration certificate was provided.

The measured lobe power, gas flow, as-run heating rate, and as-run graphite DPA, together with the adjusted gap between heat shield and capsule, were applied in the Abaqus model to obtain the best-estimate temperatures of the test train components. Comparison between the measured and calculated TC temperatures are plotted in two styles. One is that all the TCs in each cycle, and the other is one TC in all the cycles per plot. The mean of the temperature differences is 2ºC (calculated is slightly higher) and the standard deviation is 14. Since two times the standard deviation corresponds to a 95% confidence level, the calculated TC uncertainty is ±28ºC. If considering the biased mean of 2ºC, the uncertainty can be roughly considered as ±30ºC.

The calibrations of all TC data on each cycle are presented in Figure 4 through Figure 11. These figures are helpful to explain the specimen temperature distribution. In general, an axial chopped cosine temperature distribution can be seen, especially for the last four cycles.

The temperatures of one specific TC in all the cycles are presented in Figure 12 through Figure 14.These figures are helpful to view the temperature evolution over the cycles. Simulated TC temperatures are superimposed from which an overall correlation with the TC measurement can be obtained.

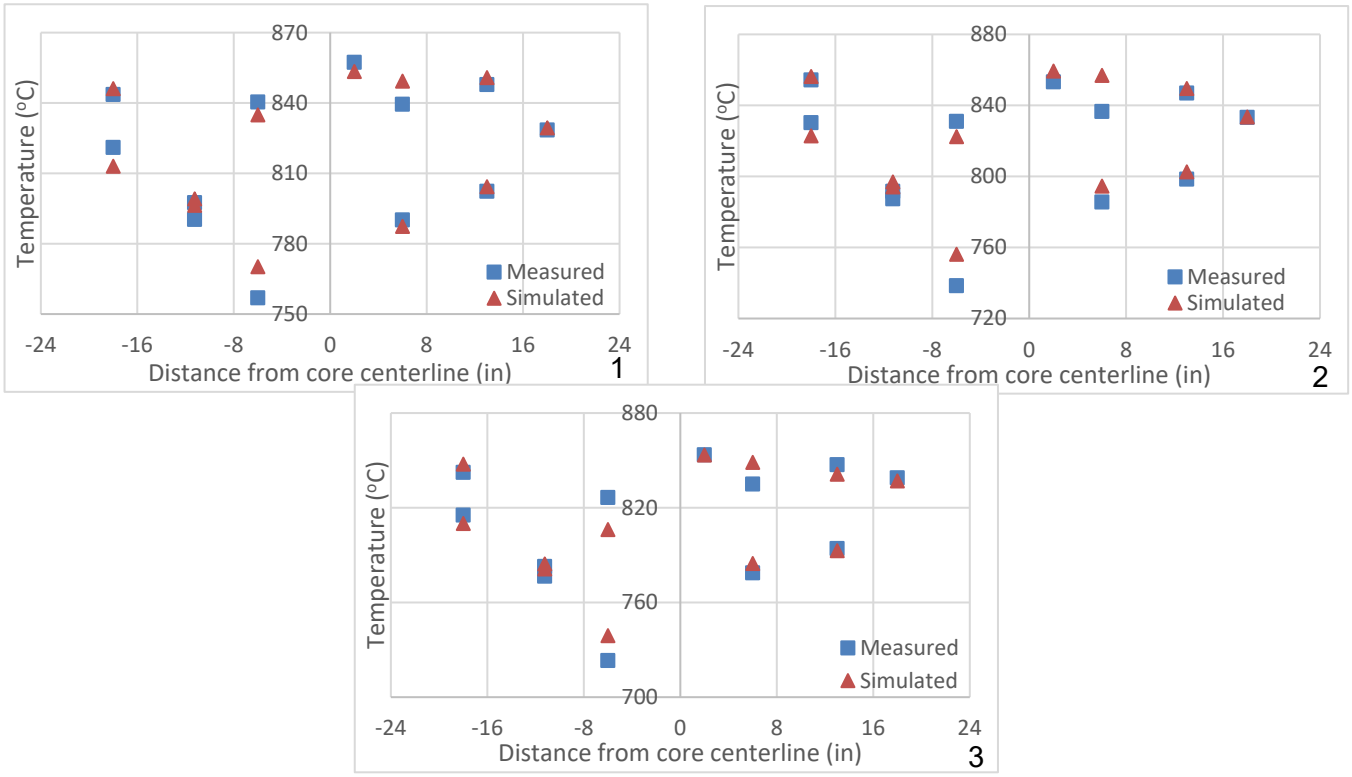

Figure 4. Measured and calculated temperatures of three selected days (1–3) in the 157D irradiation cycle.

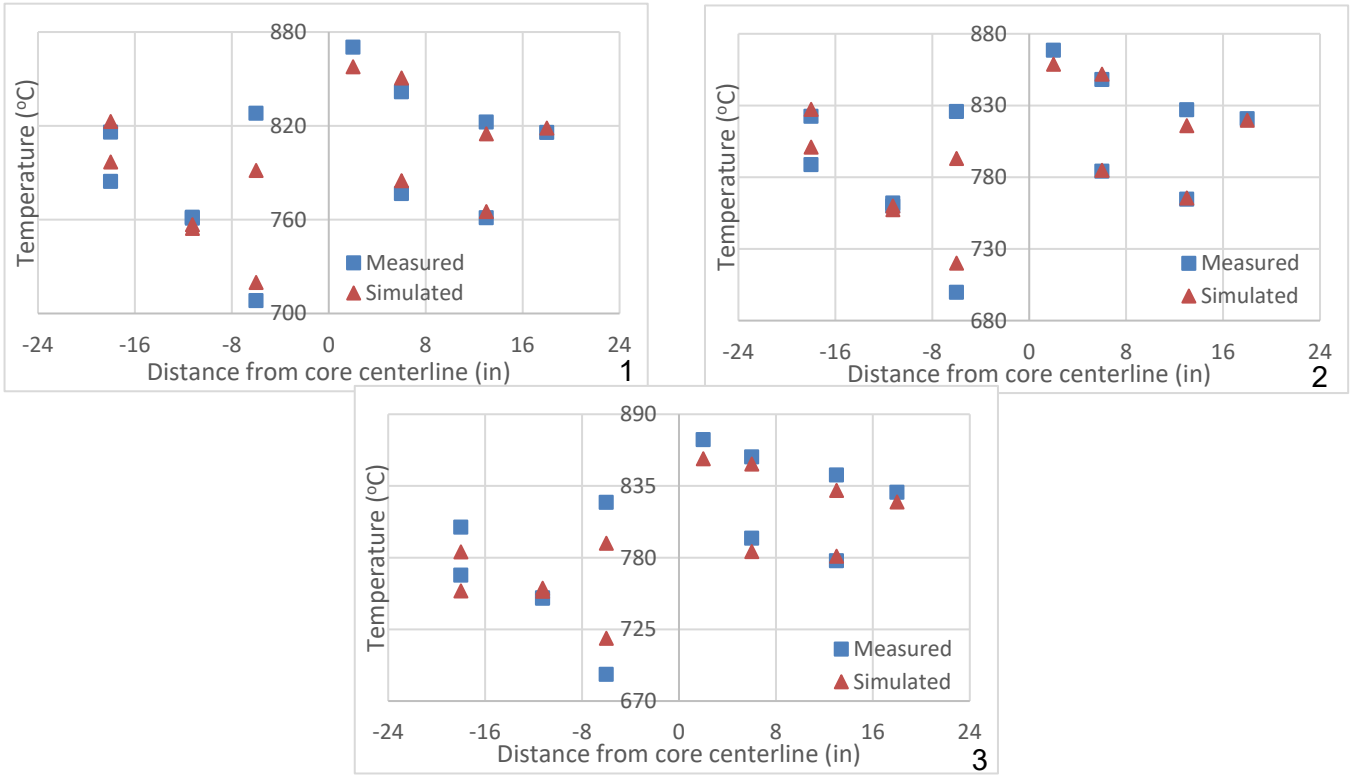

Figure 5. Measured and calculated temperatures of three selected days (1–3) in the 158A irradiation cycle.

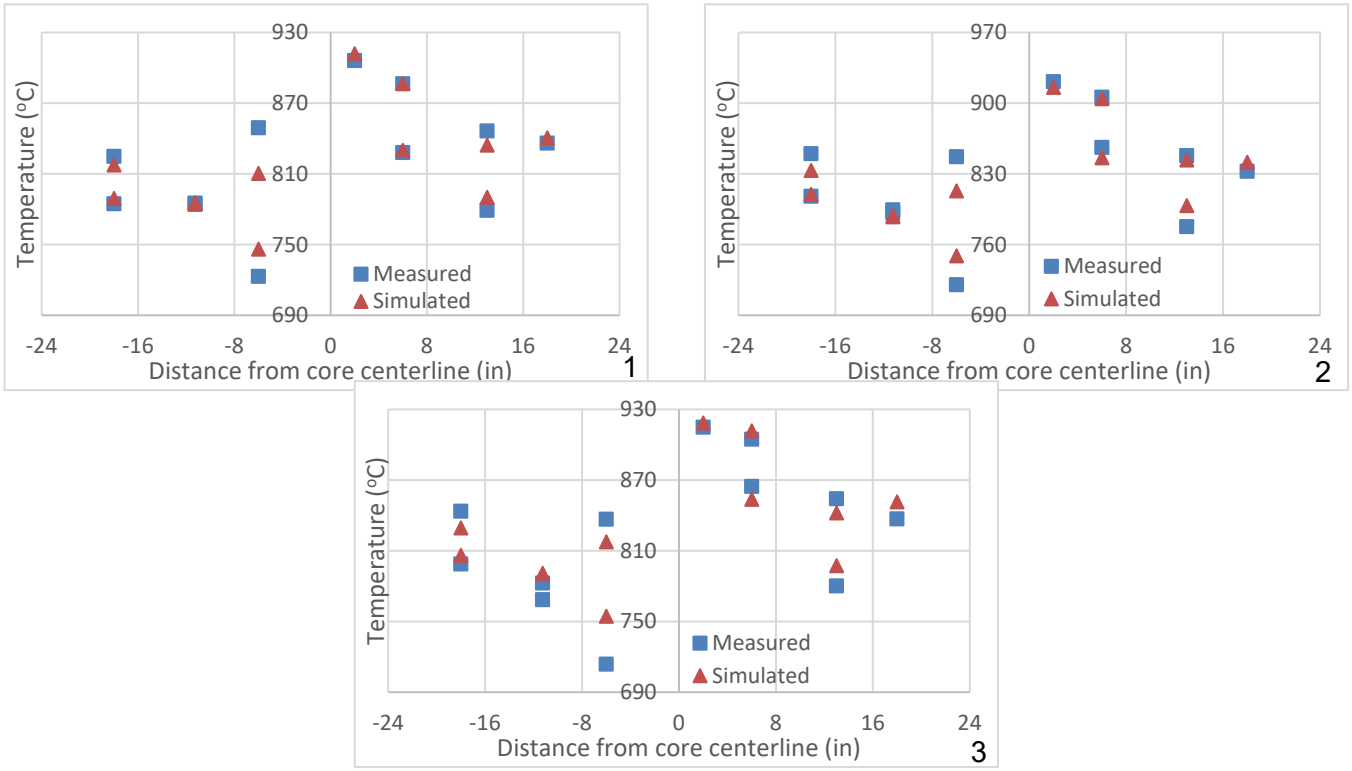

Figure 6. Measured and calculated temperatures of three selected days (1–3) in the 162A irradiation cycle.

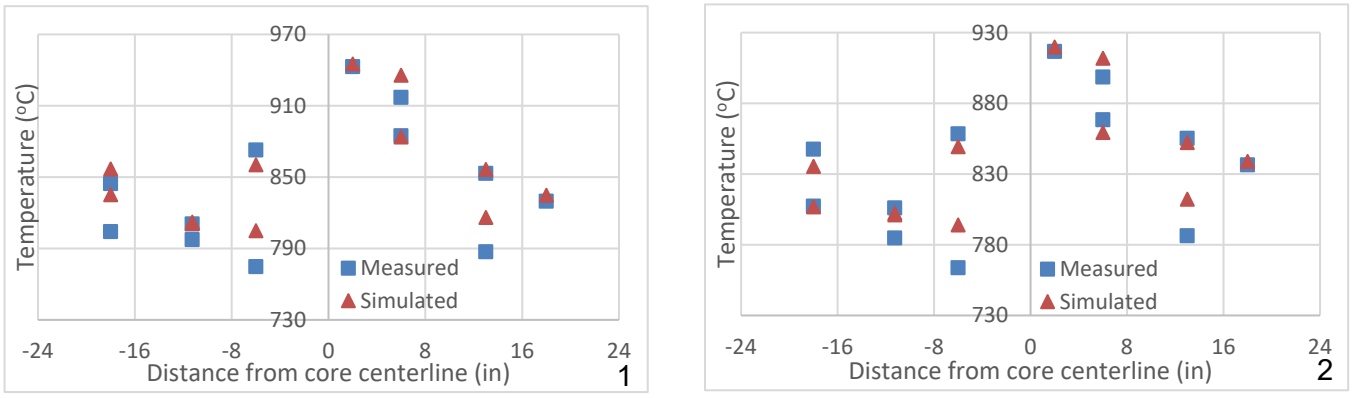

Figure 7. Measured and calculated temperatures of two selected days (1–2) in the 162B irradiation cycle.

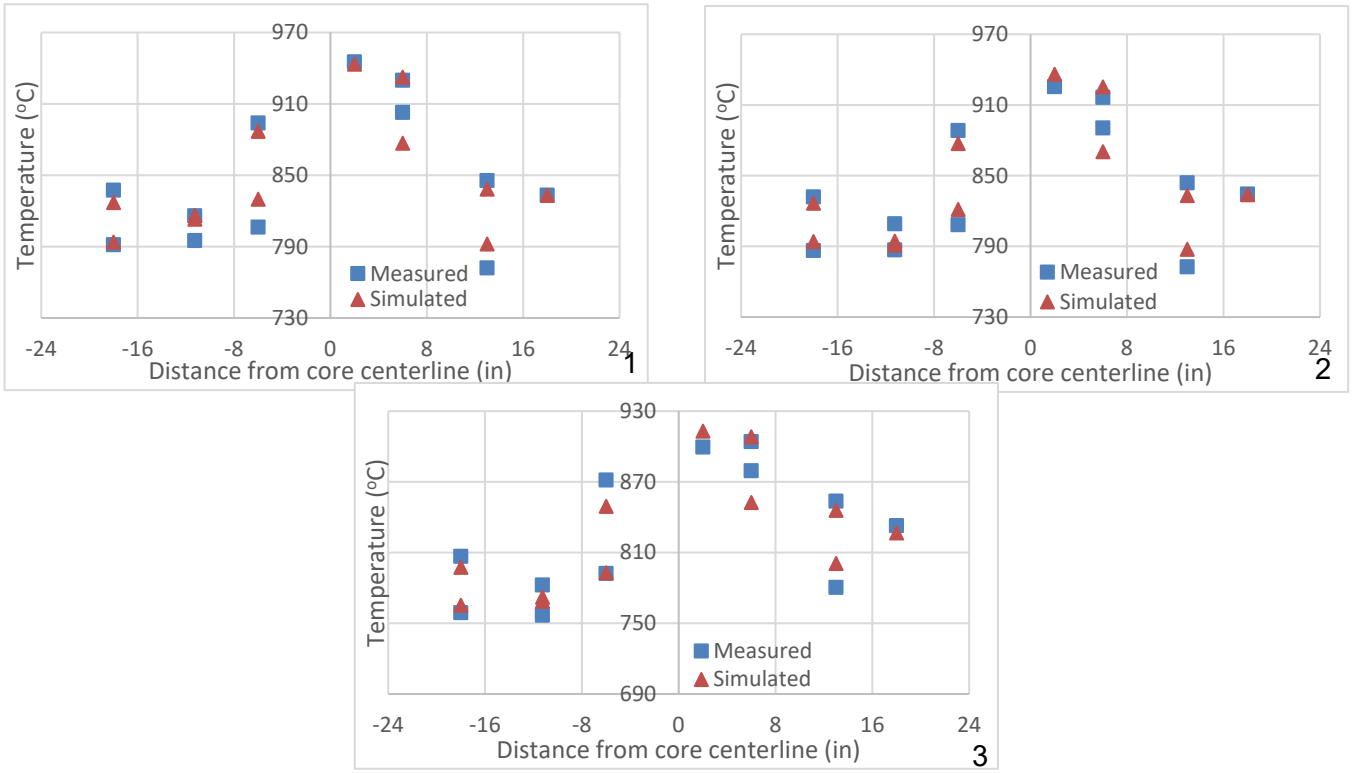

Figure 8. Measured and calculated temperatures of three selected days (1–3) in the 164A irradiation cycle.

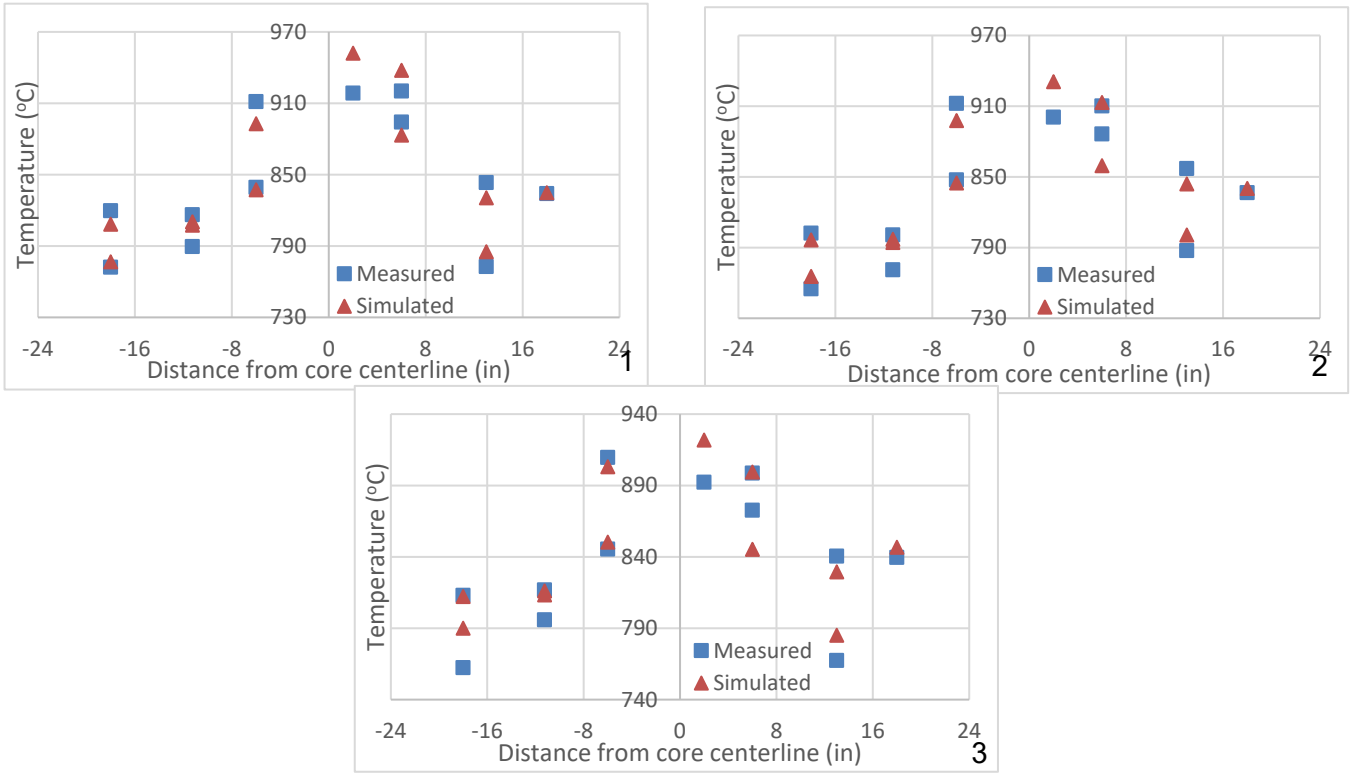

Figure 9. Measured and calculated temperatures of three selected days (1–3) in the 164B irradiation cycle.

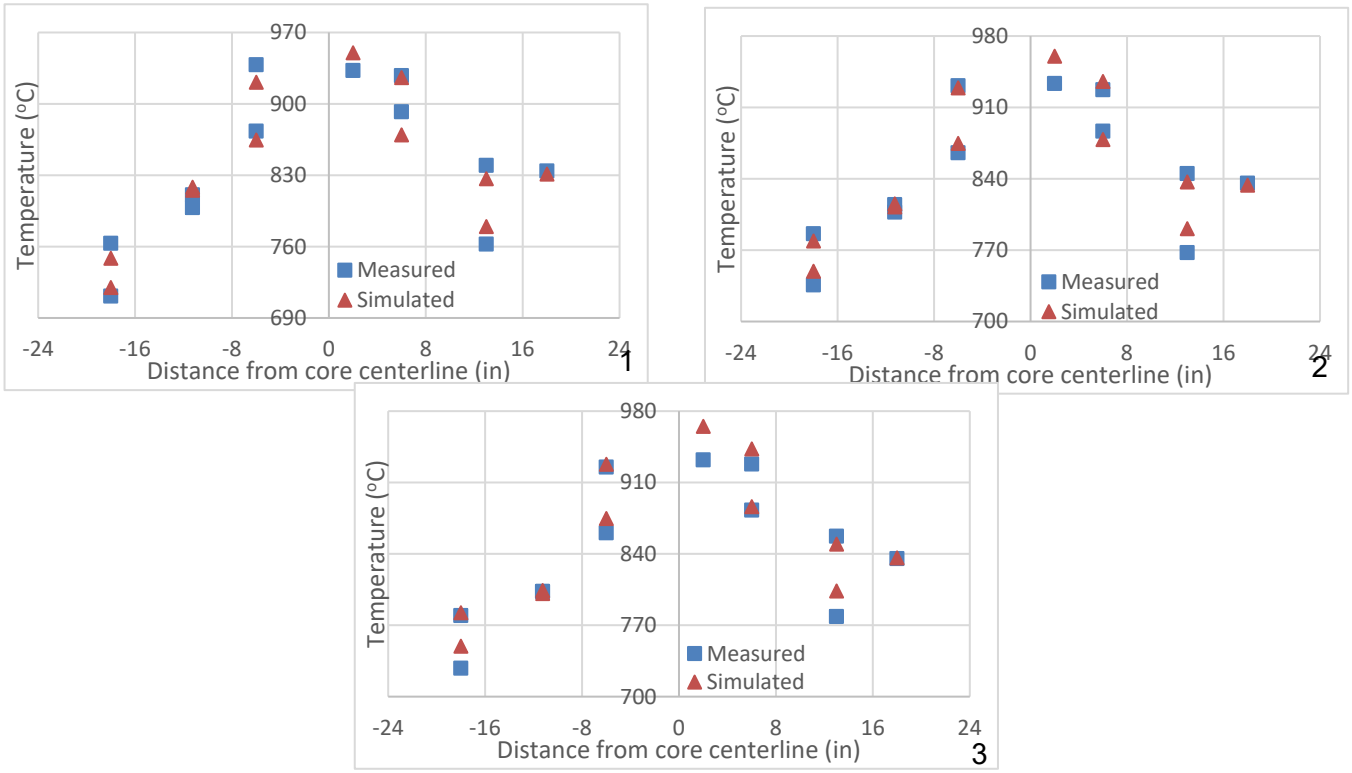

Figure 10. Measured and calculated temperatures of three selected days (1–3) in the 166A irradiation cycle.

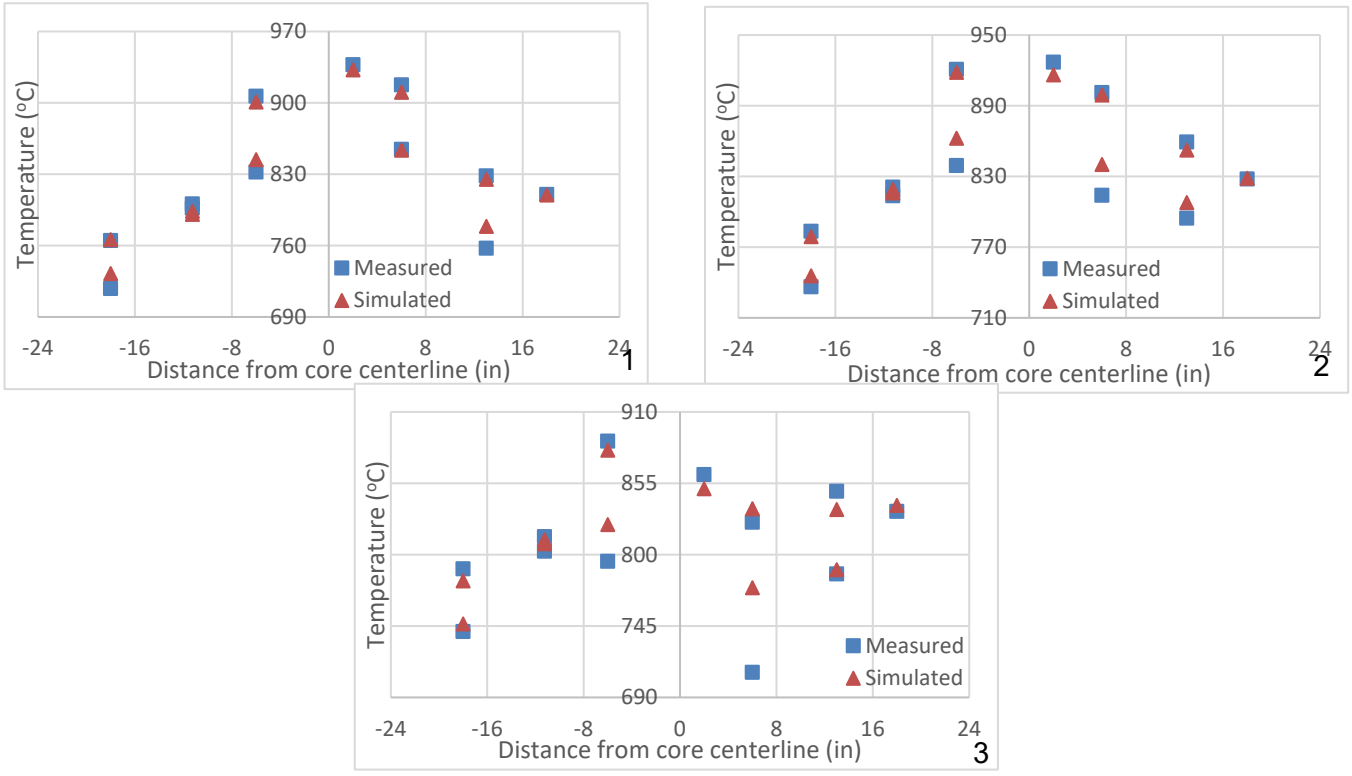

Figure 11. Measured and calculated temperatures of three selected days (1–3) in the 166B irradiation cycle.

Figure 12. Measured and calculated temperatures of TC (1–4) in all the cycles.

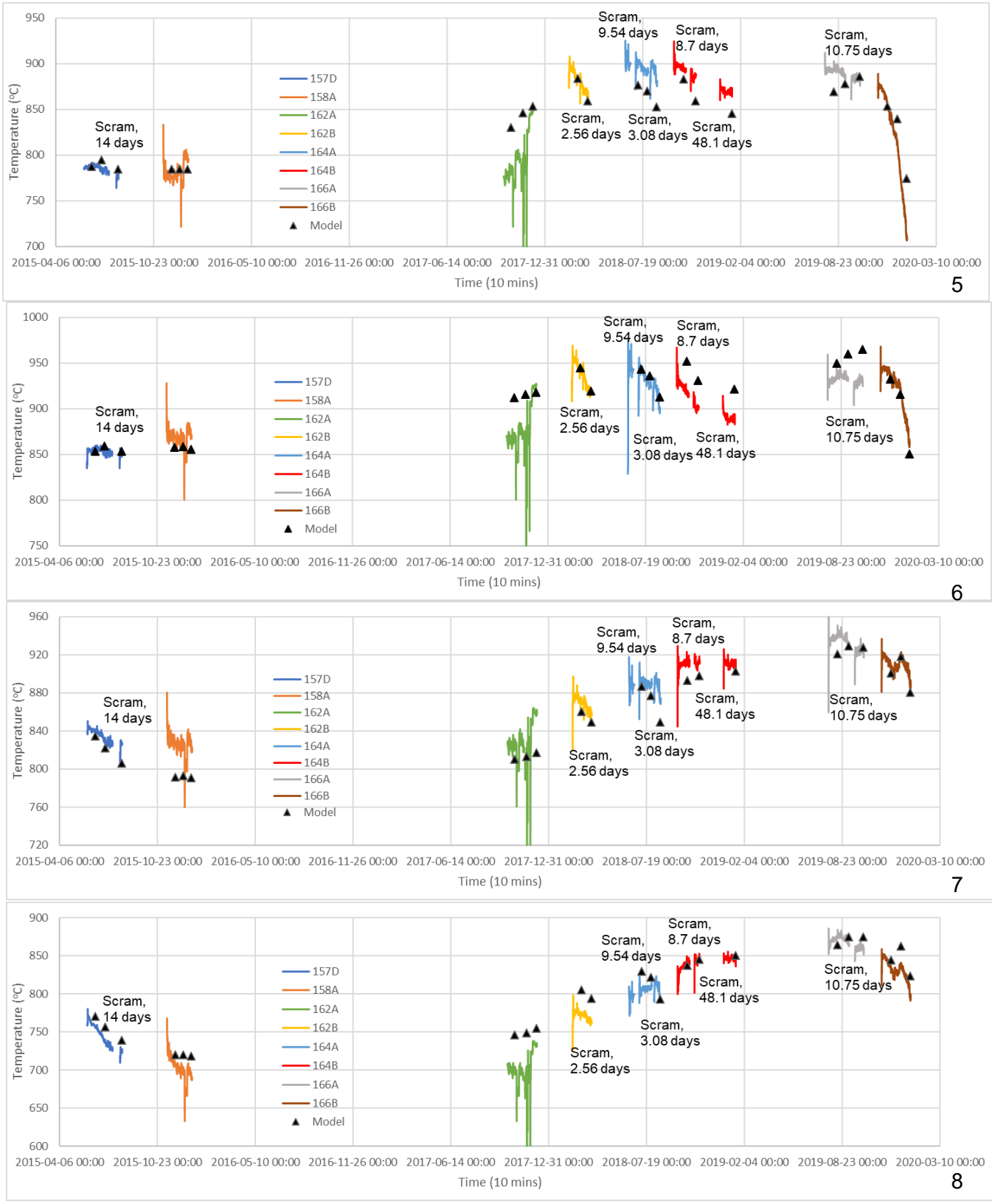

Figure 13. Measured and calculated temperatures of TC (5–8) in all the cycles.

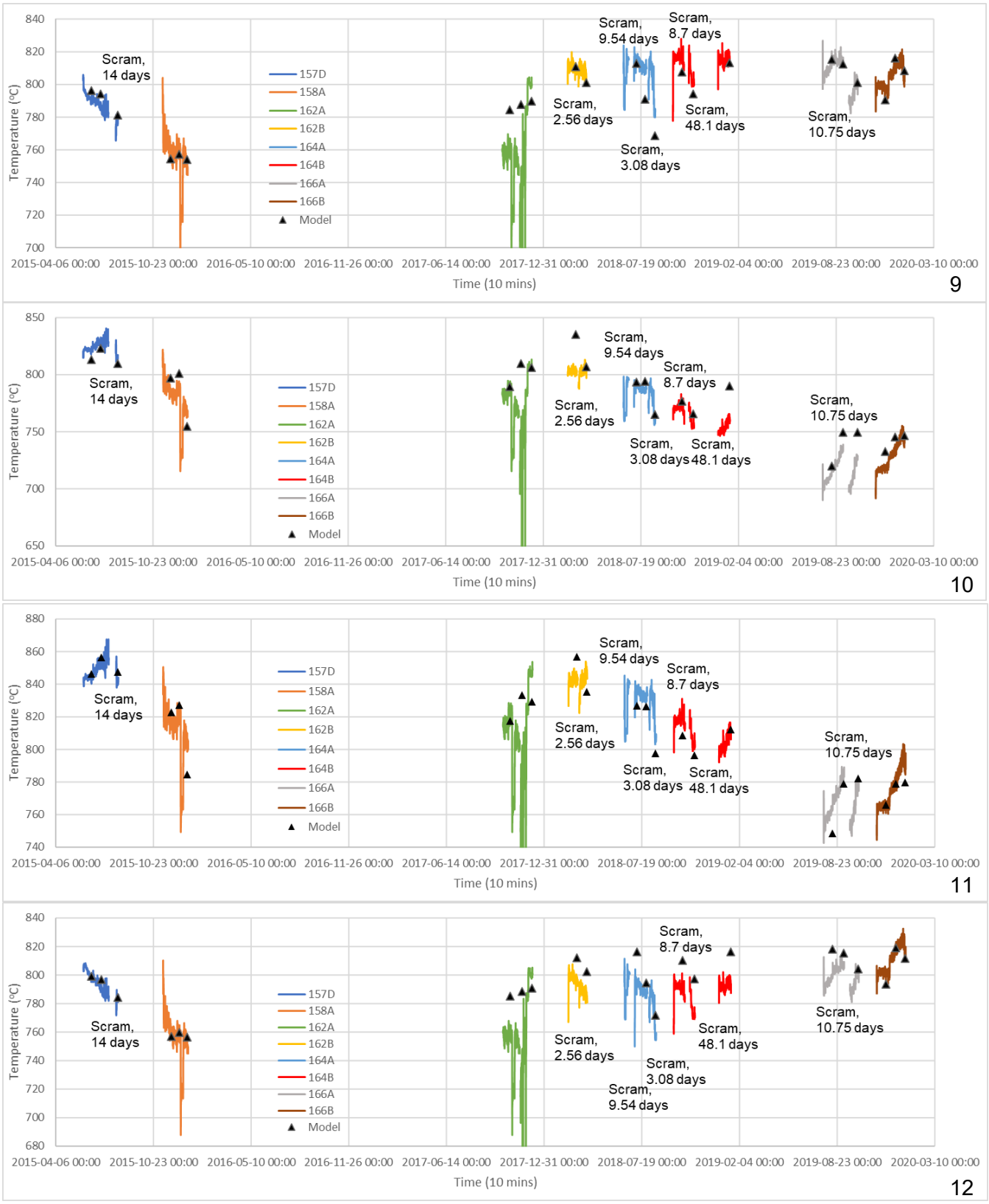

Figure 14. Measured and calculated temperatures of TC (9–12) in all the cycles.

7.4 Specimen stack temperature

With the correlated TC measurement, the axial distribution of the volume-average temperature of each specimen stack, during a selected day in each irradiation cycle, are shown in Figure 15 through Figure 22. Note that the highest temperature occurs in the center specimen stack, which is significantly hotter than the peripheral stacks. Moreover, the specimen temperature varies with elevation. An abrupt change in the temperature gradient occurs at the top of the test train due to the presence of a tungsten heater that produces a localized hot spot at that location. Temperature distribution of the specimen stacks can be viewed with the TC calibration figures. The volume-average temperature of each specimen, during three selected days in each irradiation cycle, are stored in.csv files in the storage.

The experimental requirements on the temperature control are that the volume-average and time-average temperatures of each creep specimen shall be maintained at 900°C ± 50°C (TFR-875, Requirements 1.7, 1.8, and 1.9). However, the results of this analysis show that the temperatures of the specimen stacks are outside the desired range. In general, the specimen average temperatures over the cycles vary from 800 to 900°C. The total specimen mean temperature is 838°C with a ±106°C uncertainty (two standard deviations). Specifically, the lower stack mean temperature is 818°C, upper stack mean temperature is 843°C, and center stack mean temperature is 870°C. The maximum specimen temperature occurs in the center stack, reaching close to 980°C, and the lowest occurs at the ends of the peripherical stacks, dropping to around 670°C.

The tungsten heater on top of the center stack does bring additional heat to the underlying specimen; thus, the end temperature is higher. On the top of the peripherical stacks, the temperature is lower because of no extra heating. On the bottom of the peripherical stacks, tungsten heaters exist. The bottom temperature is higher in Cycle 157D. However, for the rest seven cycles, the bottom has a lower temperature. For all the cycles, the temperature above the core center line is higher than that below the core centerline.

Specimens around the core centerline have a higher temperature than at the two ends of the core. This is especially evident in the last four cycles.

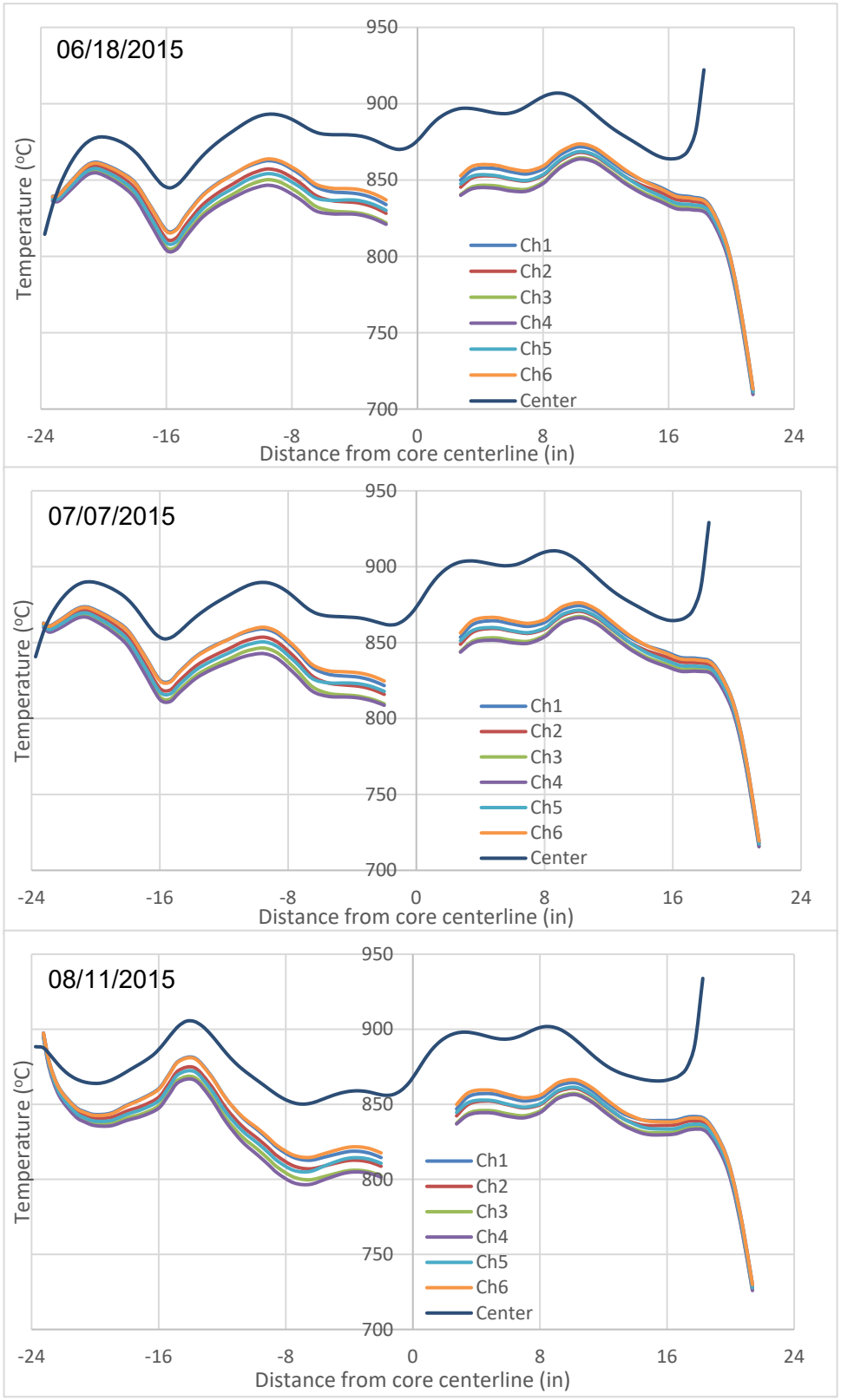

Figure 15. Temperature of specimens in three selected days in Cycle 157D.

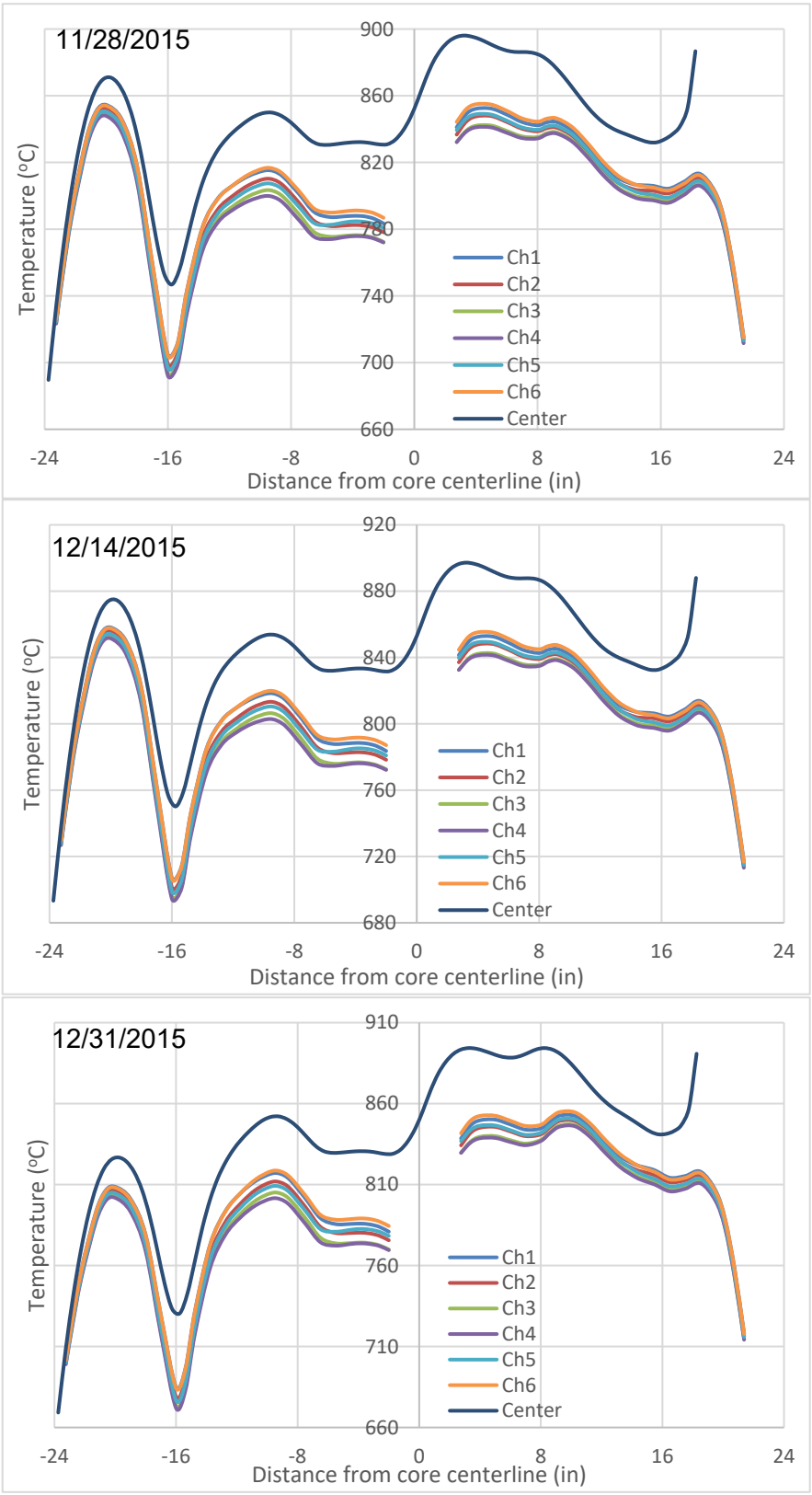

Figure 16. Temperature of specimens in three selected days in Cycle 158A.

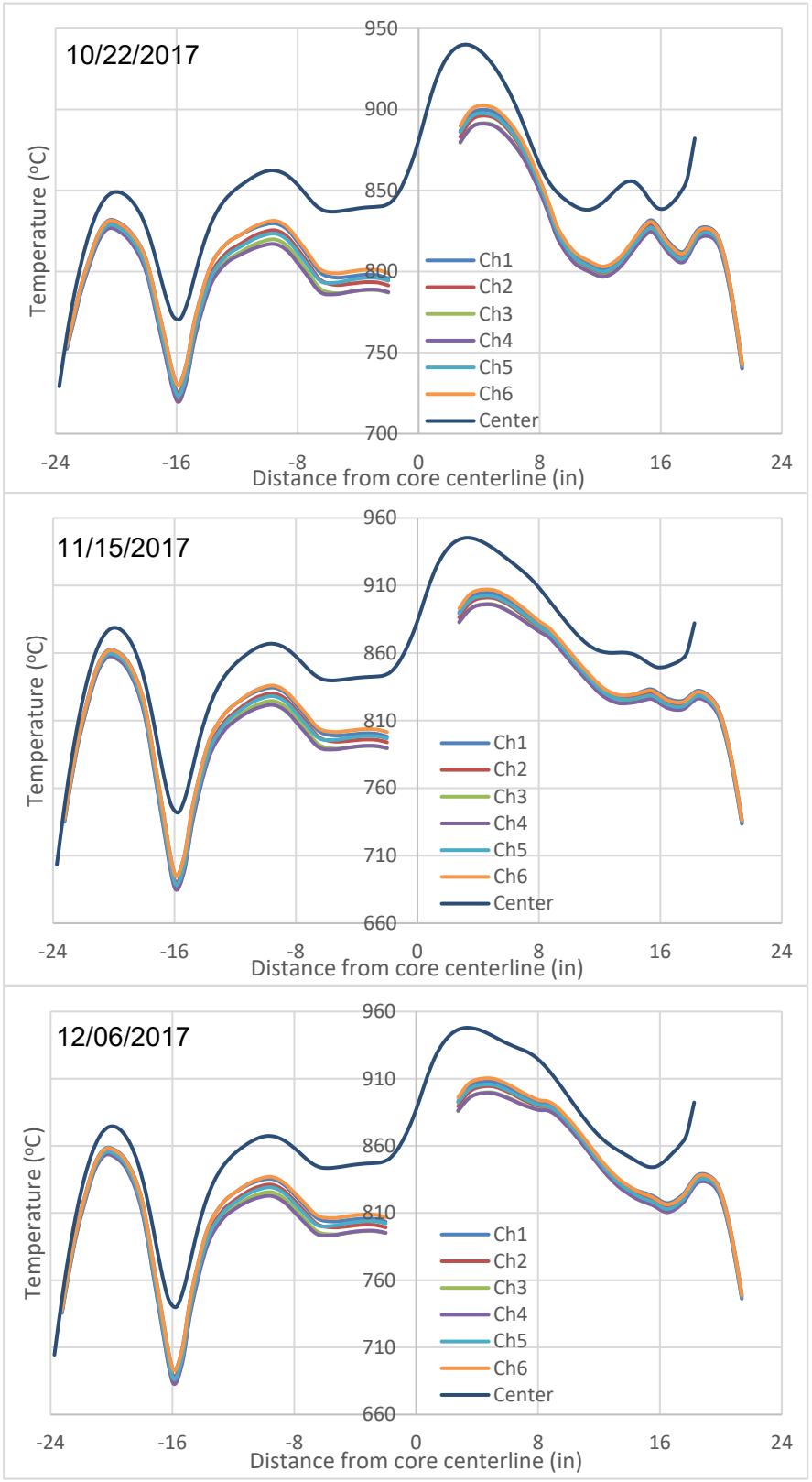

Figure 17. Temperature of specimens in three selected days in Cycle 162A.

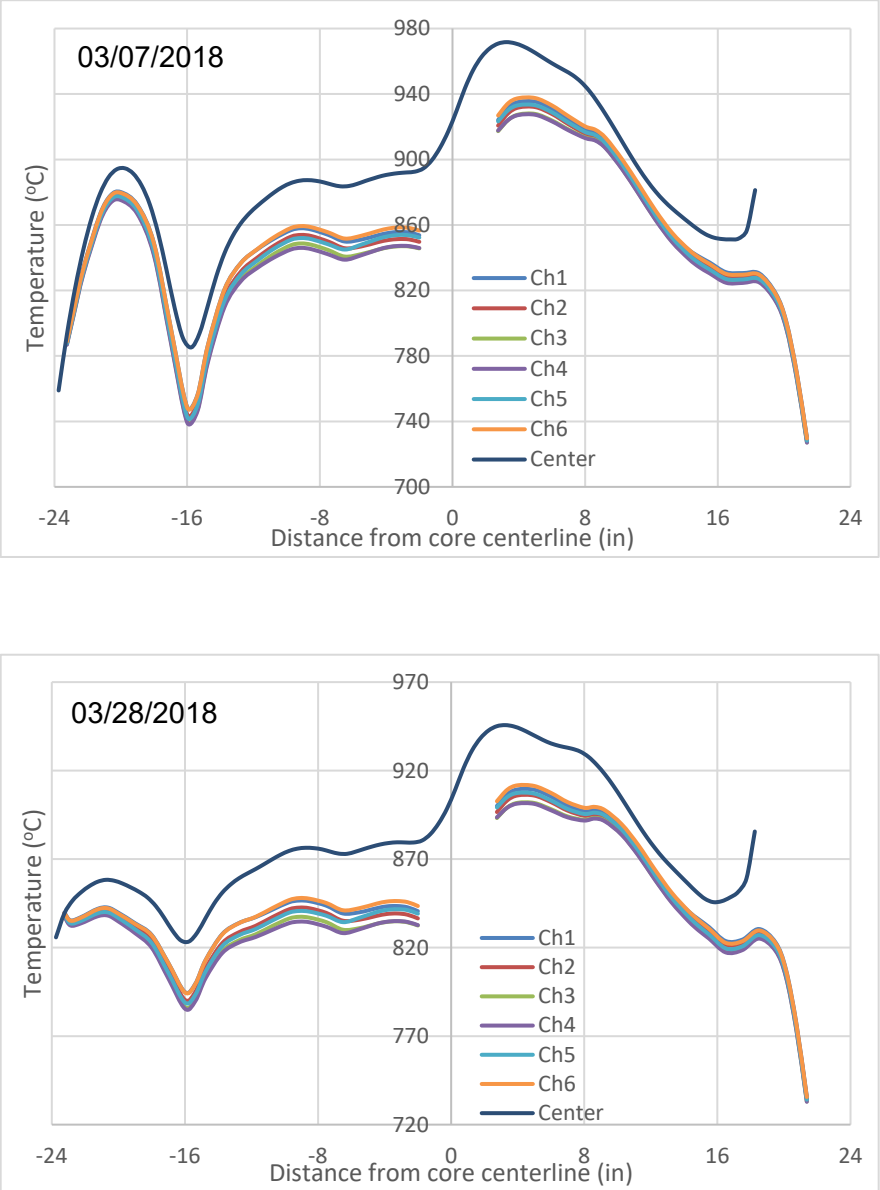

Figure 18. Temperature of specimens in three selected days in Cycle 162B.

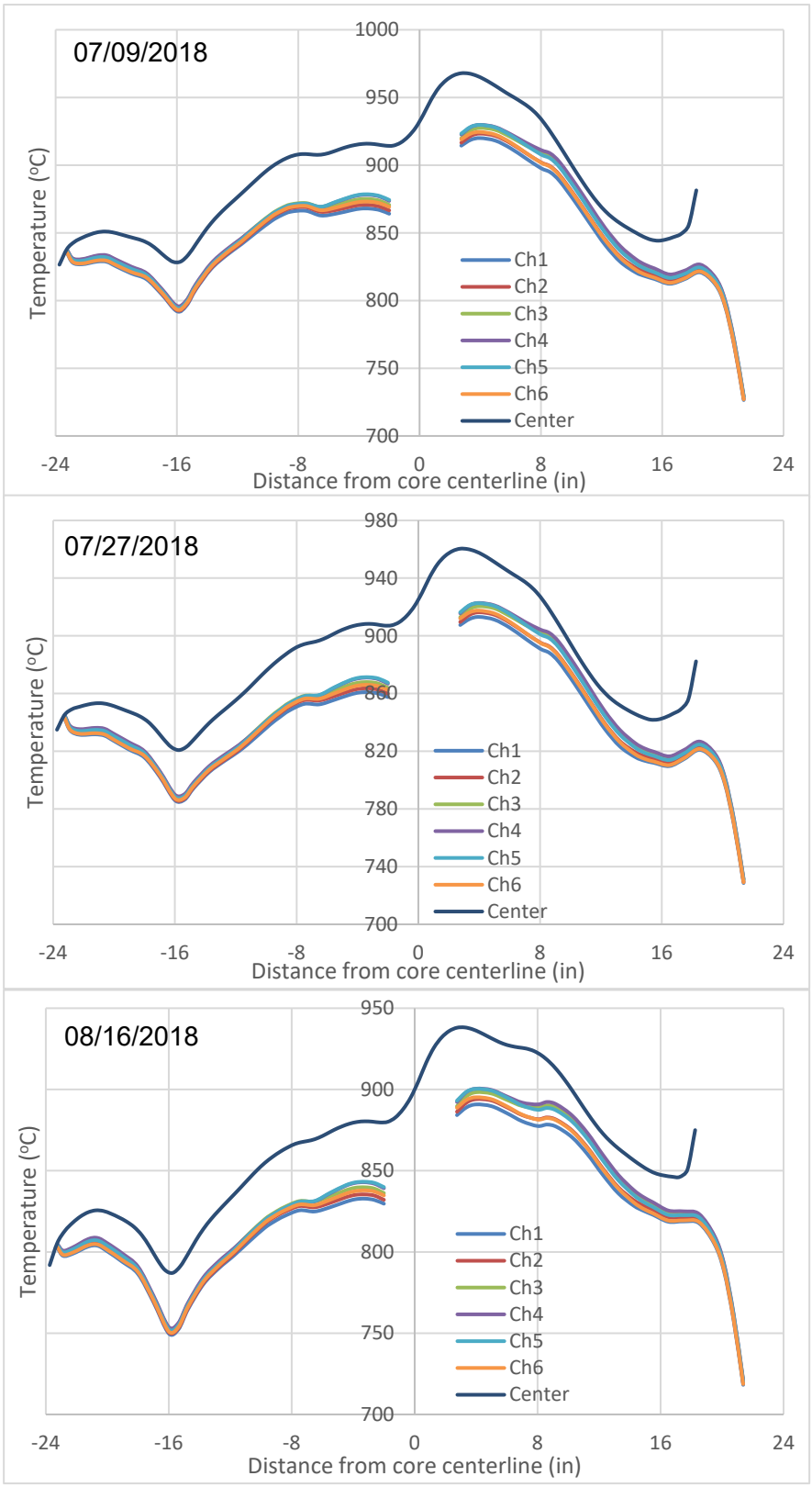

Figure 19. Temperature of specimens in three selected days in Cycle 164A.

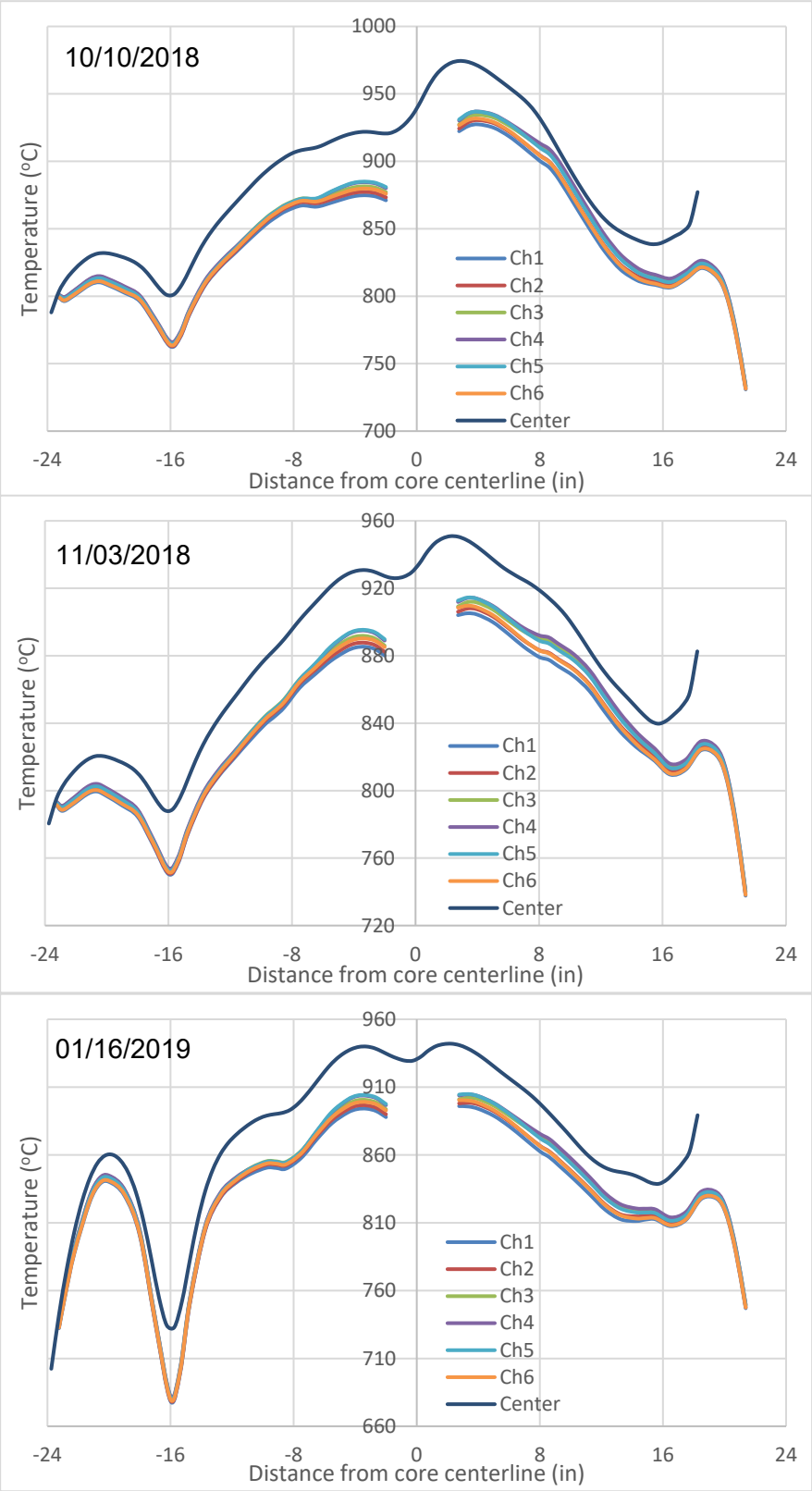

Figure 20. Temperature of specimens in three selected days in Cycle 164B.

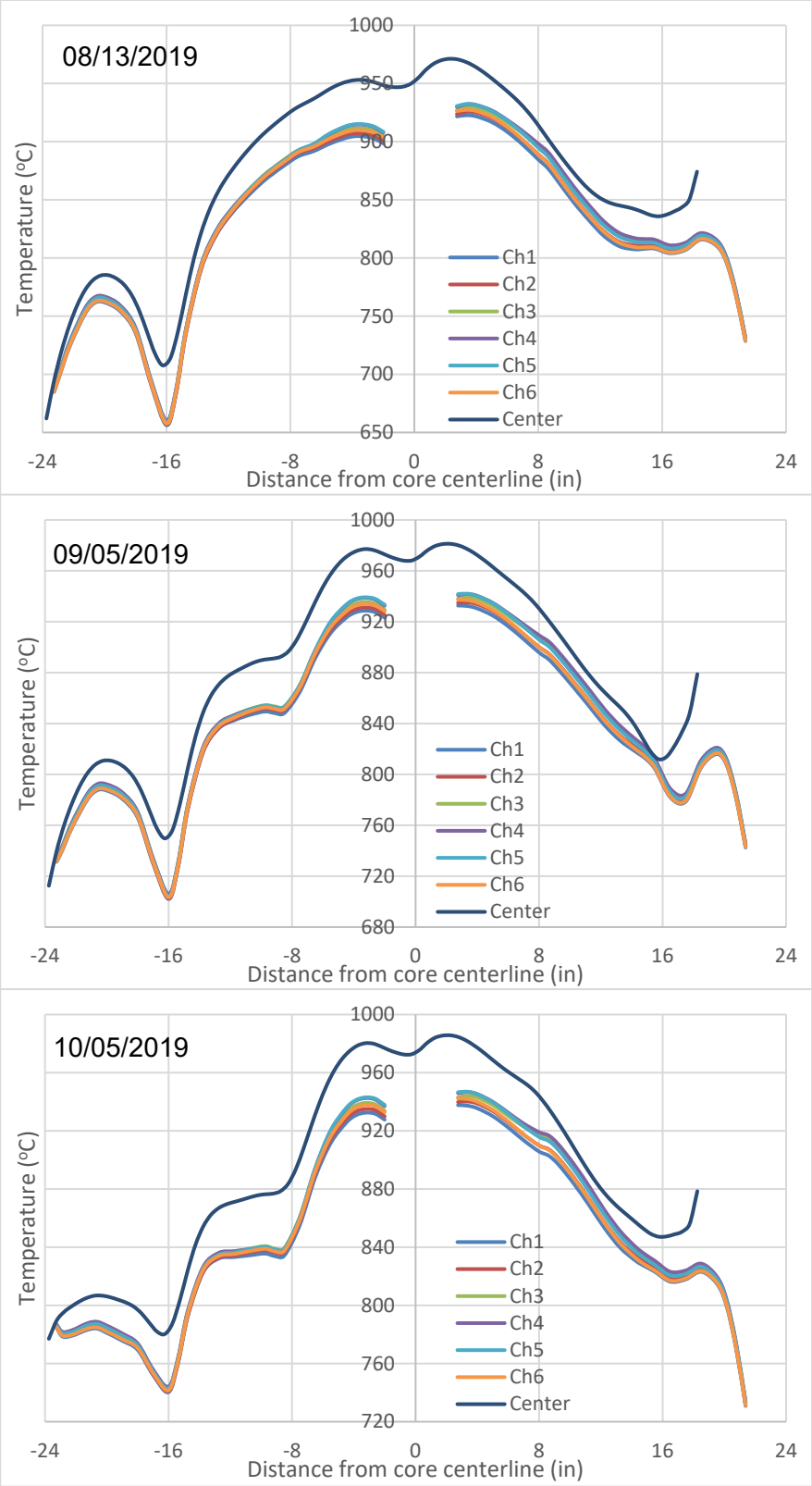

Figure 21. Temperature of specimens in three selected days in Cycle 166A.

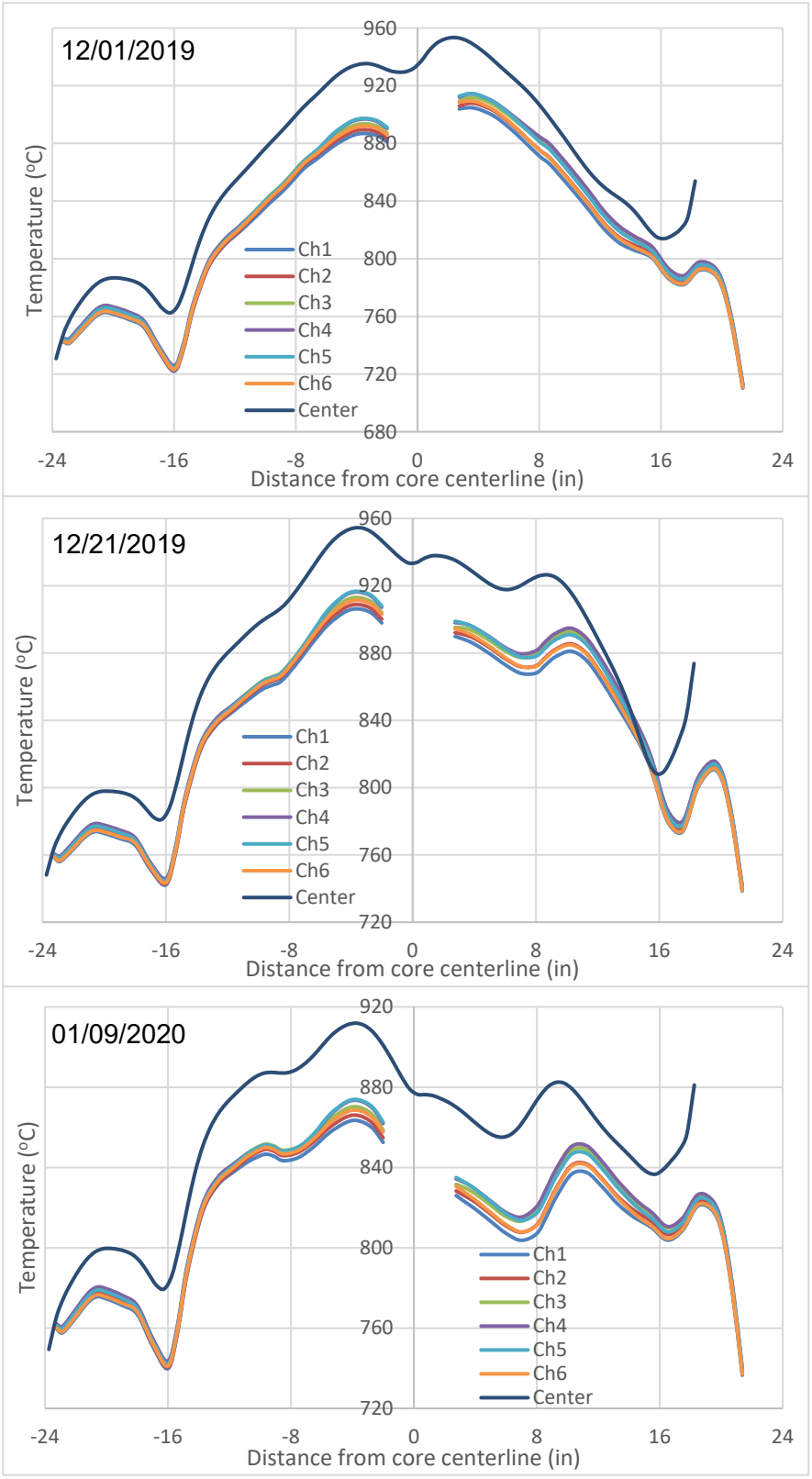

Figure 22. Temperature of specimens in three selected days in Cycle 166B.

8. STORAGE LOCATION

The ECAR, Mathcad, and Abaqus simulation files are stored at the HPC: /projects/atr_exp/AGC-4/as-run/. The files created are listed in Table 2.

Table 2. Documents and Abaqus model for the experiment.

File or Directory Name	Description
ECAR-5414.docx	This document
Under folder /Abaqus	Abaqus files for the analysis
Under folder /Appendix	Mathcad file for material & thermal analysis
Under folder /Drawings	Drawings used in this project
Under folder /Measurement_data	Data from NDMAS and the data processing file
Under folder /References	References used in this ECAR

9. REFERENCES

1. *AGC-4 Test Train for The Very High Temperature Reactor Technical Development Office (VHTR TDO)*, Idaho National Laboratory, 2014, FOR-173, Rev. 2.
2. *AGC-4 Test Train Technical and Functional Requirements*, Idaho National Laboratory, 2014, TFR-875, Rev. 0.
3. Brookman, J.V., *As-Run Physics Analysis for the AGC-4 Experiment Irradiated in the ATR*, Idaho National Laboratory, 2021, ECAR-5345, Rev. 0.
4. Windes, W.E., P.L. Winston, and W.D. Swank, *AGC-2 Disassembly Report*, Idaho National Laboratory, 2014, INL/EXT-14-32060, Rev. 0.
5. Murray, P.E., *Uncertainty Analysis of Temperature in the AGC-1 and AGC-2 Experiments*, Idaho National Laboratory, 2016, ECAR-3017, Rev. 0.
6. Murray, P.E., *Thermal Analysis of The AGC Thermocouple Experiment*, Idaho National Laboratory, 2014, ECAR-2429, Rev. 0.
7. Murray, P.E., *As-Run Thermal Analysis of The AGC-1 Experiment*, Idaho National Laboratory, 2014, ECAR-2562, Rev. 0.
8. Murray, P.E., *As-Run Thermal Analysis of The AGC-2 Experiment*, Idaho National Laboratory, 2014, ECAR-2322, Rev. 0.
9. Murray, P.E., *Validation of ABAQUS Standard 6.7-3 Heat Transfer*, Idaho National Laboratory, 2008, ECAR-131, Rev. 1.
10. Xing, C., *Thermal Analysis of the ATF-1 Experiments for Cycle 164B-1 As-Runs and 166A-1 Projections in the ATR*, Idaho National Laboratory, 2019, ECAR-4673, Rev. 0.
11. *Engineering Calculations and Analysis Report*, Idaho National Laboratory, 2018, LWP-10200, Rev. 11.

APPENDICES

Appendix A: Thermophysical properties, hydrodynamics, heat transer, and heating

A1: Thermophysical properties

Note: the density and heat capacity are not necessary for the steady state computations. The heat capacities in the past AGC models are under "constant volume" but they should be under "constant pressure". This analysis did not change them.
If the significant digits of the values in the model are different, please check this Mathcad file. The legacy model was not changed.
The model has additional materials of Macor and Zirconia that were not used. They were not deleted from the model but the material properties are not summarized here.

Thermophysical properties of 304 and 304L austenitic stainless steel (Perry's Handbook, 7th edition, Table 2-375; Machinery's Handbook, 28th edition, P378)

$$T_{S\_SST} := \begin{pmatrix} 212 \\ 932 \end{pmatrix} °F$$

$$\rho_{SST} := 0.29 \frac{lb}{in^3}$$

$$Cp_{SST} := 0.12 \frac{BTU}{lb \cdot R}$$

$$k_{304\_SST} := \begin{pmatrix} 9.4 \\ 12.4 \end{pmatrix} \frac{BTU}{hr \cdot ft \cdot R} = \begin{pmatrix} 0.78333 \\ 1.03333 \end{pmatrix} \cdot \frac{BTU}{hr \cdot in \cdot R}$$

Thermophysical properties of aluminum 6061 (Machinery's Handbook, P377)

$$\rho_{Al} := 0.098 \frac{lb}{in^3}$$

$$Cp_{Al} := 0.23 \frac{BTU}{lb \cdot R}$$

$$k_{Al} := 104 \frac{BTU}{hr \cdot ft \cdot R} = 8.67 \cdot \frac{BTU}{hr \cdot in \cdot R}$$

Thermophysical properties of tungsten (ASM Metals Handbook, Vol. 2, Properties of Pure Metals - Tungsten, ASTM B777 Class 1)

$$\rho_W := 17 \frac{gm}{cm^3} = 0.61416 \cdot \frac{lb}{in^3}$$

$$Cp_W := 0.131 \frac{J}{gm \cdot K} = 0.03129 \cdot \frac{BTU}{lb \cdot R}$$

$$T_{S\_W} := \begin{pmatrix} 500 \\ 1000 \\ 1500 \end{pmatrix} \cdot K = \begin{pmatrix} 440 \\ 1340 \\ 2240 \end{pmatrix} \cdot °F$$

$$k_W := \begin{pmatrix} 150 \\ 125 \\ 110 \end{pmatrix} \frac{W}{m \cdot K} = \begin{pmatrix} 7.22 \\ 6.02 \\ 5.3 \end{pmatrix} \cdot \frac{BTU}{hr \cdot in \cdot R}$$

Thermophysical properties of Haynes 230 nickel alloy (ASM Metals Handbook, Vol. 1, Wrought Nickel Alloys)

$$\rho_H := 8.8 \frac{gm}{cm^3} = 0.31792 \cdot \frac{lb}{in^3}$$

$$Cp_H := 0.473 \frac{J}{gm \cdot K} = 0.11297 \cdot \frac{BTU}{lb \cdot R}$$

$$T_{S\_H} := \begin{pmatrix} 21 \\ 538 \\ 871 \end{pmatrix} °C = \begin{pmatrix} 70 \\ 1000 \\ 1600 \end{pmatrix} \cdot °F$$

$$k_H := \begin{pmatrix} 8.9 \\ 18.4 \\ 24.4 \end{pmatrix} \frac{W}{m \cdot K} = \begin{pmatrix} 0.43 \\ 0.89 \\ 1.17 \end{pmatrix} \cdot \frac{BTU}{hr \cdot in \cdot R}$$

Thermophysical properties of nuclear-grade graphite

$\rho_g := 1.822 \frac{gm}{cm^3} = 0.06582 \cdot \frac{lb}{in^3}$ Density (Product Certification NBG-25 graphite, SGL Group)

$Cp_g := 5.66 \frac{cal}{mole \cdot K}$ Specific heat at 900 ºC (Perry's Handbook, 7th edition, Table 2-194)

$$\frac{Cp_g}{12 \frac{gm}{mole}} = 0.47167 \cdot \frac{BTU}{lb \cdot R}$$

Thermal conductivity of unirradiated fine-grained isotropic graphite (J.A. Vreeling, O. Wouters, J.G. van der Laan, Graphite irradiation testing for HTR technology at the High Flux Reactor in Petten, J. Nuclear Materials, 2008, 381: 68-75)

$$T_g := \begin{pmatrix} 300 \\ 400 \\ 600 \\ 800 \\ 1000 \end{pmatrix} °C = \begin{pmatrix} 572 \\ 752 \\ 1112 \\ 1472 \\ 1832 \end{pmatrix} \cdot °F$$

$$k_g := \begin{pmatrix} 95 \\ 85 \\ 72 \\ 65 \\ 60 \end{pmatrix} \frac{W}{m \cdot K} = \begin{pmatrix} 4.574 \\ 4.093 \\ 3.467 \\ 3.13 \\ 2.889 \end{pmatrix} \cdot \frac{BTU}{hr \cdot in \cdot R}$$

Experimental data on effect of neutron fluence on thermal conductivity of fine-grained isotropic graphite (J. Nuclear Materials, 2008, 381: 68-75; Tadashi Maruyama, Masaaki Harayama, Neutron irradiation effect on the thermal conductivity and dimensional change of graphite materials, J. Nuclear Materials, 1992, 195: 44-50; R.J. Price, Thermal conductivity of neutron-irradiated reactor graphites, Carbon, 1975, 13(3): 201-204). Data is given at various values of temperature and dpa (displacements per atom computed as a function of fast neutron fluence with energy >0.1 MeV)

$dpa1 := 0.13$ $T_{irr1} := 300\,°C$ $k_{g\_irr1} := 27.2 \frac{W}{m \cdot K}$

$dpa2 := 0.82$ $T_{irr2} := 400\,°C$ $k_{g\_irr2} := 26.9 \frac{W}{m \cdot K}$

$dpa3 := 1.6$ $T_{irr3} := 600\,°C$ $k_{g\_irr3} := 33 \frac{W}{m \cdot K}$

$dpa4 := 2.2$ $T_{irr4} := 1000\,°C$ $k_{g\_irr4} := 39 \frac{W}{m \cdot K}$

$dpa5 := 9$ $T_{irr5} := 800\,°C$ $k_{g\_irr5} := 37 \frac{W}{m \cdot K}$

$$dpa := \begin{pmatrix} 0.1 \\ 1 \\ 10 \end{pmatrix}$$

Displacement per atom

$$\varphi := \begin{pmatrix} 0.3 & 0.2 & 0.1 \\ 0.41 & 0.3 & 0.2 \\ 0.61 & 0.5 & 0.4 \\ 0.73 & 0.64 & 0.55 \\ 0.8 & 0.7 & 0.6 \end{pmatrix}$$

Ratio of irradiated to unirradiated thermal condutivity as a function of temperatue (rows) and dpa (columns), evaluated using the experimental data given above.

Thermal conductivity of irradiated graphite at various values of temperature and dpa

$i := 0..4$ $j := 0..2$

$$\lambda_{i,j} := \varphi_{i,j} \cdot k_{g_i}$$

$$\lambda = \begin{pmatrix} 1.37225 & 0.91483 & 0.45742 \\ 1.678 & 1.2278 & 0.81853 \\ 2.11471 & 1.73337 & 1.38669 \\ 2.28468 & 2.003 & 1.72133 \\ 2.31116 & 2.02226 & 1.73337 \end{pmatrix} \cdot \frac{BTU}{in \cdot hr \cdot R}$$

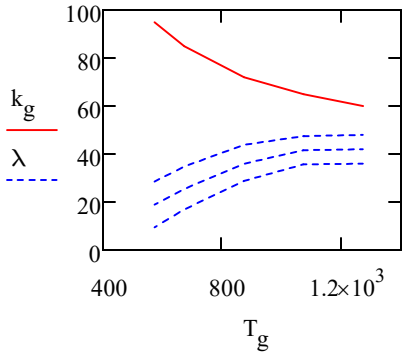

Thermophysical properties of compressed water (Perry's Handbook, Tables 2-355 and 2-356)

$P_L := 20bar = 290 \cdot psi$

$$T_{H2O} := \begin{pmatrix} 300 \\ 350 \\ 400 \end{pmatrix} K = \begin{pmatrix} 80 \\ 170 \\ 260 \end{pmatrix} \cdot °F$$

$$\rho_{H2O} := \begin{pmatrix} 994.1 \\ 968.2 \\ 929.7 \end{pmatrix} \frac{kg}{m^3} = \begin{pmatrix} 0.0359 \\ 0.035 \\ 0.0336 \end{pmatrix} \cdot \frac{lb}{in^3}$$

$$Cp_{H2O} := \begin{pmatrix} 4.17 \\ 4.19 \\ 4.25 \end{pmatrix} \frac{J}{gm \cdot K} = \begin{pmatrix} 0.996 \\ 1.001 \\ 1.015 \end{pmatrix} \cdot \frac{BTU}{lb \cdot R}$$

$$k_{H2O} := \begin{pmatrix} 0.616 \\ 0.669 \\ 0.689 \end{pmatrix} \frac{W}{m \cdot K} = \begin{pmatrix} 0.03 \\ 0.032 \\ 0.033 \end{pmatrix} \cdot \frac{BTU}{hr \cdot in \cdot R}$$

$$\mu_{H2O} := \begin{pmatrix} 0.000856 \\ 0.000371 \\ 0.000218 \end{pmatrix} \frac{N \cdot s}{m^2} = \begin{pmatrix} 0.173 \\ 0.075 \\ 0.044 \end{pmatrix} \cdot \frac{lb}{hr \cdot in}$$

$$Pr_{H2O} := \begin{pmatrix} 5.8 \\ 2.32 \\ 1.34 \end{pmatrix}$$

$$\rho_w := 0.5 \cdot \left(\rho_{H2O_0} + \rho_{H2O_1} \right) = 0.0354 \cdot \frac{lb}{in^3}$$

Thermal conductivity of helium-argon gas mixtures (Edward A. Mason, Thermal Conductivities of Rare Gas Mixtures, Physics of Fluids, 1960, 3(3):355-361; E. I. Marchenkov & A. G. Shashkov, Study of thermal conductivity of an He-Ar mixture in the temperature range of 400–1500 °K on an installation with a molybdenum measuring cell, Journal of Engineering Physics and Thermophysics, 1975, 28(6):725-731)

$$T_{gas} := \begin{pmatrix} 302 \\ 793 \\ 1173 \end{pmatrix} K = \begin{pmatrix} 84 \\ 968 \\ 1652 \end{pmatrix} \cdot °F$$

$$k_{0He100Ar} := \begin{pmatrix} 0.0182 \\ 0.0383 \\ 0.048 \end{pmatrix} \frac{W}{m \cdot K} = \begin{pmatrix} 0.00088 \\ 0.00184 \\ 0.00231 \end{pmatrix} \cdot \frac{BTU}{hr \cdot in \cdot R}$$

$$k_{10He90Ar} := \begin{pmatrix} 0.0234 \\ 0.0494 \\ 0.059 \end{pmatrix} \frac{W}{m \cdot K} = \begin{pmatrix} 0.00113 \\ 0.00238 \\ 0.00284 \end{pmatrix} \cdot \frac{BTU}{hr \cdot in \cdot R}$$

$$k_{20He80Ar} := \begin{pmatrix} 0.0294 \\ 0.0622 \\ 0.07 \end{pmatrix} \frac{W}{m \cdot K} = \begin{pmatrix} 0.00142 \\ 0.00299 \\ 0.00337 \end{pmatrix} \cdot \frac{BTU}{hr \cdot in \cdot R}$$

$$k_{30He70Ar} := \begin{pmatrix} 0.0364 \\ 0.0772 \\ 0.088 \end{pmatrix} \frac{W}{m \cdot K} = \begin{pmatrix} 0.00175 \\ 0.00372 \\ 0.00424 \end{pmatrix} \cdot \frac{BTU}{hr \cdot in \cdot R}$$

$$k_{40He60Ar} := \begin{pmatrix} 0.0451 \\ 0.0957 \\ 0.106 \end{pmatrix} \frac{W}{m \cdot K} = \begin{pmatrix} 0.00217 \\ 0.00461 \\ 0.0051 \end{pmatrix} \cdot \frac{BTU}{hr \cdot in \cdot R}$$

$$k_{50He50Ar} := \begin{pmatrix} 0.0551 \\ 0.116 \\ 0.137 \end{pmatrix} \frac{W}{m \cdot K} = \begin{pmatrix} 0.00265 \\ 0.00559 \\ 0.0066 \end{pmatrix} \cdot \frac{BTU}{hr \cdot in \cdot R}$$

$$k_{60He40Ar} := \begin{pmatrix} 0.0667 \\ 0.14 \\ 0.167 \end{pmatrix} \frac{W}{m \cdot K} = \begin{pmatrix} 0.00321 \\ 0.00674 \\ 0.00804 \end{pmatrix} \cdot \frac{BTU}{hr \cdot in \cdot R}$$

$$k_{70He30Ar} := \begin{pmatrix} 0.0809 \\ 0.169 \\ 0.223 \end{pmatrix} \frac{W}{m \cdot K} = \begin{pmatrix} 0.0039 \\ 0.00814 \\ 0.01074 \end{pmatrix} \cdot \frac{BTU}{hr \cdot in \cdot R}$$

$$k_{80He20Ar} := \begin{pmatrix} 0.0993 \\ 0.195 \\ 0.279 \end{pmatrix} \frac{W}{m \cdot K} = \begin{pmatrix} 0.00478 \\ 0.00939 \\ 0.01343 \end{pmatrix} \cdot \frac{BTU}{hr \cdot in \cdot R}$$

$$k_{90He10Ar} := \begin{pmatrix} 0.124 \\ 0.25 \\ 0.338 \end{pmatrix} \frac{W}{m \cdot K} = \begin{pmatrix} 0.00597 \\ 0.01204 \\ 0.01627 \end{pmatrix} \cdot \frac{BTU}{hr \cdot in \cdot R}$$

$$k_{100He0Ar} := \begin{pmatrix} 0.154 \\ 0.308 \\ 0.397 \end{pmatrix} \frac{W}{m \cdot K} = \begin{pmatrix} 0.00741 \\ 0.01483 \\ 0.01912 \end{pmatrix} \cdot \frac{BTU}{hr \cdot in \cdot R}$$

Thermal radiation properties of materials (for stainless steel and tungsten, Table A.11, "Fundamentals of Heat and Mass Transfer", 5th ed., F. Incropera and D. DeWitt, 2002; for graphite, European Physical J. A, 2008, 38: 167-171; for Inconel 600 (TC sheath) and Hanes 230 (heat shield), CINDAS Thermophysical Properties of Matter Database; for stainless steel coated with graphite powder, Maynard, Raymond K., "Total Hemispherical Emissivity of VHTR Candidate Materials", University of Missouri, PhD Dissertation, 2011

$\varepsilon_{SST\_lo} := 0.2$ Emissivity of clean stainless steel (304, Inconel 600, and Haynes 230)

$\varepsilon_{SST\_hi} := 0.4$ Emissivity of stainless steel coated with graphite powder

$\varepsilon_{W} := 0.1$ Emissivity of tungsten

$\varepsilon_{C} := 0.9$ Emissivity of graphite

$$\sigma := 5.67 \cdot 10^{-8} \frac{W}{m^2 \cdot K^4} = 1.18902 \times 10^{-11} \cdot \frac{BTU}{hr \cdot in^2 \cdot R^4}$$

A2 Gas gaps between capsule components

Calculate thermal expansion of capsule components

$\alpha_{graphite} := 4.5 \cdot 10^{-6} \frac{1}{K}$ Coefficient of thermal expansion of graphite (Perry's Handbook, Table 28-29)

$T_{holder} := 800\,°C$ Approximate irradiation temperature of graphite holder

$T_0 := 25\,°C$ Reference temperature

$\Delta T_{holder} := T_{holder} - T_0 = 775 \cdot \Delta°C$

$r_{o\_holder} := \frac{1}{2} \cdot 2.087in$ Maximum nominal outside radius of the holder (DWG-604551, sheets 2 and 4)

$u_{o\_holder} := \alpha_{graphite} \cdot \Delta T_{holder} \cdot r_{o\_holder} = 0.0036 \cdot in$ Radial thermal expansion at outside surface of holder

$r_{i\_holder} := 0.5 \cdot 0.51in$ Inside radius of channels in holder (DWG-604552, sheet 1 and 2)

$u_{i\_holder} := \alpha_{graphite} \cdot \Delta T_{holder} \cdot r_{i\_holder} = 0.0009 \cdot in$ Radial thermal expansion at inside surface of channels in holder

$T_{specimen} := 900\,°C$ Irradiation temperature of specimens

$\Delta T_{specimen} := T_{specimen} - T_0 = 875 \cdot \Delta°C$

$r_{o\_specimen} := 0.5 \cdot 0.49in$ Outside radius of specimens (DWG-778033 sheet 6)

$u_{o\_specimen} := \alpha_{graphite} \cdot \Delta T_{specimen} \cdot r_{o\_specimen} = 0.001 \cdot in$ Radial thermal expansion at outside surface of specimens

$u_{i\_holder} - u_{o\_specimen} = -0.00008 \cdot in$ Differential expansion between holder and specimens is negligible

$\alpha_{SST} := 17.3 \cdot 10^{-6} \frac{1}{K}$ Coefficient of thermal expansion of stainless steel (Perry's Handbook, Table 28-4)

$T_{capsule} := 160\,°C$ Irradiation temperature o capsule

$\Delta T_{capsule} := T_{capsule} - T_0 = 135 \cdot \Delta°C$ Temperature change of capsule

$r_{i\_capsule} := \frac{2.13in}{2}$ Inside radius of capsule (DWG-630434, sheet 1)

$u_{i\_capsule} := \alpha_{SST} \cdot \Delta T_{capsule} \cdot r_{i\_capsule} = 0.00249 \cdot in$ Radial thermal expansion at inside surface of capsule

Calculate location of heat shield assuming dimples on heat shield contact the inside surface of capsule
Note: Dimensions are changed on Rev. 1 from Rev. 0

$h_{dimple} := \left(\frac{2.131 + 2.127}{2} - \frac{2.108 + 2.104}{2}\right)\cdot in\cdot 0.5 = 0.0115\cdot in$ Height of dimple on heat shield (DWG-604534)

$r_{o\_hs} := r_{i\_capsule} + u_{i\_capsule} - h_{dimple} = 1.056\cdot in$ Outside radius of heat shield after contact with the inside surface of capsule

$t_{hs} := \left(\frac{2.108 + 2.104}{2} - \frac{2.1 + 2.096}{2}\right)\cdot in\cdot 0.5 = 0.004\cdot in$ Thickess of heat shield

$r_{i\_hs} := r_{o\_hs} - t_{hs} = 1.052\cdot in$ Inside radius of heat shield (this is the radius after expansion)

Calculate gas gaps between capsule and heat shield and between capsule and nubs on holder

$d_{cap\_hs} := r_{i\_capsule} + u_{i\_capsule} - r_{o\_hs} = 0.0115\cdot in$ Gas gap between capsule and heat shield. This gap is not directly use in Abaqus but appropriate gaps are used in each cycle to correlate the modeling and measurement. See conductance section below.

$r_{o\_nub} := 0.5\cdot 2.121in$ Outside radius of nubs at bottom of lower holder (DWG-604551, wheet 5, view T-T). Heat shield sits on top of the nubs

$d_{cap\_nub} := r_{i\_capsule} + u_{i\_capsule} - r_{o\_nub} - u_{o\_holder} = 0.0033\cdot in$ Gas gap between capsule and nubs

Rings on holder separate gas zones. Contact between heat shield and rings is assumed.

Calculate gas gaps between capsule and graphite insulator at top of holder, and between heat shield and graphite insulator at top of holder

$r_{o\_insulator} := 0.5\cdot 2.09in$ Ouside radius of graphite insulator at top of holder (DWG-604551, sheet 7)

$d_{cap\_insulator} := r_{i\_capsule} + u_{i\_capsule} - r_{o\_insulator} - u_{o\_holder} = 0.01885\cdot in$

Gas gap between capsule and graphite insulator at top of holder

$d_{hs\_insulator} := r_{i\_hs} - r_{o\_insulator} - u_{o\_holder} = 0.0033\cdot in$ Gas gap between heat shield and graphite insulator at top of holder

Calculate gas gaps between capsule and bottom end of holder, and between heat shield and bottom end of holder. The holder OD is no-uniform. The gaps of each step are different.

$r_{o\_bottom\_holder} := 0.5 \cdot 2.023in$ Outside radius of bottom end of lower holder (DWG-604551, sheet 4)

$d_{cap\_bottom\_holder} := r_{i\_capsule} + u_{i\_capsule} - r_{o\_bottom\_holder} - u_{o\_holder} = 0.05235 \cdot in$

Gas gap between capsule and bottom end of holder

$d_{hs\_bottom\_holder} := r_{i\_hs} - r_{o\_bottom\_holder} - u_{o\_holder} = 0.0368 \cdot in$

Gas gap between heat shield and bottom of the holder

Calculate gas gaps between holder and speciemens, holder and push rods, and holder and spacers

$r_{i\_channel} := r_{i\_holder} = 0.255 \cdot in$ Inside radius of specimen channels in holder (DWG-604552, sheets 1 and 2)

$r_{i\_TC} := \frac{(0.129 + 0.126)in}{4} = 0.0638 \cdot in$ Inside radius of TC channels in holder (DWG-604552, sheets 1, 2). Because temperature is obtained from the TC junction bead, use the radius of the beads.

$r_{o\_rod} := 0.5 \cdot 0.482in$ Outside radius of upper push rods and spacers (DWG-603523, sheet 2, -10, and -12)

$r_{o\_tc} := 0.5 \cdot 0.125in$ Outside radius of thermocouples (DWG-604554, item 64)

$d_{channel\_specimen} := r_{i\_channel} - r_{o\_specimen} = 0.01 \cdot in$ Gas gap between specimens and holder channels

$d_{channel\_rod} := r_{i\_channel} - r_{o\_rod} = 0.014 \cdot in$ Gas gap beteen spacer/push rod and the holder channel

$r_{heater} := 0.5 \cdot 0.491in$ radius of the heater, DWG-603539

$d_{channel\_heater} := r_{i\_channel} - r_{heater} = 0.0095 \cdot in$ Gap between heater and holder channel

Gas gap between thermocouple and holder may vary since the thermocouple is unlikely to be centered in the

hole. The minimum gap is assumed to be equal to 0.0005" (ECAR-2494)

$d_{TC\_hole} := 0.5\cdot(0.126 + 0.129)\cdot in = 0.1275\cdot in$ Mean diameter of TC hole in holder (DWG-604552)

$d_{TC\_gap} := d_{TC\_hole} - 2\cdot r_{o\_tc} = 0.0025\cdot in$ Mean diametrical clearance between 1/8" TC and hole

$$d_{tc\_gap} := \begin{pmatrix} 0.0005in \\ d_{TC\_gap} - 0.0005in \end{pmatrix} = \begin{pmatrix} 0.0005 \\ 0.002 \end{pmatrix}\cdot in$$

The gas line is assumed to have the TC diameter and contact the holder.

Calculate temperature control gas gaps accounting for thermal expansion of heat shield, holder, and capsule

$$r_{holder\_seg} := \begin{pmatrix} 1.975 \\ 1.991 \\ 2.003 \\ 2.023 \\ 2.039 \\ 2.051 \\ 2.06 \\ 2.068 \\ 2.074 \\ 2.077 \\ 2.082 \\ 2.087 \end{pmatrix} 0.5in$$ Outside radius of holder sections (DWG-604551, sheets 2 and 4). The ORs are sorted in an ascend order.

$d_{holder\_hs} := r_{i\_hs} - r_{holder\_seg} - u_{o\_holder} =$

0.061
0.053
0.047
0.037
0.029
0.023
0.018
0.014
0.011
0.01
0.007
0.005

$\cdot in$ Gas gaps between holder and heat shield after expansion

Include effect of change in diameter of graphite due to irradiation induced shrinkage

Effect of neutron fluence on graphite dimensions (William Windes, Data Report on PostIrradiation Dimensional Change in AGC-1 Samples, INL/EXT-12-26255, Appendix A, 2012)

$\beta := 0.00191$ This value was not found in the referenced report but used in ECAR-2494. It may be regressed somewhere.

Evaluate temperature control gas gaps at 3 dpa and 6 dpa

$dpa_{3.0} := 3$

$d_{holder\_hs\_3dpa} := d_{holder\_hs} + \beta \cdot dpa_{3.0} \cdot r_{holder\_seg} =$

	0
0	0.06651
1	0.05855
2	0.05259
3	0.04264
4	0.03469
5	0.02872
6	0.02425
7	0.02027
8	0.01729
9	0.0158
10	0.01331
11	0.01083

$\cdot in$

$dpa_{6.0} := 6$

$d_{holder\_hs\_6dpa} := d_{holder\_hs} + \beta \cdot dpa_{6.0} \cdot r_{holder\_seg} =$

	0
0	0.07216
1	0.06426
2	0.05833
3	0.04844
4	0.04053
5	0.0346
6	0.03015
7	0.0262
8	0.02323
9	0.02175
10	0.01928
11	0.01681

$\cdot in$

A3: Heat transfer coefficients/thermal conductance for conduction across gas gaps

$$T_{gas} = \begin{pmatrix} 84 \\ 968 \\ 1652 \end{pmatrix} \cdot °F$$

$ii := 0..2$ $jj := 0..1$

As showing in the DWG-604554 and explained in the attached email, there are 7 gas zones. Zones 1-5 flow in the gap between heat shield and graphite holder, divided by rings into five zones. The ring is not gas-tight and the gases in the adjacent zones may mix (ECAR-3386). In this as-run analysis, gases in some adjacent zones are averaged.
For the gap between heat shield and capsule, zone 6 provides the gas mixture. In the simulation, the actual gas mixture is not used because the gap size uncertainty is significant.The 50% Argon and Helium mixture is employed to calculate the conductances of different gap sizes. Appropriate gap size is selected to match the TC measured temperature.
Gas zone 7 flows inside the graphite holder. The actual gas mixture is used to get the gap conductance.

Gas mixtures can be found in **A6: Source power, gas flows, and DPA** section.

Use 50% Helium and 50% Argon for the general gaps

$$h_{cap\_insulator} := \frac{k_{50He50Ar}}{d_{cap\_insulator}} = \begin{pmatrix} 0.14076 \\ 0.29633 \\ 0.34998 \end{pmatrix} \cdot \frac{BTU}{in^2 \cdot hr \cdot R}$$ Gap between capsule and upper graphite insulator

$$h_{cap\_holder\_bottom} := \frac{k_{50He50Ar}}{d_{cap\_bottom\_holder}} = \begin{pmatrix} 0.05068 \\ 0.1067 \\ 0.12601 \end{pmatrix} \cdot \frac{BTU}{in^2 \cdot hr \cdot R}$$ Gap between capsule and bottom end of holder

$$h_{cap\_nub} := \frac{k_{50He50Ar}}{d_{cap\_nub}} = \begin{pmatrix} 0.79239 \\ 1.6682 \\ 1.9702 \end{pmatrix} \cdot \frac{BTU}{in^2 \cdot hr \cdot R}$$ Gap between capsule and nubs at bottom end of holder

$$h_{hs\_holder\_bottom} := \frac{k_{50He50Ar}}{d_{hs\_bottom\_holder}} = \begin{pmatrix} 0.072 \\ 0.15158 \\ 0.17902 \end{pmatrix} \cdot \frac{BTU}{in^2 \cdot hr \cdot R}$$ Gap between heat shield and bottom end of holder

$$h_{hs\_insulator} := \frac{k_{50He50Ar}}{d_{hs\_insulator}} = \begin{pmatrix} 0.79239 \\ 1.6682 \\ 1.9702 \end{pmatrix} \cdot \frac{BTU}{in^2 \cdot hr \cdot R}$$ Gap between heat shield and upper graphite insulator

These gaps are inside the holder and the conductance is changed from cycle to cycle

50% argon and 50% helium (cycle 157D)

$k_{gas\_zone7} := k_{50He50Ar}$

$h_{channel\_specimen} := \frac{k_{gas\_zone7}}{d_{channel\_specimen}} = \begin{pmatrix} 0.2653 \\ 0.55853 \\ 0.65964 \end{pmatrix} \cdot \frac{BTU}{in^2 \cdot hr \cdot R}$ Gap between specimens and holder channels

$h_{channel\_rod} := \frac{k_{gas\_zone7}}{d_{channel\_rod}} = \begin{pmatrix} 0.1895 \\ 0.39895 \\ 0.47117 \end{pmatrix} \cdot \frac{BTU}{in^2 \cdot hr \cdot R}$ Gap between spacer/push rod and holder channel

$h_{channel\_heater} := \frac{k_{gas\_zone7}}{d_{channel\_heater}} = \begin{pmatrix} 0.27926 \\ 0.58793 \\ 0.69436 \end{pmatrix} \cdot \frac{BTU}{in^2 \cdot hr \cdot R}$ Gap between heater and holder channel

$h_{tc_{ii,jj}} := \frac{k_{gas\_zone7_{ii}}}{d_{tc\_gap_{jj}}}$

Gap between holder and thermocouple

$h_{tc} = \begin{pmatrix} 5.30603 & 1.32651 \\ 11.17059 & 2.79265 \\ 13.19286 & 3.29821 \end{pmatrix} \cdot \frac{BTU}{in^2 \cdot hr \cdot R}$

For 30% Argon, 70% Helium (cycle 158A)

$k_{gas\_zone7} := k_{70He30Ar}$

$h_{channel\_specimen} := \frac{k_{gas\_zone7}}{d_{channel\_specimen}} = \begin{pmatrix} 0.38953 \\ 0.81372 \\ 1.07373 \end{pmatrix} \cdot \frac{BTU}{in^2 \cdot hr \cdot R}$ Gap between specimens and holder channels

$$h_{channel\_rod} := \frac{k_{gas\_zone7}}{d_{channel\_rod}} = \begin{pmatrix} 0.27823 \\ 0.58123 \\ 0.76695 \end{pmatrix} \cdot \frac{BTU}{in^2 \cdot hr \cdot R}$$

Gap between spacer/push rod and holder channel

$$h_{channel\_heater} := \frac{k_{gas\_zone7}}{d_{channel\_heater}} = \begin{pmatrix} 0.41003 \\ 0.85655 \\ 1.13024 \end{pmatrix} \cdot \frac{BTU}{in^2 \cdot hr \cdot R}$$

Gap between heater and holder channel

$$h_{tc_{ii,jj}} := \frac{k_{gas\_zone7_{ii}}}{d_{tc\_gap_{jj}}}$$

Gap between holder and thermocouple

$$h_{tc} = \begin{pmatrix} 7.79053 & 1.94763 \\ 16.2744 & 4.0686 \\ 21.4745 & 5.36863 \end{pmatrix} \cdot \frac{BTU}{in^2 \cdot hr \cdot R}$$

For 10% Argon, 90% Helium (cycle 162B, 164A)

$$k_{gas\_zone7} := k_{90He10Ar}$$

$$h_{channel\_specimen} := \frac{k_{gas\_zone7}}{d_{channel\_specimen}} = \begin{pmatrix} 0.59705 \\ 1.20373 \\ 1.62744 \end{pmatrix} \cdot \frac{BTU}{in^2 \cdot hr \cdot R}$$

$$h_{channel\_rod} := \frac{k_{gas\_zone7}}{d_{channel\_rod}} = \begin{pmatrix} 0.42646 \\ 0.85981 \\ 1.16246 \end{pmatrix} \cdot \frac{BTU}{in^2 \cdot hr \cdot R}$$

Gap between spacer/push rod and holder channel

$$h_{channel\_heater} := \frac{k_{gas\_zone7}}{d_{channel\_heater}} = \begin{pmatrix} 0.62847 \\ 1.26708 \\ 1.71309 \end{pmatrix} \cdot \frac{BTU}{in^2 \cdot hr \cdot R}$$

Gap between heater and holder channel

$$h_{tc_{ii,jj}} := \frac{k_{gas\_zone7_{ii}}}{d_{tc\_gap_{jj}}}$$

Gap between holder and thermocouple

$$h_{tc} = \begin{pmatrix} 11.94098 & 2.98524 \\ 24.07455 & 6.01864 \\ 32.5488 & 8.1372 \end{pmatrix} \cdot \frac{BTU}{in^2 \cdot hr \cdot R}$$

For 0% Argon, 100% Helium (all other cycles)

$$k_{gas\_zone7} := k_{100He0Ar}$$

$$h_{channel\_specimen} := \frac{k_{gas\_zone7}}{d_{channel\_specimen}} = \begin{pmatrix} 0.7415 \\ 1.48299 \\ 1.91152 \end{pmatrix} \cdot \frac{BTU}{in^2 \cdot hr \cdot R}$$

$$h_{channel\_rod} := \frac{k_{gas\_zone7}}{d_{channel\_rod}} = \begin{pmatrix} 0.52964 \\ 1.05928 \\ 1.36537 \end{pmatrix} \cdot \frac{BTU}{in^2 \cdot hr \cdot R}$$

Gap between spacer/push rod and holder channel

$$h_{channel\_heater} := \frac{k_{gas\_zone7}}{d_{channel\_heater}} = \begin{pmatrix} 0.78052 \\ 1.56104 \\ 2.01213 \end{pmatrix} \cdot \frac{BTU}{in^2 \cdot hr \cdot R}$$

Gap between heater and holder channel

$$h_{tc_{ii,jj}} := \frac{k_{gas\_zone7_{ii}}}{d_{tc\_gap_{jj}}}$$

Gap between holder and thermocouple

$$h_{tc} = \begin{pmatrix} 14.82993 & 3.70748 \\ 29.65985 & 7.41496 \\ 38.23039 & 9.5576 \end{pmatrix} \cdot \frac{BTU}{in^2 \cdot hr \cdot R}$$

Evaluate temperature control gas gap conductance using various gas mixture

$kk := 0 .. 11$

For the unirradiated graphite

Pure helium (100%)

$$h_{g_{ii,kk}} := \frac{k_{100He0Ar_{ii}}}{d_{holder\_hs_{kk}}}$$

$$h_g = \begin{pmatrix} 0.122 & 0.14 & 0.158 & 0.201 & 0.257 & 0.325 & 0.404 & 0.517 & 0.653 & 0.753 & 1.009 & 1.529 \\ 0.244 & 0.281 & 0.317 & 0.402 & 0.514 & 0.649 & 0.808 & 1.034 & 1.307 & 1.506 & 2.018 & 3.059 \\ 0.314 & 0.362 & 0.408 & 0.519 & 0.663 & 0.837 & 1.042 & 1.332 & 1.684 & 1.941 & 2.601 & 3.943 \end{pmatrix} \cdot \frac{BTU}{in^2 \cdot hr \cdot R}$$

90% Helium 10% Argon

$$h_{g_{ii,kk}} := \frac{k_{90He10Ar_{ii}}}{d_{holder\_hs_{kk}}}$$

$$h_g = \begin{pmatrix} 0.098 & 0.113 & 0.127 & 0.162 & 0.207 & 0.261 & 0.325 & 0.416 & 0.526 & 0.606 & 0.813 & 1.232 \\ 0.198 & 0.228 & 0.257 & 0.327 & 0.417 & 0.527 & 0.656 & 0.839 & 1.061 & 1.222 & 1.638 & 2.483 \\ 0.267 & 0.308 & 0.347 & 0.442 & 0.564 & 0.712 & 0.887 & 1.134 & 1.434 & 1.653 & 2.215 & 3.357 \end{pmatrix} \cdot \frac{BTU}{in^2 \cdot hr \cdot R}$$

80% Helium 20% Argon

$$h_{g_{ii,kk}} := \frac{k_{80He20Ar_{ii}}}{d_{holder\_hs_{kk}}}$$

$$h_g = \begin{bmatrix} 0.079 & 0.09 & 0.102 & 0.13 & 0.166 & 0.209 & 0.261 & 0.333 & 0.421 & 0.485 & 0.651 & 0.986 \\ 0.154 & 0.178 & 0.2 & 0.255 & 0.325 & 0.411 & 0.512 & 0.654 & 0.827 & 0.953 & 1.278 & 1.937 \\ 0.221 & 0.254 & 0.287 & 0.365 & 0.466 & 0.588 & 0.732 & 0.936 & 1.184 & 1.364 & 1.828 & 2.771 \end{bmatrix} \cdot \frac{BTU}{in^2 \cdot hr \cdot R}$$

70% Helium 30% Argon

$$h_{g_{ii,kk}} := \frac{k_{70He30Ar_{ii}}}{d_{holder\_hs_{kk}}}$$

$$h_g = \begin{bmatrix} 0.064 & 0.074 & 0.083 & 0.106 & 0.135 & 0.17 & 0.212 & 0.271 & 0.343 & 0.396 & 0.53 & 0.803 \\ 0.134 & 0.154 & 0.174 & 0.221 & 0.282 & 0.356 & 0.443 & 0.567 & 0.717 & 0.826 & 1.107 & 1.678 \\ 0.176 & 0.203 & 0.229 & 0.291 & 0.372 & 0.47 & 0.585 & 0.748 & 0.946 & 1.09 & 1.461 & 2.215 \end{bmatrix} \cdot \frac{BTU}{in^2 \cdot hr \cdot R}$$

60% Helium 40% Argon

$$h_{g_{ii,kk}} := \frac{k_{60He40Ar_{ii}}}{d_{holder\_hs_{kk}}}$$

$$h_g = \begin{bmatrix} 0.053 & 0.061 & 0.069 & 0.087 & 0.111 & 0.141 & 0.175 & 0.224 & 0.283 & 0.326 & 0.437 & 0.662 \\ 0.111 & 0.128 & 0.144 & 0.183 & 0.234 & 0.295 & 0.367 & 0.47 & 0.594 & 0.684 & 0.917 & 1.39 \\ 0.132 & 0.152 & 0.172 & 0.218 & 0.279 & 0.352 & 0.438 & 0.56 & 0.709 & 0.816 & 1.094 & 1.659 \end{bmatrix} \cdot \frac{BTU}{in^2 \cdot hr \cdot R}$$

50% Helium 50% Argon

$$h_{g_{ii,kk}} := \frac{k_{50He50Ar_{ii}}}{d_{holder\_hs_{kk}}}$$

$$h_g = \begin{bmatrix} 0.044 & 0.05 & 0.057 & 0.072 & 0.092 & 0.116 & 0.145 & 0.185 & 0.234 & 0.269 & 0.361 & 0.547 \\ 0.092 & 0.106 & 0.119 & 0.152 & 0.194 & 0.244 & 0.304 & 0.389 & 0.492 & 0.567 & 0.76 & 1.152 \\ 0.108 & 0.125 & 0.141 & 0.179 & 0.229 & 0.289 & 0.36 & 0.46 & 0.581 & 0.67 & 0.898 & 1.361 \end{bmatrix} \cdot \frac{BTU}{in^2 \cdot hr \cdot R}$$

40% Helium 60% Argon

$$h_{g_{ii,kk}} := \frac{k_{40He60Ar_{ii}}}{d_{holder\_hs_{kk}}}$$

$$h_g = \begin{bmatrix} 0.036 & 0.041 & 0.046 & 0.059 & 0.075 & 0.095 & 0.118 & 0.151 & 0.191 & 0.221 & 0.296 & 0.448 \\ 0.076 & 0.087 & 0.098 & 0.125 & 0.16 & 0.202 & 0.251 & 0.321 & 0.406 & 0.468 & 0.627 & 0.95 \\ 0.084 & 0.097 & 0.109 & 0.139 & 0.177 & 0.223 & 0.278 & 0.356 & 0.45 & 0.518 & 0.695 & 1.053 \end{bmatrix} \cdot \frac{BTU}{in^2 \cdot hr \cdot R}$$

30% Helium 70% Argon

$$h_{g_{ii,kk}} := \frac{k_{30He70Ar_{ii}}}{d_{holder\_hs_{kk}}}$$

$$h_g = \begin{bmatrix} 0.029 & 0.033 & 0.037 & 0.048 & 0.061 & 0.077 & 0.096 & 0.122 & 0.154 & 0.178 & 0.239 & 0.362 \\ 0.061 & 0.07 & 0.079 & 0.101 & 0.129 & 0.163 & 0.203 & 0.259 & 0.328 & 0.377 & 0.506 & 0.767 \\ 0.07 & 0.08 & 0.09 & 0.115 & 0.147 & 0.185 & 0.231 & 0.295 & 0.373 & 0.43 & 0.577 & 0.874 \end{bmatrix} \cdot \frac{BTU}{in^2 \cdot hr \cdot R}$$

20% Helium 80% Argon

$$h_{g_{ii,kk}} := \frac{k_{20He80Ar_{ii}}}{d_{holder\_hs_{kk}}}$$

$$h_g = \begin{bmatrix} 0.023 & 0.027 & 0.03 & 0.038 & 0.049 & 0.062 & 0.077 & 0.099 & 0.125 & 0.144 & 0.193 & 0.292 \\ 0.049 & 0.057 & 0.064 & 0.081 & 0.104 & 0.131 & 0.163 & 0.209 & 0.264 & 0.304 & 0.408 & 0.618 \\ 0.055 & 0.064 & 0.072 & 0.091 & 0.117 & 0.148 & 0.184 & 0.235 & 0.297 & 0.342 & 0.459 & 0.695 \end{bmatrix} \cdot \frac{BTU}{in^2 \cdot hr \cdot R}$$

10% Helium 90% Argon

$$h_{g_{ii,kk}} := \frac{k_{10He90Ar_{ii}}}{d_{holder\_hs_{kk}}}$$

$$h_g = \begin{bmatrix} 0.019 & 0.021 & 0.024 & 0.031 & 0.039 & 0.049 & 0.061 & 0.079 & 0.099 & 0.114 & 0.153 & 0.232 \\ 0.039 & 0.045 & 0.051 & 0.065 & 0.082 & 0.104 & 0.13 & 0.166 & 0.21 & 0.242 & 0.324 & 0.491 \\ 0.047 & 0.054 & 0.061 & 0.077 & 0.098 & 0.124 & 0.155 & 0.198 & 0.25 & 0.288 & 0.387 & 0.586 \end{bmatrix} \cdot \frac{BTU}{in^2 \cdot hr \cdot R}$$

0% Helium 100% Argon

$$h_{g_{ii,kk}} := \frac{k_{0He100Ar_{ii}}}{d_{holder\_hs_{kk}}}$$

$$h_g = \begin{bmatrix} 0.014 & 0.017 & 0.019 & 0.024 & 0.03 & 0.038 & 0.048 & 0.061 & 0.077 & 0.089 & 0.119 & 0.181 \\ 0.03 & 0.035 & 0.039 & 0.05 & 0.064 & 0.081 & 0.101 & 0.129 & 0.163 & 0.187 & 0.251 & 0.38 \\ 0.038 & 0.044 & 0.049 & 0.063 & 0.08 & 0.101 & 0.126 & 0.161 & 0.204 & 0.235 & 0.315 & 0.477 \end{bmatrix} \cdot \frac{BTU}{in^2 \cdot hr \cdot R}$$

Control gas gap conductane with the effect of irradiation induced shrinkage of graphite at 3 dpa

100% Helium 0% Argon

$$h_{g_{ii,kk}} := \frac{k_{100He0Ar_{ii}}}{d_{holder\_hs\_3dpa_{kk}}}$$

$$h_g = \begin{bmatrix} 0.111 & 0.127 & 0.141 & 0.174 & 0.214 & 0.258 & 0.306 & 0.366 & 0.429 & 0.469 & 0.557 & 0.685 \\ 0.223 & 0.253 & 0.282 & 0.348 & 0.428 & 0.516 & 0.612 & 0.732 & 0.858 & 0.939 & 1.114 & 1.37 \\ 0.287 & 0.326 & 0.363 & 0.448 & 0.551 & 0.665 & 0.788 & 0.943 & 1.106 & 1.21 & 1.436 & 1.765 \end{bmatrix} \cdot \frac{BTU}{in^2 \cdot hr \cdot R}$$

90% Helium 10% Argon

$$h_{g_{ii,kk}} := \frac{k_{90He10Ar_{ii}}}{d_{holder\_hs\_3dpa_{kk}}}$$

$$h_g = \begin{bmatrix} 0.09 & 0.102 & 0.114 & 0.14 & 0.172 & 0.208 & 0.246 & 0.295 & 0.345 & 0.378 & 0.448 & 0.551 \\ 0.181 & 0.206 & 0.229 & 0.282 & 0.347 & 0.419 & 0.496 & 0.594 & 0.696 & 0.762 & 0.904 & 1.112 \\ 0.245 & 0.278 & 0.309 & 0.382 & 0.469 & 0.567 & 0.671 & 0.803 & 0.941 & 1.03 & 1.222 & 1.503 \end{bmatrix} \cdot \frac{BTU}{in^2 \cdot hr \cdot R}$$

80% Helium 20% Argon

$$h_{g_{ii,kk}} := \frac{k_{80He20Ar_{ii}}}{d_{holder\_hs\_3dpa_{kk}}}$$

$$h_g = \begin{bmatrix} 0.072 & 0.082 & 0.091 & 0.112 & 0.138 & 0.166 & 0.197 & 0.236 & 0.277 & 0.303 & 0.359 & 0.442 \\ 0.141 & 0.16 & 0.179 & 0.22 & 0.271 & 0.327 & 0.387 & 0.463 & 0.543 & 0.594 & 0.705 & 0.867 \\ 0.202 & 0.229 & 0.255 & 0.315 & 0.387 & 0.468 & 0.554 & 0.663 & 0.777 & 0.85 & 1.009 & 1.241 \end{bmatrix} \cdot \frac{BTU}{in^2 \cdot hr \cdot R}$$

70% Helium 30% Argon

$$h_{g_{ii,kk}} := \frac{k_{70He30Ar_{ii}}}{d_{holder\_hs\_3dpa_{kk}}}$$

$$h_g = \begin{bmatrix} 0.059 & 0.067 & 0.074 & 0.091 & 0.112 & 0.136 & 0.161 & 0.192 & 0.225 & 0.247 & 0.293 & 0.36 \\ 0.122 & 0.139 & 0.155 & 0.191 & 0.235 & 0.283 & 0.336 & 0.401 & 0.471 & 0.515 & 0.611 & 0.752 \\ 0.161 & 0.183 & 0.204 & 0.252 & 0.31 & 0.374 & 0.443 & 0.53 & 0.621 & 0.68 & 0.807 & 0.992 \end{bmatrix} \cdot \frac{BTU}{in^2 \cdot hr \cdot R}$$

60% Helium 40% Argon

$$h_{g_{ii,kk}} := \frac{k_{60He40Ar_{ii}}}{d_{holder\_hs\_3dpa_{kk}}}$$

$$h_g = \begin{bmatrix} 0.048 & 0.055 & 0.061 & 0.075 & 0.093 & 0.112 & 0.132 & 0.158 & 0.186 & 0.203 & 0.241 & 0.297 \\ 0.101 & 0.115 & 0.128 & 0.158 & 0.194 & 0.235 & 0.278 & 0.333 & 0.39 & 0.427 & 0.506 & 0.623 \\ 0.121 & 0.137 & 0.153 & 0.189 & 0.232 & 0.28 & 0.332 & 0.397 & 0.465 & 0.509 & 0.604 & 0.743 \end{bmatrix} \cdot \frac{BTU}{in^2 \cdot hr \cdot R}$$

50% Helium 50% Argon

$$h_{g_{ii,kk}} := \frac{k_{50He50Ar_{ii}}}{d_{holder\_hs\_3dpa_{kk}}}$$

$$h_g = \begin{bmatrix} 0.04 & 0.045 & 0.05 & 0.062 & 0.076 & 0.092 & 0.109 & 0.131 & 0.153 & 0.168 & 0.199 & 0.245 \\ 0.084 & 0.095 & 0.106 & 0.131 & 0.161 & 0.194 & 0.23 & 0.276 & 0.323 & 0.354 & 0.42 & 0.516 \\ 0.099 & 0.113 & 0.125 & 0.155 & 0.19 & 0.23 & 0.272 & 0.325 & 0.382 & 0.418 & 0.495 & 0.609 \end{bmatrix} \cdot \frac{BTU}{in^2 \cdot hr \cdot R}$$

40% Helium 60% Argon

$$h_{g_{ii,kk}} := \frac{k_{40He60Ar_{ii}}}{d_{holder\_hs\_3dpa_{kk}}}$$

$$h_g = \begin{bmatrix} 0.033 & 0.037 & 0.041 & 0.051 & 0.063 & 0.076 & 0.09 & 0.107 & 0.126 & 0.137 & 0.163 & 0.201 \\ 0.069 & 0.079 & 0.088 & 0.108 & 0.133 & 0.16 & 0.19 & 0.227 & 0.267 & 0.292 & 0.346 & 0.426 \\ 0.077 & 0.087 & 0.097 & 0.12 & 0.147 & 0.178 & 0.21 & 0.252 & 0.295 & 0.323 & 0.383 & 0.471 \end{bmatrix} \cdot \frac{BTU}{in^2 \cdot hr \cdot R}$$

30% Helium 70% Argon

$$h_{g_{ii,kk}} := \frac{k_{30He70Ar_{ii}}}{d_{holder\_hs\_3dpa_{kk}}}$$

$h_g =$

0.026	0.03	0.033	0.041	0.051	0.061	0.072	0.086	0.101	0.111	0.132	0.162
0.056	0.063	0.071	0.087	0.107	0.129	0.153	0.183	0.215	0.235	0.279	0.343
0.064	0.072	0.081	0.099	0.122	0.148	0.175	0.209	0.245	0.268	0.318	0.391

$\cdot \frac{BTU}{in^2 \cdot hr \cdot R}$

20% Helium 80% Argon

$$h_{g_{ii,kk}} := \frac{k_{20He80Ar_{ii}}}{d_{holder\_hs\_3dpa_{kk}}}$$

$h_g =$

0.021	0.024	0.027	0.033	0.041	0.049	0.058	0.07	0.082	0.09	0.106	0.131
0.045	0.051	0.057	0.07	0.086	0.104	0.123	0.148	0.173	0.19	0.225	0.277
0.051	0.058	0.064	0.079	0.097	0.117	0.139	0.166	0.195	0.213	0.253	0.311

$\cdot \frac{BTU}{in^2 \cdot hr \cdot R}$

10% Helium 90% Argon

$$h_{g_{ii,kk}} := \frac{k_{10He90Ar_{ii}}}{d_{holder\_hs\_3dpa_{kk}}}$$

$h_g =$

0.017	0.019	0.021	0.026	0.032	0.039	0.046	0.056	0.065	0.071	0.085	0.104
0.036	0.041	0.045	0.056	0.069	0.083	0.098	0.117	0.138	0.151	0.179	0.22
0.043	0.049	0.054	0.067	0.082	0.099	0.117	0.14	0.164	0.18	0.213	0.262

$\cdot \frac{BTU}{in^2 \cdot hr \cdot R}$

0% Helium 100% Argon

$$h_{g_{ii,kk}} := \frac{k_{0He100Ar_{ii}}}{d_{holder\_hs\_3dpa_{kk}}}$$

$h_g =$

0.013	0.015	0.017	0.021	0.025	0.031	0.036	0.043	0.051	0.055	0.066	0.081
0.028	0.031	0.035	0.043	0.053	0.064	0.076	0.091	0.107	0.117	0.139	0.17
0.035	0.039	0.044	0.054	0.067	0.08	0.095	0.114	0.134	0.146	0.174	0.213

$\cdot \frac{BTU}{in^2 \cdot hr \cdot R}$

Control gas gap conductane with the effect of irradiation induced shrinkage of graphite at 6 dpa

100% Helium 0% Argon

$$h_{g_{ii,kk}} := \frac{k_{100He0Ar_{ii}}}{d_{holder\_hs\_6dpa_{kk}}}$$

$h_g =$

	0.103	0.115	0.127	0.153	0.183	0.214	0.246	0.283	0.319	0.341	0.385	0.441
	0.206	0.231	0.254	0.306	0.366	0.429	0.492	0.566	0.638	0.682	0.769	0.882
	0.265	0.297	0.328	0.395	0.472	0.552	0.634	0.73	0.823	0.879	0.992	1.137

$\cdot \frac{BTU}{in^2 \cdot hr \cdot R}$

90% Helium 10% Argon

$$h_{g_{ii,kk}} := \frac{k_{90He10Ar_{ii}}}{d_{holder\_hs\_6dpa_{kk}}}$$

$h_g =$

	0.083	0.093	0.102	0.123	0.147	0.173	0.198	0.228	0.257	0.275	0.31	0.355
	0.167	0.187	0.206	0.248	0.297	0.348	0.399	0.459	0.518	0.553	0.624	0.716
	0.226	0.253	0.279	0.336	0.402	0.47	0.54	0.621	0.701	0.748	0.844	0.968

$\cdot \frac{BTU}{in^2 \cdot hr \cdot R}$

80% Helium 20% Argon

$$h_{g_{ii,kk}} := \frac{k_{80He20Ar_{ii}}}{d_{holder\_hs\_6dpa_{kk}}}$$

$h_g =$

	0.066	0.074	0.082	0.099	0.118	0.138	0.159	0.183	0.206	0.22	0.248	0.284
	0.13	0.146	0.161	0.194	0.232	0.271	0.311	0.358	0.404	0.432	0.487	0.559
	0.186	0.209	0.23	0.277	0.331	0.388	0.446	0.513	0.578	0.618	0.697	0.799

$\cdot \frac{BTU}{in^2 \cdot hr \cdot R}$

70% Helium 30% Argon

$$h_{g_{ii,kk}} := \frac{k_{70He30Ar_{ii}}}{d_{holder\_hs\_6dpa_{kk}}}$$

$h_g =$

	0.054	0.061	0.067	0.08	0.096	0.113	0.129	0.149	0.168	0.179	0.202	0.232
	0.113	0.127	0.14	0.168	0.201	0.235	0.27	0.311	0.35	0.374	0.422	0.484
	0.149	0.167	0.184	0.222	0.265	0.31	0.356	0.41	0.462	0.494	0.557	0.639

$\cdot \frac{BTU}{in^2 \cdot hr \cdot R}$

60% Helium 40% Argon

$$h_{g_{ii,kk}} := \frac{k_{60He40Ar_{ii}}}{d_{holder\_hs\_6dpa_{kk}}}$$

	0.045	0.05	0.055	0.066	0.079	0.093	0.107	0.123	0.138	0.148	0.167	0.191

BTU

$h_g =$

0.093	0.105	0.116	0.139	0.166	0.195	0.224	0.257	0.29	0.31	0.35	0.401
0.111	0.125	0.138	0.166	0.198	0.232	0.267	0.307	0.346	0.37	0.417	0.478

$\cdot \frac{\text{BTU}}{\text{in}^2 \cdot \text{hr} \cdot \text{R}}$

50% Helium 50% Argon

$$h_{g_{ii,kk}} := \frac{k_{50He50Ar_{ii}}}{d_{holder\_hs\_6dpa_{kk}}}$$

$h_g =$

0.037	0.041	0.045	0.055	0.065	0.077	0.088	0.101	0.114	0.122	0.138	0.158
0.077	0.087	0.096	0.115	0.138	0.161	0.185	0.213	0.24	0.257	0.29	0.332
0.091	0.103	0.113	0.136	0.163	0.191	0.219	0.252	0.284	0.303	0.342	0.392

$\cdot \frac{\text{BTU}}{\text{in}^2 \cdot \text{hr} \cdot \text{R}}$

40% Helium 60% Argon

$$h_{g_{ii,kk}} := \frac{k_{40He60Ar_{ii}}}{d_{holder\_hs\_6dpa_{kk}}}$$

$h_g =$

0.03	0.034	0.037	0.045	0.054	0.063	0.072	0.083	0.093	0.1	0.113	0.129
0.064	0.072	0.079	0.095	0.114	0.133	0.153	0.176	0.198	0.212	0.239	0.274
0.071	0.079	0.088	0.105	0.126	0.148	0.169	0.195	0.22	0.235	0.265	0.304

$\cdot \frac{\text{BTU}}{\text{in}^2 \cdot \text{hr} \cdot \text{R}}$

30% Helium 70% Argon

$$h_{g_{ii,kk}} := \frac{k_{30He70Ar_{ii}}}{d_{holder\_hs\_6dpa_{kk}}}$$

$h_g =$

0.024	0.027	0.03	0.036	0.043	0.051	0.058	0.067	0.075	0.081	0.091	0.104
0.052	0.058	0.064	0.077	0.092	0.107	0.123	0.142	0.16	0.171	0.193	0.221
0.059	0.066	0.073	0.087	0.105	0.122	0.141	0.162	0.182	0.195	0.22	0.252

$\cdot \frac{\text{BTU}}{\text{in}^2 \cdot \text{hr} \cdot \text{R}}$

20% Helium 80% Argon

$$h_{g_{ii,kk}} := \frac{k_{20He80Ar_{ii}}}{d_{holder\_hs\_6dpa_{kk}}}$$

$$h_g = \begin{pmatrix} 0.02 & 0.022 & 0.024 & 0.029 & 0.035 & 0.041 & 0.047 & 0.054 & 0.061 & 0.065 & 0.073 & 0.084 \\ 0.042 & 0.047 & 0.051 & 0.062 & 0.074 & 0.087 & 0.099 & 0.114 & 0.129 & 0.138 & 0.155 & 0.178 \\ 0.047 & 0.052 & 0.058 & 0.07 & 0.083 & 0.097 & 0.112 & 0.129 & 0.145 & 0.155 & 0.175 & 0.201 \end{pmatrix} \cdot \frac{BTU}{in^2 \cdot hr \cdot R}$$

10% Helium 90% Argon

$$h_{g_{ii,kk}} := \frac{k_{10He90Ar_{ii}}}{d_{holder\_hs\_6dpa_{kk}}}$$

$$h_g = \begin{pmatrix} 0.016 & 0.018 & 0.019 & 0.023 & 0.028 & 0.033 & 0.037 & 0.043 & 0.048 & 0.052 & 0.058 & 0.067 \\ 0.033 & 0.037 & 0.041 & 0.049 & 0.059 & 0.069 & 0.079 & 0.091 & 0.102 & 0.109 & 0.123 & 0.142 \\ 0.039 & 0.044 & 0.049 & 0.059 & 0.07 & 0.082 & 0.094 & 0.108 & 0.122 & 0.131 & 0.147 & 0.169 \end{pmatrix} \cdot \frac{BTU}{in^2 \cdot hr \cdot R}$$

0% Helium 100% Argon

$$h_{g_{ii,kk}} := \frac{k_{0He100Ar_{ii}}}{d_{holder\_hs\_6dpa_{kk}}}$$

$$h_g = \begin{pmatrix} 0.012 & 0.014 & 0.015 & 0.018 & 0.022 & 0.025 & 0.029 & 0.033 & 0.038 & 0.04 & 0.045 & 0.052 \\ 0.026 & 0.029 & 0.032 & 0.038 & 0.045 & 0.053 & 0.061 & 0.07 & 0.079 & 0.085 & 0.096 & 0.11 \\ 0.032 & 0.036 & 0.04 & 0.048 & 0.057 & 0.067 & 0.077 & 0.088 & 0.099 & 0.106 & 0.12 & 0.138 \end{pmatrix} \cdot \frac{BTU}{in^2 \cdot hr \cdot R}$$

Assume the gap between capsule and heat shield varies from 0.001" to 0.02". Some cycles may need additional higher or lower conductance.

$d_{cap\_hs\_001} := 0.001in$

$$h_{cap\_hs\_001} := \frac{k_{50He50Ar}}{d_{cap\_hs\_001}} = \begin{pmatrix} 2.65302 \\ 5.5853 \\ 6.59643 \end{pmatrix} \cdot \frac{BTU}{in^2 \cdot hr \cdot R}$$

$d_{cap\_hs\_002} := 0.002in$

$$h_{cap\_hs\_002} := \frac{k_{50He50Ar}}{d_{cap\_hs\_002}} = \begin{pmatrix} 1.32651 \\ 2.79265 \\ 3.29821 \end{pmatrix} \cdot \frac{BTU}{in^2 \cdot hr \cdot R}$$

$d_{cap\_hs\_003} := 0.003in$

$$h_{cap\_hs\_003} := \frac{k_{50He50Ar}}{d_{cap\_hs\_003}} = \begin{pmatrix} 0.88434 \\ 1.86177 \\ 2.19881 \end{pmatrix} \cdot \frac{BTU}{in^2 \cdot hr \cdot R}$$

$d_{cap\_hs\_004} := 0.004in$

$$h_{cap\_hs\_004} := \frac{k_{50He50Ar}}{d_{cap\_hs\_004}} = \begin{pmatrix} 0.66325 \\ 1.39632 \\ 1.64911 \end{pmatrix} \cdot \frac{BTU}{in^2 \cdot hr \cdot R}$$

$d_{cap\_hs\_005} := 0.005in$

$d_{cap\_hs\_006} := 0.006in$

$\begin{pmatrix} 0.5306 \end{pmatrix}$ $\begin{pmatrix} 0.44217 \end{pmatrix}$

$$h_{cap\_hs\_005} := \frac{k_{50He50Ar}}{d_{cap\_hs\_005}} = \begin{pmatrix} \\ 1.11706 \\ 1.31929 \end{pmatrix} \cdot \frac{BTU}{in^2 \cdot hr \cdot R} \qquad h_{cap\_hs\_006} := \frac{k_{50He50Ar}}{d_{cap\_hs\_006}} = \begin{pmatrix} \\ 0.93088 \\ 1.0994 \end{pmatrix} \cdot \frac{BTU}{in^2 \cdot hr \cdot R}$$

$d_{cap\_hs\_007} := 0.007in$ $d_{cap\_hs\_008} := 0.008in$

$$h_{cap\_hs\_007} := \frac{k_{50He50Ar}}{d_{cap\_hs\_007}} = \begin{pmatrix} 0.379 \\ 0.7979 \\ 0.94235 \end{pmatrix} \cdot \frac{BTU}{in^2 \cdot hr \cdot R} \qquad h_{cap\_hs\_008} := \frac{k_{50He50Ar}}{d_{cap\_hs\_008}} = \begin{pmatrix} 0.33163 \\ 0.69816 \\ 0.82455 \end{pmatrix} \cdot \frac{BTU}{in^2 \cdot hr \cdot R}$$

$d_{cap\_hs\_009} := 0.009in$ $d_{cap\_hs\_010} := 0.01in$

$$h_{cap\_hs\_009} := \frac{k_{50He50Ar}}{d_{cap\_hs\_009}} = \begin{pmatrix} 0.29478 \\ 0.62059 \\ 0.73294 \end{pmatrix} \cdot \frac{BTU}{in^2 \cdot hr \cdot R} \qquad h_{cap\_hs\_010} := \frac{k_{50He50Ar}}{d_{cap\_hs\_010}} = \begin{pmatrix} 0.2653 \\ 0.55853 \\ 0.65964 \end{pmatrix} \cdot \frac{BTU}{in^2 \cdot hr \cdot R}$$

$d_{cap\_hs\_011} := 0.011in$ $d_{cap\_hs\_012} := 0.012in$

$$h_{cap\_hs\_011} := \frac{k_{50He50Ar}}{d_{cap\_hs\_011}} = \begin{pmatrix} 0.24118 \\ 0.50775 \\ 0.59968 \end{pmatrix} \cdot \frac{BTU}{in^2 \cdot hr \cdot R} \qquad h_{cap\_hs\_012} := \frac{k_{50He50Ar}}{d_{cap\_hs\_012}} = \begin{pmatrix} 0.22108 \\ 0.46544 \\ 0.5497 \end{pmatrix} \cdot \frac{BTU}{in^2 \cdot hr \cdot R}$$

$d_{cap\_hs\_013} := 0.013in$ $d_{cap\_hs\_014} := 0.014in$

$$h_{cap\_hs\_013} := \frac{k_{50He50Ar}}{d_{cap\_hs\_013}} = \begin{pmatrix} 0.20408 \\ 0.42964 \\ 0.50742 \end{pmatrix} \cdot \frac{BTU}{in^2 \cdot hr \cdot R} \qquad h_{cap\_hs\_014} := \frac{k_{50He50Ar}}{d_{cap\_hs\_014}} = \begin{pmatrix} 0.1895 \\ 0.39895 \\ 0.47117 \end{pmatrix} \cdot \frac{BTU}{in^2 \cdot hr \cdot R}$$

$d_{cap\_hs\_015} := 0.015in$ $d_{cap\_hs\_016} := 0.016in$

$$h_{cap\_hs\_015} := \frac{k_{50He50Ar}}{d_{cap\_hs\_015}} = \begin{pmatrix} 0.17687 \\ 0.37235 \\ 0.43976 \end{pmatrix} \cdot \frac{BTU}{in^2 \cdot hr \cdot R} \qquad h_{cap\_hs\_016} := \frac{k_{50He50Ar}}{d_{cap\_hs\_016}} = \begin{pmatrix} 0.16581 \\ 0.34908 \\ 0.41228 \end{pmatrix} \cdot \frac{BTU}{in^2 \cdot hr \cdot R}$$

$d_{cap\_hs\_017} := 0.017in$ $d_{cap\_hs\_018} := 0.018in$

$$h_{cap\_hs\_017} := \frac{k_{50He50Ar}}{d_{cap\_hs\_017}} = \begin{pmatrix} 0.15606 \\ 0.32855 \\ 0.38803 \end{pmatrix} \cdot \frac{BTU}{in^2 \cdot hr \cdot R} \qquad h_{cap\_hs\_018} := \frac{k_{50He50Ar}}{d_{cap\_hs\_018}} = \begin{pmatrix} 0.14739 \\ 0.31029 \\ 0.36647 \end{pmatrix} \cdot \frac{BTU}{in^2 \cdot hr \cdot R}$$

$d_{cap\_hs\_019} := 0.019in$ $d_{cap\_hs\_020} := 0.02in$

$$h_{cap\_hs\_019} := \frac{k_{50He50Ar}}{d_{cap\_hs\_019}} = \begin{pmatrix} 0.13963 \\ 0.29396 \\ 0.34718 \end{pmatrix} \cdot \frac{BTU}{in^2 \cdot hr \cdot R} \qquad h_{cap\_hs\_020} := \frac{k_{50He50Ar}}{d_{cap\_hs\_020}} = \begin{pmatrix} 0.13265 \\ 0.27926 \\ 0.32982 \end{pmatrix} \cdot \frac{BTU}{in^2 \cdot hr \cdot R}$$

Insert more points

$d_{cap\_hs\_0013} := 0.0013in$ $d_{cap\_hs\_0024} := 0.0024in$

$$h_{cap\_hs\_0013} := \frac{k_{50He50Ar}}{d_{cap\_hs\_0013}} = \begin{pmatrix} 2.04078 \\ 4.29638 \\ 5.07418 \end{pmatrix} \cdot \frac{BTU}{in^2 \cdot hr \cdot R} \qquad h_{cap\_hs\_0024} := \frac{k_{50He50Ar}}{d_{cap\_hs\_0024}} = \begin{pmatrix} 1.10542 \\ 2.32721 \\ 2.74851 \end{pmatrix} \cdot \frac{BTU}{in^2 \cdot hr \cdot R}$$

$d_{cap\_hs\_0034} := 0.0034in$

$h_{cap\_hs\_0034} := \frac{k_{50He50Ar}}{d_{cap\_hs\_0034}} = \begin{pmatrix} 0.7803 \\ 1.64273 \\ 1.94013 \end{pmatrix} \cdot \frac{BTU}{in^2 \cdot hr \cdot R}$

$d_{cap\_hs\_0045} := 0.0045in$

$h_{cap\_hs\_0045} := \frac{k_{50He50Ar}}{d_{cap\_hs\_0045}} = \begin{pmatrix} 0.58956 \\ 1.24118 \\ 1.46587 \end{pmatrix} \cdot \frac{BTU}{in^2 \cdot hr \cdot R}$

$d_{cap\_hs\_0055} := 0.0055in$

$h_{cap\_hs\_0055} := \frac{k_{50He50Ar}}{d_{cap\_hs\_0055}} = \begin{pmatrix} 0.48237 \\ 1.01551 \\ 1.19935 \end{pmatrix} \cdot \frac{BTU}{in^2 \cdot hr \cdot R}$

$d_{cap\_hs\_0065} := 0.0065in$

$h_{cap\_hs\_0065} := \frac{k_{50He50Ar}}{d_{cap\_hs\_0065}} = \begin{pmatrix} 0.40816 \\ 0.85928 \\ 1.01484 \end{pmatrix} \cdot \frac{BTU}{in^2 \cdot hr \cdot R}$

$d_{cap\_hs\_0075} := 0.0075in$

$h_{cap\_hs\_0075} := \frac{k_{50He50Ar}}{d_{cap\_hs\_0075}} = \begin{pmatrix} 0.35374 \\ 0.74471 \\ 0.87952 \end{pmatrix} \cdot \frac{BTU}{in^2 \cdot hr \cdot R}$

$d_{cap\_hs\_0085} := 0.0085in$

$h_{cap\_hs\_0085} := \frac{k_{50He50Ar}}{d_{cap\_hs\_0085}} = \begin{pmatrix} 0.31212 \\ 0.65709 \\ 0.77605 \end{pmatrix} \cdot \frac{BTU}{in^2 \cdot hr \cdot R}$

$d_{cap\_hs\_0095} := 0.0095in$

$h_{cap\_hs\_0095} := \frac{k_{50He50Ar}}{d_{cap\_hs\_0095}} = \begin{pmatrix} 0.27926 \\ 0.58793 \\ 0.69436 \end{pmatrix} \cdot \frac{BTU}{in^2 \cdot hr \cdot R}$

$d_{cap\_hs\_0105} := 0.0105in$

$h_{cap\_hs\_0105} := \frac{k_{50He50Ar}}{d_{cap\_hs\_0105}} = \begin{pmatrix} 0.25267 \\ 0.53193 \\ 0.62823 \end{pmatrix} \cdot \frac{BTU}{in^2 \cdot hr \cdot R}$

$d_{cap\_hs\_0003} := 0.0003in$

$d_{cap\_hs\_022} := 0.022in$

$$h_{cap\_hs\_0003} := \frac{k_{50He50Ar}}{d_{cap\_hs\_0003}} = \begin{pmatrix} 8.84339 \\ 18.61766 \\ 21.98809 \end{pmatrix} \cdot \frac{BTU}{in^2 \cdot hr \cdot R}$$

$$h_{cap\_hs\_022} := \frac{k_{50He50Ar}}{d_{cap\_hs\_022}} = \begin{pmatrix} 0.12059 \\ 0.25388 \\ 0.29984 \end{pmatrix} \cdot \frac{BTU}{in^2 \cdot hr \cdot R}$$

$$d_{cap\_hs\_025} := 0.025in$$

$$h_{cap\_hs\_025} := \frac{k_{50He50Ar}}{d_{cap\_hs\_025}} = \begin{pmatrix} 0.10612 \\ 0.22341 \\ 0.26386 \end{pmatrix} \cdot \frac{BTU}{in^2 \cdot hr \cdot R}$$

$$d_{cap\_hs\_029} := 0.029in$$

$$h_{cap\_hs\_029} := \frac{k_{50He50Ar}}{d_{cap\_hs\_029}} = \begin{pmatrix} 0.09148 \\ 0.1926 \\ 0.22746 \end{pmatrix} \cdot \frac{BTU}{in^2 \cdot hr \cdot R}$$

A4: Turbulent forced convection in the annulus between capsule and chopped dummy in-pile tube

$T_{inlet} := 125\,°F$

Primary coolant inlet temperature and pressure

$P_{inlet} := 360psi$

$\Delta p := 77psi$

Core pressure drop for 2-pump operation

$$T_{film} := \begin{pmatrix} 125 \\ 170 \\ 260 \end{pmatrix} °F$$

$$\rho := \begin{bmatrix} 0.5\cdot\left(\rho_{H2O_0} + \rho_{H2O_1}\right) \\ \rho_{H2O_1} \\ \rho_{H2O_2} \end{bmatrix} = \begin{pmatrix} 0.0354 \\ 0.035 \\ 0.0336 \end{pmatrix} \cdot \frac{lb}{in^3}$$

$$Cp := \begin{bmatrix} 0.5\cdot\left(Cp_{H2O_0} + Cp_{H2O_1}\right) \\ Cp_{H2O_1} \\ Cp_{H2O_2} \end{bmatrix} = \begin{pmatrix} 0.998 \\ 1.001 \\ 1.015 \end{pmatrix} \cdot \frac{BTU}{lb\cdot R}$$

$$k := \begin{bmatrix} 0.5\cdot\left(k_{H2O_0} + k_{H2O_1}\right) \\ k_{H2O_1} \\ k_{H2O_2} \end{bmatrix} = \begin{pmatrix} 0.031 \\ 0.032 \\ 0.033 \end{pmatrix} \cdot \frac{BTU}{hr\cdot in\cdot R}$$

$$\mu := \begin{bmatrix} 0.5\cdot\left(\mu_{H2O_0} + \mu_{H2O_1}\right) \\ \mu_{H2O_1} \\ \mu_{H2O_2} \end{bmatrix} = \begin{pmatrix} 0.124 \\ 0.075 \\ 0.044 \end{pmatrix} \cdot \frac{lb}{hr\cdot in}$$

$$Pr := \begin{bmatrix} 0.5\cdot\left(Pr_{H2O_0} + Pr_{H2O_1}\right) \\ Pr_{H2O_1} \\ Pr_{H2O_2} \end{bmatrix} = \begin{pmatrix} 4.06 \\ 2.32 \\ 1.34 \end{pmatrix}$$

Hydrodynamics in the annulus between capsule and chopped dummy in-pile tube

$D_{o\_c} := 2.505in$ Outside diameter of capsule, DWG-630434

$D_{i\_d} := 2.625in$ Inside diameter of dummy in-pile tube (DWG-443027, sheet 3, OD is 2.875"). However, according to the material spec, it is 2.624". The 2.625" will not be changed in the analysis.

$D_{hy} := D_{i\_d} - D_{o\_c} = 0.12\cdot in$ Hydraulic diameter of annulus

$A_f := 0.25\pi\cdot\left(D_{o\_c} + D_{i\_d}\right)\cdot D_{hy} = 0.48349\cdot in^2$ Flow area of annulus

$L_f := 145in$ Length of annulus(elevations on DWG-604554, sheet 4 and DWG-443027, sheet 1). This length is from ECAR-2494

$V_f := 214.097\,\frac{in}{s}$ Initially assumed flow velocity

$$Re := \frac{\left(\rho_0\cdot D_{hy}\cdot V_f\right)}{\mu_0} = 26508$$

$\varepsilon := 250\cdot 10^{-6}in$ Wall roughness (Perry's Handbook, Table 6-1)

$$f := \left[-4\cdot\log\left[\frac{0.27\cdot\varepsilon}{D_{hy}} + \left(\frac{7}{Re}\right)^{0.9}\right]\right]^{-2} = 0.00726$$

Turbulent Fanning friction factor for rough tubes (Perry's Handbook, Eq. 6-39)

$K_c := 0.5$ Maximum loss coefficient for sudde contraction (Perry's Handbook, Eq. 6-91)

$K_e := 1.0$ Maximum loss coefficient for sudde enlargement (Perry's Handbook, Eq. 6-95)

$K_f := \frac{4 \cdot f \cdot L_f}{D_{hy}} = 35.09459$ Loss coefficient for pipe friction (Perry's Handbook, Eq. 6-32)

Bernoulli equation (Perry's Handbook, Eq. 6-90)

$V_f := \sqrt{\frac{2 \cdot \Delta p}{\rho_0 \cdot (K_c + K_e + K_f)}} = 214.09672 \cdot \frac{in}{s}$ Checks

$Q_f := V_f \cdot A_f = 26.88672 \cdot \frac{gal}{min}$

$m_f := \rho_0 \cdot V_f = 27320 \cdot \frac{lb}{in^2 \cdot hr}$ This is the mass flux to the Abaqus model

Heat transfer coefficient for turbulent forced convection in an annulus

Colburn correlation (Perry's Handbook, Eq. 5-50c, using film temperature method to account for fluid property variation)

$Re_f := \frac{\rho \cdot D_{hy} \cdot V_f}{\mu} = \begin{pmatrix} 26508 \\ 43256 \\ 70688 \end{pmatrix}$

Nusselt number (applies to both surface of annulus)

$ii := 0 .. 2$

$Nu_{ii} := 0.023 \cdot (Re_{f_{ii}})^{0.8} \cdot (Pr_{ii})^{0.33}$

$Nu = \begin{pmatrix} 126.25397 \\ 155.30261 \\ 191.93246 \end{pmatrix}$

$h_{ii} := \frac{Nu_{ii} \cdot k_{ii}}{D_{hy}}$

$h = \begin{pmatrix} 32.55 \\ 41.69 \\ 53.06 \end{pmatrix} \cdot \frac{BTU}{hr \cdot in^2 \cdot R}$ $T_{film} = \begin{pmatrix} 125 \\ 170 \\ 260 \end{pmatrix} \cdot °F$

Heat transfer coefficient to Abaqus. This coefficient is not applied on the convective boundary, which requires wall temperaure, but on the contact that needs film temperature.

A5: Nuclear heating rates

Average heating rate at east lobe power over the 8 irradiation cycles is 20.8 MW from ECAR-5345.
A cosine function is used to represent the axial heating profile. In some cases, the heating rates are averaged over azimuthal segments.

Note:The regressed cosine distributions are different from component to component. In the Abaqus model, an unsymmetric distribution derived from previous AGC series experiment will be used. Thus the amplitude of each component is applied as the heat load in the model but the distributions will not be used.

Heating rates of stainless steel capsule/pressure boundary (Table 9 in ECAR-5345)

x (in)	$q_{capsule}$ (W/gm)
−24	1.976666667
−23	2.34
−22	2.733333333
−21	3.101666667
−20	3.461666667
−19	3.823333333
−18	4.203333333
−17	4.561666667
−16	4.896666667
−15	5.185
−14	5.485
−13	5.746666667
−12	6.016666667
−11	6.256666667
−10	6.456666667
−9	6.656666667
−8	6.801666667
−7	6.951666667
−6	7.076666667
−5	7.186666667
−4	7.263333333
−3	7.306666667
−2	7.36
−1	7.386666667
0	7.365
1	7.341666667
2	7.308333333
3	7.233333333

4	7.146666667
5	7.006666667
6	6.89
7	6.721666667
8	6.541666667
9	6.346666667
10	6.131666667
11	5.876666667
12	5.605
13	5.306666667
14	4.99
15	4.668333333
16	4.34
17	3.983333333
18	3.585
19	3.151666667
20	2.731666667
21	2.301666667
22	1.821666667
23	1.423333333
24	1.123333333

$f(x,a,b,c) := a\cdot\cos[b\cdot(x + c)]$

Axial heating profile

$$g_s := \begin{pmatrix} 10 \\ 0.05 \\ 1 \end{pmatrix}$$

Initial guess of regression coefficients

$$s_f := \text{genfit}\left(\frac{x}{in}, \frac{q_{capsule}}{\frac{W}{gm}}, g_s, f\right)$$

Calculate regression coefficiets for heating profile

$$s_f = \begin{pmatrix} 7.43117 \\ 0.05679 \\ 0.91192 \end{pmatrix}$$

$$P_{SST} := \rho_{SST}\cdot s_{f_0}\cdot\frac{W}{gm} = 3335\cdot\frac{BTU}{hr\cdot in^3}$$

Peak heating rate of Capsule to Abaqus (Gas line uses this value also in ECAR-2494)

$$F_f(x) := f\left(x, s_{f_0}, s_{f_1}, s_{f_2}\right)$$

Plot comparing calculated heating data to heating data fitted to a cosine function

$$z := \frac{x}{in}$$

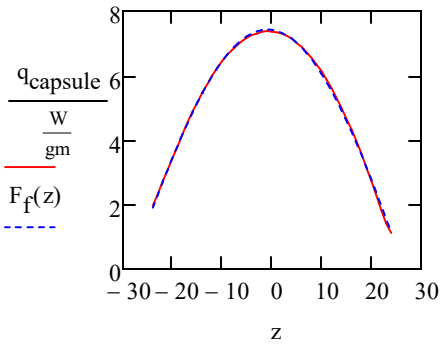

Heating rates of Haynes 230 heat shield (Table 10 in ECAR-5345)

x (in)	q_{shield} ($\frac{W}{gm}$)
–24	2.976666667
–23	3.768333333
–22	4.42
–21	5.028333333
–20	5.628333333
–19	6.213333333
–18	6.775
–17	7.363333333
–16	7.851666667
–15	8.333333333
–14	8.82
–13	9.258333333
–12	9.605
–11	9.983333333
–10	10.32
–9	10.59
–8	10.75166667
–7	11.005
–6	11.19333333
–5	11.38
–4	11.44333333
–3	11.49333333
–2	11.60333333
–1	11.59166667
0	11.53833333
1	11.50333333
2	11.42166667
3	11.30333333
4	11.13833333
5	10.93833333
6	10.69666667
7	10.46
8	10.12666667
9	9.811666667
10	9.411666667
11	9.073333333
12	8.591666667
13	8.091666667
14	7.628333333
15	7.126666667

15	7.126666667
16	6.505
17	6.001666667
18	5.316666667
19	4.576666667
20	3.938333333
21	3.191666667
22	2.483333333
23	1.9
24	1.483333333

Repeat the regression process

$$f(x,a,b,c) := a\cdot\cos[b\cdot(x+c)]$$

$$g_s := \begin{pmatrix} 10 \\ 0.05 \\ 1 \end{pmatrix}$$

$$s_f := \text{genfit}\left(\frac{x}{in}, \frac{q_{shield}}{\frac{W}{gm}}, g_s, f\right)$$

$$s_f = \begin{pmatrix} 11.69611 \\ 0.05726 \\ 1.29859 \end{pmatrix}$$

$$P_{shield} := \rho_H \cdot s_{f_0} \cdot \frac{W}{gm} = 5755 \cdot \frac{BTU}{hr\cdot in^3}$$

Peak heating rate of Heat Shield to Abaqus

$$F_f(x) := f\left(x, s_{f_0}, s_{f_1}, s_{f_2}\right)$$

Plot comparing calculated heating data to heating data fitted to a cosine function

$z := \frac{x}{in}$

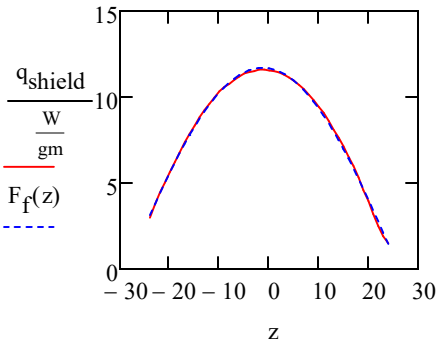

Heat rates of graphite holder (Table 11 in ECAR-5345)

–24	1.598333333
–23	1.975
–22	2.265
–21	2.576666667
–20	2.871666667
–19	3.185
–18	3.495
–17	3.79
–16	4.066666667
–15	4.315
–14	4.55
–13	4.77
–12	4.985
–11	5.18
–10	5.348333333
–9	5.515
–8	5.653333333
–7	5.763333333
–6	5.86
–5	5.936666667
–4	6.013333333
–3	6.06
–2	6.101666667
–1	6.11

$$x := \begin{pmatrix} 0 \\ 1 \\ 2 \\ 3 \\ 4 \\ 5 \\ 6 \\ 7 \\ 8 \\ 9 \\ 10 \\ 11 \\ 12 \\ 13 \\ 14 \\ 15 \\ 16 \\ 17 \\ 18 \\ 19 \\ 20 \\ 21 \\ 22 \\ 23 \\ 24 \end{pmatrix} \text{in} \qquad q_{holder} := \begin{pmatrix} 6.111666667 \\ 6.081666667 \\ 6.056666667 \\ 5.995 \\ 5.933333333 \\ 5.845 \\ 5.736666667 \\ 5.598333333 \\ 5.441666667 \\ 5.28 \\ 5.108333333 \\ 4.893333333 \\ 4.676666667 \\ 4.433333333 \\ 4.183333333 \\ 3.916666667 \\ 3.633333333 \\ 3.346666667 \\ 3.028333333 \\ 2.681666667 \\ 2.345 \\ 2.066666667 \\ 1.731666667 \\ 1.413333333 \\ 1.136666667 \end{pmatrix} \frac{W}{gm}$$

$$f(x, a, b, c) := a \cdot \cos[b \cdot (x + c)]$$

$$g_s := \begin{pmatrix} 10 \\ 0.05 \\ 1 \end{pmatrix}$$

$$s_c := \text{genfit}\left(\frac{x}{in}, \frac{q_{holder}}{\frac{W}{gm}}, g_s, f\right)$$

$$s_f = \begin{pmatrix} 6.14982 \\ 0.05617 \\ 0.77001 \end{pmatrix}$$

$P_{holder} := \rho_g \cdot s_{f_0} \cdot \frac{W}{gm} = 627 \cdot \frac{BTU}{hr \cdot in^3}$ Peak heating rate of Holder to Abaqus

$F_f(x) := f\left(x, s_{f_0}, s_{f_1}, s_{f_2}\right)$

Plot comparing calculated heating data to heating data fitted to a cosine function

$z := \frac{x}{in}$

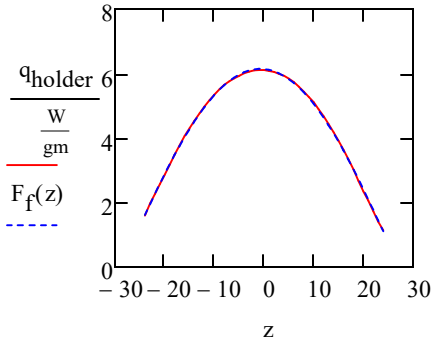

Heating rates of graphite samples are considered separately for each channel. In addition, the experiment was rotated 180º after 4 cycles. Thus 1<->4; 2<->5; and 3<->6

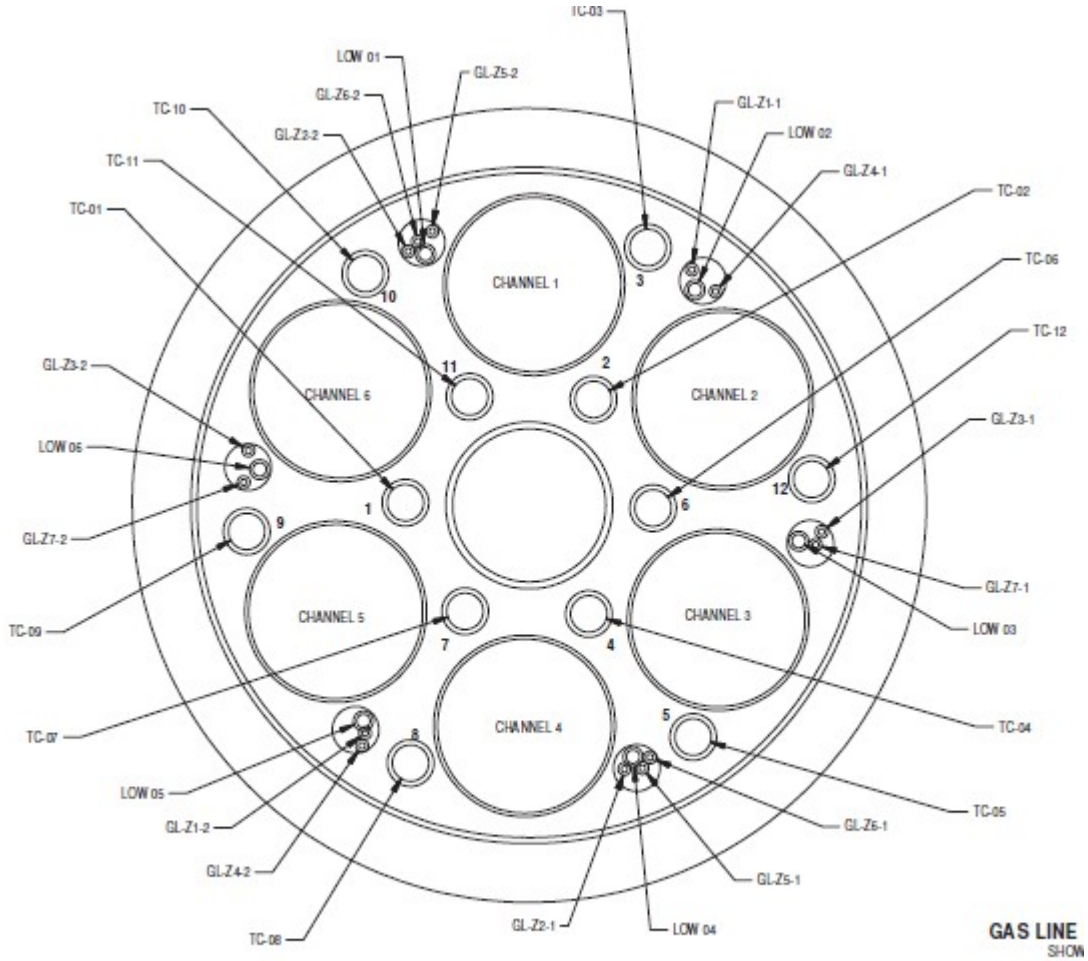

THERMOCOUPLE AND GAS LINE LOADING DIAGRAM
(LOOKING FROM TOP DOWN)
SHOWN FOR CLARITY
SCALE: 4/1

GAS LINE
SHOW

GAS LINE	
UPPER CYLINDER 01-1	
UPPER CYLINDER 02-1	
UPPER CYLINDER 03-1	

x (in)	q_{center} (W/gm)	q_{c1} (W/gm)	q_{c2} (W/gm)
–23	2.14	2.33	2.23
–22	2.44	2.66	2.55
–21	2.74	3.01	2.88
–20	3.02	3.32	3.18
–19	3.34	3.68	3.51
–18	3.65	3.98	3.82
–17	3.95	4.32	4.1
–16	4.18	4.57	4.4
–15	4.44	4.85	4.63
–14	4.65	5.08	4.87
–13	4.88	5.32	5.06
–12	5.07	5.54	5.29
–11	5.23	5.74	5.45
–10	5.4	5.89	5.64
–9	5.54	6.05	5.76
–8	5.62	6.2	5.86
–7	5.77	6.3	5.98
–6	5.85	6.39	6.08
–5	5.91	6.45	6.15
–4	6.01	6.56	6.21
–3	6.03	6.54	6.25
–2	6.04	6.6	6.29
–1	6.03	6.59	6.31
0	6.02	6.57	6.32
1	6.04	6.59	6.23
2	6	6.55	6.25
3	5.94	6.53	6.19
4	5.88	6.42	6.09
5	5.77	6.32	6.01
6	5.66	6.18	5.91
7	5.55	6.05	5.78
8	5.38	5.91	5.65
9	5.23	5.74	5.52
10	5.09	5.57	5.31
11	4.87	5.35	5.1
12	4.66	5.1	4.84
13	4.4	4.84	4.63
14	4.18	4.58	4.34
15	3.93	4.29	4.12
16	3.64	4	3.82

16	3.64	4	3.82
17	3.34	3.67	3.5
18	3.03	3.33	3.17
19	2.76	2.99	2.79
20	2.25	2.61	2.46
21	2.08	2.26	2.14
22	1.72	1.85	1.79
23	1.42	1.5	1.43

$q_{c3} :=$	$q_{c4} :=$	$q_{c5} :=$	$q_{c6} :=$
2.04	1.93	2.07	2.26
2.34	2.24	2.36	2.61
2.64	2.52	2.69	2.93
2.91	2.8	2.97	3.22
3.21	3.09	3.27	3.58
3.48	3.34	3.6	3.89
3.79	3.62	3.88	4.19
4.03	3.84	4.12	4.49
4.23	4.08	4.36	4.77
4.47	4.28	4.6	4.99
4.66	4.5	4.82	5.23
4.84	4.67	5.01	5.47
5	4.84	5.21	5.66
5.17	4.97	5.36	5.83
5.29	5.09	5.49	5.99
5.39	5.21	5.64	6.1
5.49	5.33	5.71	6.25
5.61	5.38	5.81	6.35
5.62	5.47	5.9	6.41
5.71	5.51	5.95	6.5
5.77	5.57	6.02	6.51
5.79	5.59	6.03	6.55
5.8	5.58	6.04	6.56
5.78	5.59	6.02	6.54
5.75	5.54	5.95	6.56
5.71	5.53	5.94	6.49
5.66	5.49	5.9	6.48
5.6	5.41	5.84	6.34
5.52	5.33	5.74	6.24

$\frac{W}{gm}$ $\frac{W}{gm}$ $\frac{W}{gm}$ $\frac{W}{gm}$

5.39	5.22	5.65	6.11
5.32	5.13	5.51	6
5.19	4.96	5.35	5.82
5.02	4.82	5.19	5.67
4.89	4.67	5.02	5.44
4.66	4.47	4.79	5.24
4.48	4.28	4.59	5.02
4.23	4.02	4.36	4.75
4.01	3.81	4.13	4.48
3.78	3.59	3.86	4.21
3.5	3.32	3.57	3.93
3.21	3.05	3.28	3.56
2.9	2.78	2.96	3.24
2.54	2.4	2.57	2.86
2.21	2.13	2.32	2.55
1.98	1.91	2.01	2.2
1.67	1.6	1.68	1.81
1.36	1.31	1.36	1.47

$$f(x,a,b,c) := a\cdot\cos[b\cdot(x + c)]$$

$$g_s := \begin{pmatrix} 10 \\ 0.05 \\ 1 \end{pmatrix}$$

For the center channel specimens

$$s_f := \text{genfit}\left(\frac{x}{in}, \frac{q_{center}}{\frac{W}{gm}}, g_s, f\right)$$

$$s_f = \begin{pmatrix} 6.11182 \\ 0.05523 \\ 1.05774 \end{pmatrix}$$

$$P_{center} := \rho_g \cdot s_{f_0} \cdot \frac{W}{gm} = 623 \cdot \frac{BTU}{hr \cdot in^3}$$

$$F_f(x) := f\left(x, s_{f_0}, s_{f_1}, s_{f_2}\right)$$

Plot comparing calculated heating data to heating data fitted to a cosine function

$$z := \frac{x}{in}$$

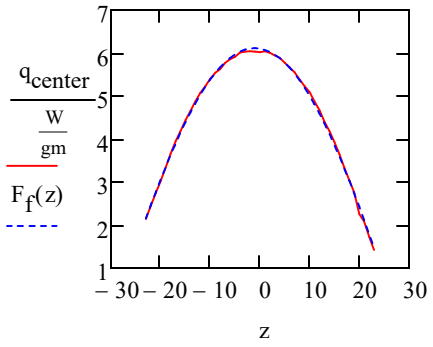

For the channel1 specimens

$$s_f := genfit\left(\frac{x}{in}, \frac{q_{c1}}{\frac{W}{gm}}, g_s, f\right)$$

$$s_f = \begin{pmatrix} 6.68218 \\ 0.05518 \\ 1.04407 \end{pmatrix}$$

$$P_{c1} := \rho_g \cdot s_{f_0} \cdot \frac{W}{gm} = 681 \cdot \frac{BTU}{hr \cdot in^3}$$

$$F_f(x) := f\left(x, s_{f_0}, s_{f_1}, s_{f_2}\right)$$

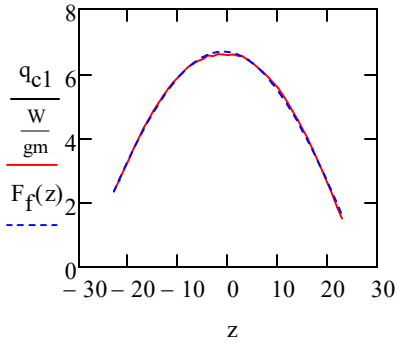

For the channel2 specimens

$$s_f := \text{genfit}\left(\frac{x}{in}, \frac{q_{c2}}{\frac{W}{gm}}, g_s, f\right)$$

$$s_f = \begin{pmatrix} 6.36718 \\ 0.05514 \\ 1.0619 \end{pmatrix}$$

$$P_{c2} := \rho_g \cdot s_{f_0} \cdot \frac{W}{gm} = 649 \cdot \frac{BTU}{hr \cdot in^3}$$

$$F_f(x) := f\left(x, s_{f_0}, s_{f_1}, s_{f_2}\right)$$

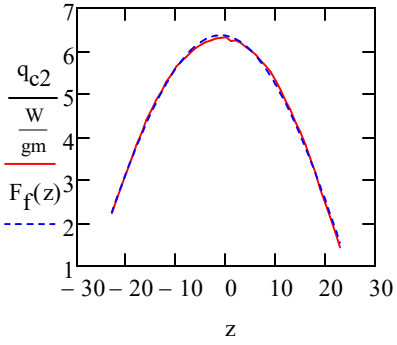

For the channel3 specimens

$$s_f := \text{genfit}\left(\frac{x}{in}, \frac{q_{c3}}{\frac{W}{gm}}, g_s, f\right)$$

$$s_f = \begin{pmatrix} 5.84389 \\ 0.05515 \\ 1.05506 \end{pmatrix}$$

$$P_{c3} := \rho_g \cdot s_{f_0} \cdot \frac{W}{gm} = 595 \cdot \frac{BTU}{hr \cdot in^3}$$

$$F_f(x) := f\left(x, s_{f_0}, s_{f_1}, s_{f_2}\right)$$

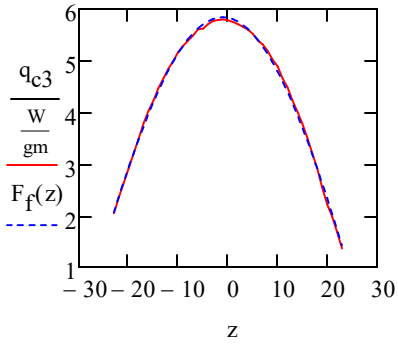

For the channel4 specimens

$$s_f := \text{genfit}\left(\frac{x}{in}, \frac{q_{c4}}{\frac{W}{gm}}, g_s, f\right)$$

$$s_f = \begin{pmatrix} 5.63655 \\ 0.05541 \\ 1.07785 \end{pmatrix}$$

$$P_{c4} := \rho_g \cdot s_{f_0} \cdot \frac{W}{gm} = 574 \cdot \frac{BTU}{hr \cdot in^3}$$

$$F_f(x) := f\left(x, s_{f_0}, s_{f_1}, s_{f_2}\right)$$

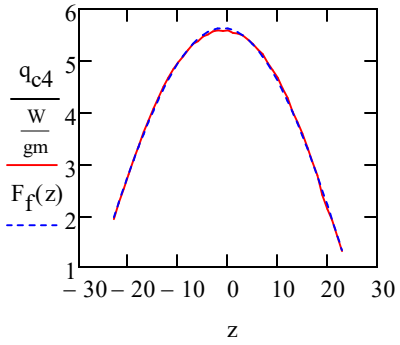

For the channel5 specimens

$$s_f := \text{genfit}\left(\frac{x}{in}, \frac{q_{c5}}{\frac{W}{gm}}, g_s, f\right)$$

$$s_f = \begin{pmatrix} 6.07829 \\ 0.05568 \\ 1.05501 \end{pmatrix}$$

$$P_{c5} := \rho_g \cdot s_{f_0} \cdot \frac{W}{gm} = 619 \cdot \frac{BTU}{hr \cdot in^3}$$

$$F_f(x) := f\left(x, s_{f_0}, s_{f_1}, s_{f_2}\right)$$

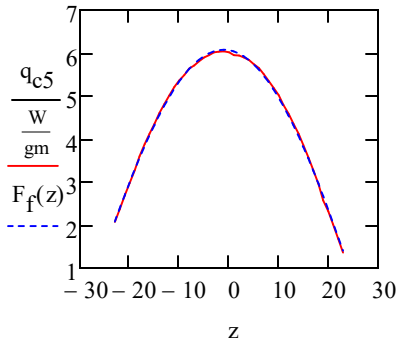

For the channel6 specimens

$$s_f := \text{genfit}\left(\frac{x}{in}, \frac{q_{c6}}{\frac{W}{gm}}, g_s, f\right)$$

$$s_f = \begin{pmatrix} 6.61886 \\ 0.05564 \\ 1.03925 \end{pmatrix}$$

$$P_{c6} := \rho_g \cdot s_{f_0} \cdot \frac{W}{gm} = 674 \cdot \frac{BTU}{hr \cdot in^3}$$

$$F_f(x) := f\left(x, s_{f_0}, s_{f_1}, s_{f_2}\right)$$

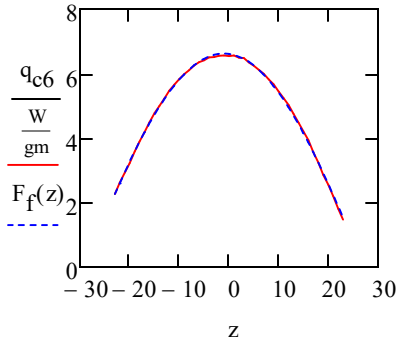

In summary, for the first 4 cycles, from 157D, 158A, 162A, to 162B, the heat rates are:

$$P_{center} = 623 \cdot \frac{BTU}{hr \cdot in^3} \quad P_{c1} = 681 \cdot \frac{BTU}{hr \cdot in^3} \quad P_{c2} = 649 \cdot \frac{BTU}{hr \cdot in^3} \quad P_{c3} = 595 \cdot \frac{BTU}{hr \cdot in^3}$$

$$P_{c4} = 574 \cdot \frac{BTU}{hr \cdot in^3} \quad P_{c5} = 619 \cdot \frac{BTU}{hr \cdot in^3} \quad P_{c6} = 674 \cdot \frac{BTU}{hr \cdot in^3}$$

In the second 4 cycles, from 164A, 164B, 166A, and 166B, the heat rates are:

$$P_{center} = 623 \cdot \frac{BTU}{hr \cdot in^3} \quad P_{nc1} := P_{c4} = 574 \cdot \frac{BTU}{hr \cdot in^3} \quad P_{nc2} := P_{c5} = 619 \cdot \frac{BTU}{hr \cdot in^3} \quad P_{nc3} := P_{c6} = 674 \cdot \frac{BTU}{hr \cdot in^3}$$

$$P_{nc4} := P_{c1} = 681 \cdot \frac{BTU}{hr \cdot in^3} \quad P_{nc5} := P_{c2} = 649 \cdot \frac{BTU}{hr \cdot in^3} \quad P_{nc6} := P_{c3} = 595 \cdot \frac{BTU}{hr \cdot in^3}$$

Heating rates of coolant (Table 14 in ECAR-5345)

−24	3.27
−23	3.41
−22	4.32
−21	5.09
−20	5.82
−19	6.53
−18	7.23
−17	7.96
−16	8.66
−15	9.3
−14	9.87
−13	10.38
−12	10.86
−11	11.38
−10	11.84
−9	12.24
−8	12.55
−7	12.87
−6	13.11
−5	13.33
−4	13.51
−3	13.68

$$x := \begin{pmatrix} -3 \\ -2 \\ -1 \\ 0 \\ 1 \\ 2 \\ 3 \\ 4 \\ 5 \\ 6 \\ 7 \\ 8 \\ 9 \\ 10 \\ 11 \\ 12 \\ 13 \\ 14 \\ 15 \\ 16 \\ 17 \\ 18 \\ 19 \\ 20 \\ 21 \\ 22 \\ 23 \\ 24 \end{pmatrix} \text{in} \qquad q_{coolant} := \begin{pmatrix} 13.68 \\ 13.77 \\ 13.87 \\ 13.89 \\ 13.89 \\ 13.86 \\ 13.77 \\ 13.67 \\ 13.54 \\ 13.32 \\ 13.03 \\ 12.74 \\ 12.41 \\ 12.07 \\ 11.66 \\ 11.2 \\ 10.64 \\ 10.1 \\ 9.52 \\ 8.95 \\ 8.33 \\ 7.66 \\ 6.91 \\ 6.1 \\ 5.36 \\ 4.67 \\ 3.94 \\ 3.19 \end{pmatrix} \frac{W}{gm}$$

$$f(x,a,b,c) := a \cdot \cos[b \cdot (x + c)]$$

$$g_s := \begin{pmatrix} 10 \\ 0.05 \\ 1 \end{pmatrix}$$

For the coolant

$$s_f := \text{genfit}\left(\frac{x}{in}, \frac{q_{coolant}}{\frac{W}{gm}}, g_s, f\right)$$

$$s_f = \begin{pmatrix} 14.0123 \\ 0.05621 \\ -0.23458 \end{pmatrix}$$

$$P_{coolant} := \rho_{0.} \cdot s_{f_0} \cdot \frac{W}{gm} = 769 \cdot \frac{BTU}{hr \cdot in^3}$$

Peak heating rate of Coolant to Abaqus

$$F_f(x) := f\left(x, s_{f_0}, s_{f_1}, s_{f_2}\right)$$

Plot comparing calculated heating data to heating data fitted to a cosine function

$$z := \frac{x}{in}$$

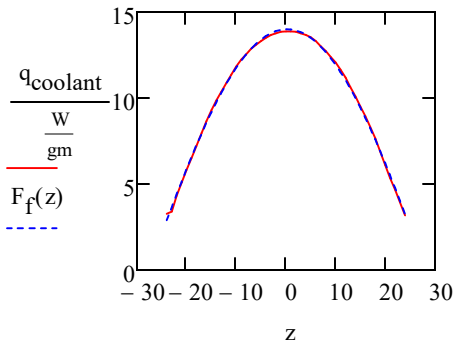

Heating rates of Thermocouple (TC) (Table 12 and 13 in ECAR-5345)

Density of the TC (composite material consisting of inconel sheath, MgO insulation, and wires) needs to be calculated. Technical specifications for mineral insulated cable are found on item 64 of DWG-604554.

12	.125-NS-1600-H-UNG	THERMOCOUPLE, TYPE N, Ø1/8 OD X 21 FT LG INCONEL SHEATH	IDAHO LABS	64

$$D_{o\_tc} := 0.125in$$

Outside diameter o thermocouple sheath

$D_{i\_tc} := 0.093in$ Inside diameter of thermocouple sheath

$A_{sheath} := 0.25\pi\cdot\left(D_{o\_tc}^{2} - D_{i\_tc}^{2}\right) = 0.0055\cdot in^{2}$ Cross sectional area of sheath

$D_{wire} := 0.025in$ Diameter of thermocouple wire

$A_{wire} := 2\cdot\pi\cdot\frac{D_{wire}^{2}}{4}$ Cross sectional area of 2 wires

$D_{i\_ins} := \sqrt{4\cdot\frac{A_{wire}}{\pi}} = 0.03536\cdot in$ Equivalent inside diameter of insulation or the equivalent diameter of the two wires

$A_{ins} := 0.25\pi\cdot\left(D_{i\_tc}^{2} - D_{i\_ins}^{2}\right) = 0.0058\cdot in^{2}$ Cross sectional area of insulation. The insulation is between the wires and sheath

$\rho_{metal} := 8.4\frac{gm}{cm^{3}}$ Density of Inconel 600 sheath and type N TC wires (ASM Metals Handbook Vol. 1 Wrough Nickel Alloys)

$\rho_{MgO} := 3.65\frac{gm}{cm^{3}}$ Density of Inconel MgO insulation (Perry's Handbook, 7th edition, Table 2-382)

$\rho_{tc} := \frac{\rho_{metal}\cdot\left(A_{sheath} + A_{wire}\right) + \rho_{MgO}\cdot A_{ins}}{A_{sheath} + A_{wire} + A_{ins}} = 6.1507\cdot\frac{gm}{cm^{3}}$ Density of themocouple

TCs 10 and 11 are the longest that reaches to -18" with respect to the core centerline. TCs 9 and 12 reach -11.25", TCs 7 and 8 reach -6", TC 6 reaches 2", TCs 4 and 5 reach 6", TCs 2 and 3 reach 13", and TC 1 reaches 18" with respect to core centerline. (DWG-604554)

Heat rates of TCs 10 and 11 are averaged from -18" to the top of the top of the core.

$$x := \begin{pmatrix} -18 \\ -17 \\ -16 \\ -15 \\ -14 \\ -13 \\ -12 \\ -11 \\ -10 \\ -9 \\ -8 \\ -7 \\ -6 \\ -5 \\ -4 \\ -3 \\ -2 \\ -1 \\ 0 \\ 1 \\ 2 \\ 3 \\ 4 \\ 5 \\ 6 \\ 7 \\ 8 \\ 9 \\ 10 \\ 11 \\ 12 \\ 13 \\ 14 \\ 15 \\ 16 \\ 17 \\ 18 \end{pmatrix} \text{in} \qquad q_{TC} := \begin{pmatrix} 4.43 \\ 4.84 \\ 5.195 \\ 5.49 \\ 5.795 \\ 6.06 \\ 6.4 \\ 6.625 \\ 6.825 \\ 7.07 \\ 7.215 \\ 7.405 \\ 7.485 \\ 7.66 \\ 7.69 \\ 7.79 \\ 7.815 \\ 7.755 \\ 7.8 \\ 7.725 \\ 7.75 \\ 7.67 \\ 7.525 \\ 8.665 \\ 8.47 \\ 8.32 \\ 8.055 \\ 7.81 \\ 7.51 \\ 7.145 \\ 6.895 \\ 6.545 \\ 6.12 \\ 5.71 \\ 5.34 \\ 4.89 \\ 4.345 \end{pmatrix} \frac{W}{gm}$$

$$\begin{pmatrix} 19 \\ 20 \\ 21 \\ 22 \\ 23 \\ 24 \end{pmatrix} \qquad \begin{pmatrix} 3.71 \\ 3.25 \\ 2.725 \\ 2.19 \\ 1.725 \\ 1.35 \end{pmatrix}$$

$$f(x, a, b, c) := a \cdot \cos[b \cdot (x + c)]$$

$$g_s := \begin{pmatrix} 10 \\ 0.05 \\ 1 \end{pmatrix}$$

$$s_f := \text{genfit}\left(\frac{x}{in}, \frac{q_{TC}}{\frac{W}{gm}}, g_s, f\right)$$

$$s_f = \begin{pmatrix} 8.27585 \\ 0.05739 \\ -0.2754 \end{pmatrix}$$

$$P_{TC} := \rho_{tc} \cdot s_{f_0} \cdot \frac{W}{gm} = 2846 \cdot \frac{BTU}{hr \cdot in^3}$$ TC amplitude

$$F_f(x) := f\left(x, s_{f_0}, s_{f_1}, s_{f_2}\right)$$

Plot comparing calculated heating data to heating data fitted to a cosine function

$$z := \frac{x}{in}$$

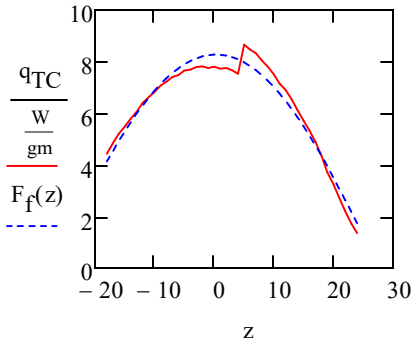

The shortest TC is at 18" above the core centerline. At this location we can compare each individual TC with the average heat rate in the regression. The ratio will be applied to the TC amplitude calculated above for the individual TC heat rate.

$x_{36} = 18 \cdot in$ index "36" in the location vector is 18"

$q_{ref} := q_{TC_{36}} = 4.345 \cdot \frac{W}{gm}$ This is the reference heat rate

Get the TC heat rate at 18" from Table 12 and 13 in ECAR-5345

$$\gamma_{TC01} := \frac{\left(4.21 \frac{W}{gm}\right)}{q_{ref}} = 0.96893 \qquad \gamma_{TC02} := \frac{\left(4.2 \frac{W}{gm}\right)}{q_{ref}} = 0.96663 \qquad \gamma_{TC03} := \frac{\left(4.39 \frac{W}{gm}\right)}{q_{ref}} = 1.01036$$

$$\gamma_{TC04} := \frac{\left(2.89 \frac{W}{gm}\right)}{q_{ref}} = 0.66513 \qquad \gamma_{TC05} := \frac{\left(3.8 \frac{W}{gm}\right)}{q_{ref}} = 0.87457 \qquad \gamma_{TC06} := \frac{\left(4.11 \frac{W}{gm}\right)}{q_{ref}} = 0.94591$$

$$\gamma_{TC07} := \frac{\left(3.98 \frac{W}{gm}\right)}{q_{ref}} = 0.916 \qquad \gamma_{TC08} := \frac{\left(3.82 \frac{W}{gm}\right)}{q_{ref}} = 0.87917 \qquad \gamma_{TC09} := \frac{\left(4.12 \frac{W}{gm}\right)}{q_{ref}} = 0.94822$$

$$\gamma_{TC10} := \frac{\left(4.41 \frac{W}{gm}\right)}{q_{ref}} = 1.01496 \qquad \gamma_{TC11} := \frac{\left(4.28 \frac{W}{gm}\right)}{q_{ref}} = 0.98504 \qquad \gamma_{TC12} := \frac{\left(4.1 \frac{W}{gm}\right)}{q_{ref}} = 0.94361$$

For the first 4 cycles, the peak heating rate of each TC

$$P_{TC01} := \gamma_{TC01} \cdot P_{TC} = 2758 \cdot \frac{BTU}{hr \cdot in^3}$$

$$P_{TC02} := \gamma_{TC02} \cdot P_{TC} = 2751 \cdot \frac{BTU}{hr \cdot in^3}$$

$$P_{TC03} := \gamma_{TC03} \cdot P_{TC} = 2876 \cdot \frac{BTU}{hr \cdot in^3}$$

$$P_{TC04} := \gamma_{TC04} \cdot P_{TC} = 1893 \cdot \frac{BTU}{hr \cdot in^3}$$

$$P_{TC05} := \gamma_{TC05} \cdot P_{TC} = 2489 \cdot \frac{BTU}{hr \cdot in^3}$$

$$P_{TC06} := \gamma_{TC06} \cdot P_{TC} = 2692 \cdot \frac{BTU}{hr \cdot in^3}$$

$$P_{TC07} := \gamma_{TC07} \cdot P_{TC} = 2607 \cdot \frac{BTU}{hr \cdot in^3}$$

$$P_{TC08} := \gamma_{TC08} \cdot P_{TC} = 2502 \cdot \frac{BTU}{hr \cdot in^3}$$

$$P_{TC09} := \gamma_{TC09} \cdot P_{TC} = 2699 \cdot \frac{BTU}{hr \cdot in^3}$$

$$P_{TC10} := \gamma_{TC10} \cdot P_{TC} = 2889 \cdot \frac{BTU}{hr \cdot in^3}$$

$$P_{TC11} := \gamma_{TC11} \cdot P_{TC} = 2804 \cdot \frac{BTU}{hr \cdot in^3}$$

$$P_{TC12} := \gamma_{TC12} \cdot P_{TC} = 2686 \cdot \frac{BTU}{hr \cdot in^3}$$

After the test train is rotated by 180º, the thermocouples are switched. TC1<->TC6; TC2<->TC7; TC3<->TC8; TC4<->TC11; TC5<->TC10; and TC9<->TC12

Peak heat rate for the second 4 cycles

$$q_{TC01} := \gamma_{TC06} \cdot P_{TC} = 2692 \cdot \frac{BTU}{hr \cdot in^3}$$

$$q_{TC02} := \gamma_{TC07} \cdot P_{TC} = 2607 \cdot \frac{BTU}{hr \cdot in^3}$$

$$q_{TC03} := \gamma_{TC08} \cdot P_{TC} = 2502 \cdot \frac{BTU}{hr \cdot in^3}$$

$$q_{TC04} := \gamma_{TC11} \cdot P_{TC} = 2804 \cdot \frac{BTU}{hr \cdot in^3}$$

$$q_{TC05} := \gamma_{TC10} \cdot P_{TC} = 2889 \cdot \frac{BTU}{hr \cdot in^3}$$

$$q_{TC06} := \gamma_{TC01} \cdot P_{TC} = 2758 \cdot \frac{BTU}{hr \cdot in^3}$$

$$q_{TC07} := \gamma_{TC02} \cdot P_{TC} = 2751 \cdot \frac{BTU}{hr \cdot in^3}$$

$$q_{TC08} := \gamma_{TC03} \cdot P_{TC} = 2876 \cdot \frac{BTU}{hr \cdot in^3}$$

$$q_{TC09} := \gamma_{TC12} \cdot P_{TC} = 2686 \cdot \frac{BTU}{hr \cdot in^3}$$

$$q_{TC10} := \gamma_{TC05} \cdot P_{TC} = 2489 \cdot \frac{BTU}{hr \cdot in^3}$$

$$q_{TC11} := \gamma_{TC04} \cdot P_{TC} = 1893 \cdot \frac{BTU}{hr \cdot in^3}$$

$$q_{TC12} := \gamma_{TC09} \cdot P_{TC} = 2699 \cdot \frac{BTU}{hr \cdot in^3}$$

Adjusting heating rate profile by splitting into separate profiles below and above core mid-plane. The resulting profile will be unsymmetric. This can improve the temperature calculation in the AGC tests. See ECAR-2562 and ECAR-2322.

In the past ECARs, this distribution is used (see ECAR-2494)

$$P_{norm}(x) := \cos[0.056\cdot(x + 0.9)]$$

Integrate normalized heating profile

$$I := \int_{-27.5}^{27.5} P_{norm}(x)\,dx\cdot in = 35.65202\cdot in$$

$L := 27.5in - (-27.5in) = 55\cdot in$ Length of integral of integration

$\gamma := \frac{I}{L} = 0.64822$ Ratio of average heating to maximum heating

$P_{norm\_below}(x) := \cos[0.051\cdot(x + 0.9)]$

$P_{norm\_above}(x) := \cos[0.06\cdot(x + 0.9)]$

These two unsymmetric heating rate distributions will be used for all components whose heating rates are non-uniform axially.

$$I_{below} := \int_{-27.5}^{0} P_{norm\_below}(x)\,dx\cdot in = 20.05944\cdot in$$

$$I_{above} := \int_{0}^{27.5} P_{norm\_above}(x)\,dx\cdot in = 15.61946\cdot in$$

$I - I_{below} - I_{above} = -0\cdot in$ The symmetric and unsymmetric distributions have the same integral.

Define array of coordinate for plotting

$i := 0..24$

$\zeta_i := -24 + 2\cdot i$ $P := P_{norm}(\zeta)$

$j := 0..12$ $k := 13..24$

$P_{adj_j} := P_{norm\_below}(\zeta_j)$ $P_{adj_k} := P_{norm\_above}(\zeta_k)$

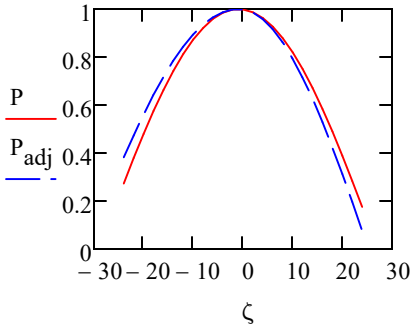

Tungsten heaters are on the top of the center specimen stack and bottom of the lower specimen stacks
Heating rates of tungsten pieces will use uniform values because they are short (Table 15 in ECAR-5345)

$q_{W\_bottom} := 3.036666667 \frac{W}{gm}$ Average over the 6 bottom heaters

$q_{W\_center\_top} := 4.23 \frac{W}{gm}$ The heater is at the top of the center specimen stack

Since unsymmetric heat distribution is used, factors will be applied to the heating rates based on the location

$x_{bottom} := -23.75$ DWG-604553, sheet 2, item 16. Bottom of the heater is 78' (-24" from core centerline) and the heater is 0.5" tall (DWG-604539)

$$\beta_{bottom} := \frac{P_{norm\_below}(x_{bottom})}{P_{norm}(x_{bottom})} = 1.37385$$

$P_{W\_bottom} := \beta_{bottom} \cdot \rho_W \cdot q_{W\_bottom} = 3966. \frac{BTU}{hr \cdot in^3}$ This is end-cap-lower in Abaqus

$x_{top} := 19.25$ DWG-604553, sheet 8, item 15. Top of the heater is 44'-24"=20" from core centerline) and the heater is 1.5" tall (DWG-604539)

$$\beta_{top} := \frac{P_{norm\_above}(x_{top})}{P_{norm}(x_{top})} = 0.82679$$

$P_{W\_top} := \beta_{top} \cdot \rho_W \cdot q_{W\_center\_top} = 3324. \frac{BTU}{hr \cdot in^3}$ This is the end-cap-center in Abaqus

A6: Source power, gas flows, and DPA

Graphite DPA as a function of irradiation time

$$t := \begin{pmatrix} 0 \\ 59.7 \\ 111.9 \\ 173.9 \\ 212.4 \\ 267.3 \\ 331.4 \\ 393.9 \\ 453.9 \end{pmatrix} \text{day}$$

Accumulative Effect Full Power Days (EFPDs) from cycle 157D to 166B, Table 1 of ECAR-5345

$$DPA := \begin{pmatrix} 0 \\ 0.590 \\ 1.439 \\ 2.304 \\ 2.698 \\ 3.223 \\ 3.853 \\ 4.673 \\ 5.549 \end{pmatrix}$$

Maximum DPA from cycle 157D to 166B. The value is averaged from the 7 stacks in Table 32 of ECAR-5345

$$t_d := \frac{t}{\text{day}}$$

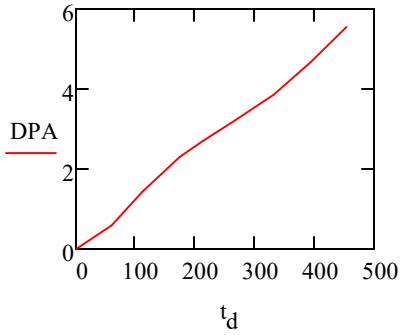

DPA at selected days during each cycle is calculated using the linear interpolation and EFPD at that day. The quantities (TC temperature, gas mixture, lobe power) at the selected days are averaged over the 24 hrs period.
Note: The unsymmetric chopped cosine function was applied to the DPA as well.
See the Excel sheets for recorded data processing

$$EFPD_{157D} := \begin{pmatrix} 19.2 \\ 38.3 \\ 59.0 \end{pmatrix} day$$

Cycle 157D, data are averaged to 6/18/2015 at 12:00; 7/7/2015 at 12:00; and 8/11/2015 at 11:00

$$DPA_{157D} := DPA_0 + \left(DPA_1 - DPA_0\right) \cdot \frac{EFPD_{157D} - t_0}{t_1 - t_0} = \begin{pmatrix} 0.19 \\ 0.38 \\ 0.58 \end{pmatrix}$$

$$EFPD_{158A} := \begin{pmatrix} 77.1 \\ 93.5 \\ 110.2 \end{pmatrix} day$$

Cycle 158A, data are averaged to 11/28/2015 at 12:00; 12/14/2015 at 20:50; and 12/31/2015 at 10:50

$$DPA_{158A} := DPA_1 + \left(DPA_2 - DPA_1\right) \cdot \frac{EFPD_{158A} - t_1}{t_2 - t_1} = \begin{pmatrix} 0.87 \\ 1.14 \\ 1.41 \end{pmatrix}$$

$$EFPD_{162A} := \begin{pmatrix} 128.2 \\ 151.9 \\ 172.9 \end{pmatrix} day$$

Cycle 162A, data are averaged to 10/22/2017 at 21:00; 11/15/2017 at 12:00; and 12/6/2017 at 12:00

$$DPA_{162A} := DPA_2 + \left(DPA_3 - DPA_2\right) \cdot \frac{EFPD_{162A} - t_2}{t_3 - t_2} = \begin{pmatrix} 1.67 \\ 2 \\ 2.29 \end{pmatrix}$$

$$EFPD_{162B} := \begin{pmatrix} 192.9 \\ 211.6 \end{pmatrix} day$$

Cycle 162B, data are averaged to 3/7/2018 at 12:00; and 3/28/2017 at 12:00

$$DPA_{162B} := DPA_3 + \left(DPA_4 - DPA_3\right)\cdot\frac{EFPD_{162B} - t_3}{t_4 - t_3} = \begin{pmatrix} 2.5 \\ 2.69 \end{pmatrix}$$

$$EFPD_{164A} := \begin{pmatrix} 230.7 \\ 249.0 \\ 266.2 \end{pmatrix} day$$

Cycle 164A, data are averaged to 7/9/2018 at 12:00; 7/27/2018 at 12:00; and 8/16/2018 at 12:00

$$DPA_{164A} := DPA_4 + \left(DPA_5 - DPA_4\right)\cdot\frac{EFPD_{164A} - t_4}{t_5 - t_4} = \begin{pmatrix} 2.87 \\ 3.05 \\ 3.21 \end{pmatrix}$$

$$EFPD_{164B} := \begin{pmatrix} 288.5 \\ 304.0 \\ 330.2 \end{pmatrix} day$$

Cycle 164B, data are averaged to 10/10/2018 at 12:00; 11/3/2018 at 12:00; and 1/16/2019 at 12:00

$$DPA_{164B} := DPA_5 + \left(DPA_6 - DPA_5\right)\cdot\frac{EFPD_{164B} - t_5}{t_6 - t_5} = \begin{pmatrix} 3.43 \\ 3.58 \\ 3.84 \end{pmatrix}$$

$$EFPD_{166A} := \begin{pmatrix} 350.4 \\ 373.9 \\ 393.0 \end{pmatrix} day$$

Cycle 166A, data are averaged to 8/13/2019 at 8:50; 9/5/2019 at 19:00; and 10/5/2019 at 12:00

$$DPA_{166A} := DPA_6 + \left(DPA_7 - DPA_6\right)\cdot\frac{EFPD_{166A} - t_6}{t_7 - t_6} = \begin{pmatrix} 4.1 \\ 4.41 \\ 4.66 \end{pmatrix}$$

$$EFPD_{166B} := \begin{pmatrix} 414.5 \\ 434.2 \\ 452.9 \end{pmatrix} day$$

Cycle 166B, data are averaged to 12/1/2019 at 12:00; 12/21/2019 at 12:00; and 1/9/2020 at 12:00

$$DPA_{166B} := DPA_7 + \left(DPA_8 - DPA_7\right)\cdot\frac{EFPD_{166B} - t_7}{t_8 - t_7} = \begin{pmatrix} 4.97 \\ 5.26 \\ 5.53 \end{pmatrix}$$

Control gas for the zones at the selected time
Zones 1 thru 5 are defined on DWG-604554. Zone 6 represents a long gap between heat shield and capsule. Zone 7 is inside the graphite holder. Gas in zone 6 was not used but the appropriate conductance was selected for better correlation.

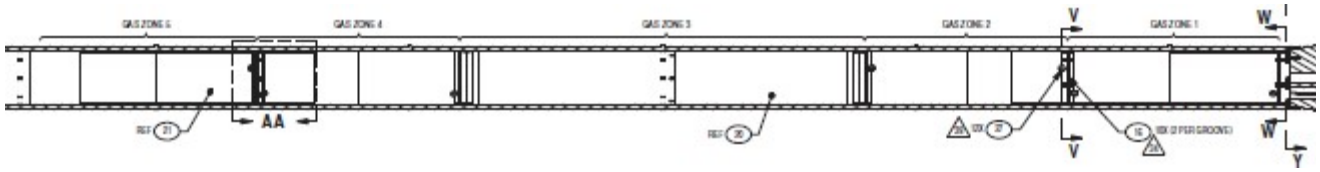

Gases in some zones were taken by averaging the adjacent zones. See the Excel file

Cycle 157D

"Ar fraction"	"Zone1"	"Zone2"	"Zone3"	"Zone4"	"Zone5"	"zone7"	"Days in cycle"	"Power"
"2015-06-18 12:00"	0.7	0.0	0.6	0.0	0.4	0.5	19.2	21.2
"2015-07-07 12:00"	0.7	0.0	0.4	0.0	0.3	0.5	38.3	21.0
"2015-08-11 11:00"	0.2	0.7	0.0	0.0	0.0	0.5	59.0	21.1

Cycle 158A

"Ar fraction"	"Zone1"	"Zone2"	"Zone3"	"Zone4"	"Zone5"	"zone7"	"Days in cycle"	"Power"
"2015-11-28 12:00"	0.8	0.2	0.0	0.0	0.3	0.3	17.4	22.5
"2015-12-14 20:50"	0.8	0.2	0.0	0.0	0.3	0.3	33.8	22.4
"2015-12-31 10:50"	0.7	0.1	0.0	0.0	0.3	0.3	50.5	22.2

Cycle 162A

"Ar fraction"	"Zone1"	"Zone2"	"Zone3"	"Zone4"	"Zone5"	"zone7"	"Days in cycle"	"Power"
"2017-10-22 21:00"	0.7	0.2	0.0	0.6	0.4	0.0	16.3	22.2
"2017-11-15 12:00"	0.8	0.2	0.0	0.3	0.4	0.0	40.0	22.2
"2017-12-06 12:00"	0.8	0.3	0.1	0.0	0.5	0.0	61.0	21.8

Cycle 162B

"Ar fraction"	"Zone1"	"Zone2"	"Zone3"	"Zone4"	"Zone5"	"zone7"	"Days in cycle"	"Power"
"2018-03-07 12:00"	0.9	0.4	0.1	0.0	0.3	0.1	19.0	19.0
"2018-03-28 12:00"	0.7	0.3	0.3	0.0	0.5	0.1	37.7	18.9

Cycle 164A

"Ar fraction"	"Zone1"	"Zone2"	"Zone3"	"Zone4"	"Zone5"	"zone7"	"Days in cycle"	"Power"
"2018-07-09 12:00"	0.6	0.0	0.1	0.0	0.3	0.1	18.3	20.6
"2018-07-27 12:00"	0.6	0.0	0.1	0.0	0.3	0.1	36.6	20.3
"2018-08-16 12:00"	0.6	0.0	0.4	0.0	0.1	0.1	53.8	20.2

Cycle 164B

"Ar fraction"	"Zone1"	"Zone2"	"Zone3"	"Zone4"	"Zone5"	"zone7"	"Days in cycle"	"Power"
"2018-10-10 12:00"	0.6	0.0	0.1	0.0	0.3	0.0	21.2	20.8
"2018-11-03 12:00"	0.6	0.0	0.7	0.0	0.5	0.0	36.7	20.2
"2019-01-16 12:00"	0.8	0.6	0.0	0.3	0.5	0.0	62.9	20.4

Cycle 166A

"Ar fraction"	"Zone1"	"Zone2"	"Zone3"	"Zone4"	"Zone5"	"zone7"	"Days in cycle"	"Power"
"2019-08-13 08:50"	0.6	0.2	0.0	0.2	0.3	0.0	19.0	21.4
"2019-09-05 19:00"	0.6	0.6	0.0	0.2	0.6	0.0	42.5	21.5
"2019-10-05 12:00"	0.5	0.6	0.2	0.0	0.3	0.0	61.6	21.2

Cycle 166B

"Ar fraction"	"Zone1"	"Zone2"	"Zone3"	"Zone4"	"Zone5"	"zone7"	"Days in cycle"	"Power"
"2019-12-01 12:00"	0.5	0.2	0.0	0.2	0.4	0.0	20.6	21.2
"2019-12-21 12:00"	0.5	0.4	0.3	0.0	0.6	0.0	40.3	21.2
"2020-01-09 12:00"	0.5	0.4	0.2	0.0	0.4	0.0	59.0	21.2

Re: AGC

DE Douglas E. Stacey
To Changhu Xing; Michael E. Davenport
Tue 2:10 PM

That is correct!

Douglas Stacey
Irradiation Experiment Design Engineer | Experiment Design C660
douglas.stacey@inl.gov | work: 208-526-1078 | cell: 208-821-2182
Idaho National Laboratory | 1955 Fremont Ave. | Idaho Falls, ID | 83415

From: Changhu Xing <Changhu.Xing@inl.gov>
Sent: Tuesday, February 2, 2021 12:44 PM
To: Douglas E. Stacey <douglas.stacey@inl.gov>; Michael E. Davenport <michael.davenport@inl.gov>
Subject: RE: AGC

Thanks. It's hard to see from the drawing but it's much easier from your explanation. Here is my understanding:

Gas zones 1 thru 5 are between heat shield and graphite holder, separated by the rings
Gas zone 6 is between heat shield and capsule, one whole gap
Gas zone 7 is for all inside the graphite holder.

From: Douglas E. Stacey <douglas.stacey@inl.gov>
Sent: Tuesday, February 2, 2021 12:36 PM
To: Michael E. Davenport <michael.davenport@inl.gov>; Changhu Xing <Changhu.Xing@inl.gov>
Subject: Re: AGC

Zone 6: Is the annulus between the heat shield and the outer capsule wall, going the full length of the upper and lower graphite specimen holders. Drawing 604554, Sheet 6, view P, shows one of the gas lines for zone 6 exiting the lower specimen holder just below the bottom edge of the heat shield.

Zone 7: Two of the gas lines go the entire length of the graphite holders and come out the bottom of the lower graphite holder. The two lines were then bent with two 90 degree bends and then stuck into blind holes. Look at drawing 604554, sheet 6, Section W-W. You can see the two tubes coming out the bottom and then being bent 180 degrees inward into blind holes. Drawing 604551, sheet 5, View T-T shows the depth of the two blind holes to only be .145". I was told that the gas from these two lines is meant to flow back up through the gas line holes and specimen holes machined in the graphite holders. I guess you could say zone 7 consists of all the void spaces inside of the two graphite specimen holders.